Republic of Iraq

Ministry of Higher Education and

Scientific Research

University of Babylon

College of Science

Department of physics

Optical and Electrical Characterization of some Phthalocyanines and their Derivatives Thin Films

A thesis

Submitted to the Physics Department, College of Science, University of Babylon in Partial Fulfillment of the Requirements for the Degree of Master of Science in Physics

By

Atheer Abbas Shatti Zappy

B.Sc. in Physics /2003

Supervised by

Asst. Prof.

Asst. Prof. Dr Hikmat Adnan Jawad Banimuslem

2022 A.D. 1444 A.H.

بسم الله الرحمن الرحيم

((يَرْفَعِ اللَّهُ الَّذِينَ آمَنُوا مِنكُمْ

وَالَّذِينَ أُوتُوا الْعِلْمَ دَرَجَاتٍ))

صدق الله العلي العظيم

سورة المجادلة | الآية 11

Supervisor`s certificate

I certify that this dissertation**(Optical and Electrical Characterization of some Phthalocyanines and their Derivatives Thin Films) by Atheer**
Signature **:**

Supervisor **: Dr. Hikmat Adnan Jawad**

Title **: Assistant Professor**

Affiliation **:**Department of Physics- College of Science- University of Babylon

Date **: / / 2022**

Recommendation of Head of Physics Department

In view of the available recommendations, I forward this thesis for

Debate by the examining committee**.**
Signature **:**

Name **: Dr. Samira A. Mahdi**

Title **: assistant Professor**

Affiliation **: Head of Department of Physics-College of Science–University of Babylon**

Date **: / / 2022**

Examining Committee Certificate

We certify that we have read this thesis entitled " **Optical and Electrical Characterization of some Phthalocyanines and their Derivatives Thin Films"** and as an examining committee , examined the M. Sc student " in its content and that, in our opinion it meets the standard of a thesis for the degree of Master of in science of physics.

Signature:

Name: **Dr. Abdulazeez O. Mousa**

Title: Professor

Affiliation: University of Babylon College of Science

Department of Physics

Date : / / **2022**

(Chairman)

Signature:

Name: **Dr. Khalid Haneen Abass**

Title: Professor

Affiliation: University of Babylon College of Education of Pure Science

Department of Physics

Date : / / **2022**

(Member)

Signature:

Name: **Dr. Hisham Mohammed Ail**

Title: Assistant Professor

Affiliation: University of Al- Qadisiyah College of Education

Department of Physics

Date : / / **2022**

(Member)

Signature:

Name: **Dr. Hikmat Adnan Jawad**

Title: Assistant Professor

Affiliation: University of Babylon College of Science

Department of Physics

Date : / / **2022**

(Member and Supervisor)

Approved by the college committee on graduate studies :

Signature:

Name: **Dr. Faez Ali Rashid AL- Maamori**

Title: **Professor**

Affiliation: Dean of the College of Science-University of Babylon

Date: \ \ 2022

Dedication

To everyone who gave us hope and confidence to reach what we want…

To everyone who encouraged us to continue…

To everyone who repeated to us calls for success…

Atheer

Acknowledgments

Firstly, I should thank my Almighty (Allah) for helping me in completing my dissertation.

I would like to express my thanks, gratitude and appreciation to my supervisor Asst. Prof. Dr. Hikmat Adnan Jawad Banimuslem for suggesting this topic for me and for his extinguished efforts, sound advice and guidance that have helped in smoothing out every difficulty encountered during my work. Many thanks to the deanery of the college of science at Babylon University and the Department of Physics for offering me the opportunity to complete my dissertation. My great thanks are expressed to all my friends. Finally, many thanks and gratefulness to all my family members who always support me and alleviate difficulties I have faced during my work.

Atheer

Summary

Full literature review and theoretical principles related the project have been discussed through the first and second chapter of this dissertation. Background of the most important fundamental that followed building up this work has also been provide.

Morphology of samples surface has been investigated by atomic force microscopy and revealed that zinc phthalocyanine shows rougher films than copper phthalocyanine because zinc atom is larger in diameter than copper resulting in hindering the movement of the entire molecule and then the alignment on the film surface.

Optical properties and energy gap calculation were studied utilizing UV-Visible absorption spectroscopy. The red shift in the absorption band in case of thin films indicated that phthalocyanines tend to make aggregation of dimer and trimer in comparison to solution where only monomers exist. energy gap calculations show that the copper phthalocyanine (CuPc) films and zinc phthalocyanine films (ZnPc) having band gaps of 3.87 eV and 3.93 eV respectively and the transition of charge carriers is direct transition.

Electrical characterization has been conducted using Kiethely semiconductor system and the temperature dependence conductivity measurements revealed that phthalocyanine films have two region of activation energies arising from two conduction mechanisms.

Detection of some gases has been carried out using resistive based sensor measurements. ZnPc has shown no obvious behavior towards gases, while CuPc was selective to NO_2 gas and shown very high sensitivity and reversibility

Contents

List of symbols and Abbreviations

Abbreviation	Description
MPcs	Metal Phthalocyanines
FETs	field-effect transistors
Pcs	Phthalocyanines
CuPc	Copper phthalocyanine
ZnPc	Zinc phthalocyanine
H_2Pc	Metal-free phthalocyanine
K	Kelvin
LED	Light emitting displays
$CHCL_3$	Chloroform
UV	Ultraviolet radiation
LB	Langmuir-Blodgett
C.B.	Conduction band
V.B.	Valence band
LC	Liquid crystalline
HOMO	Higher occupied molecular orbital
LUMO	Lower unoccupied molecular orbital
$h\upsilon$	Photon energy
h	Plank's constant
υ	The incident photon frequency
E_g	Energy gap
λ_{max}	The maximum wavelength
I_0	The incident photon intensity
I_T	The transmitted photon intensity
α	Absorption coefficient
A_b	Absorption

r	Constant which takes the values (1/2, 3/2, 2, and 3)
n	Refractive index
c	Light velocity
Re	Reflectance
T_r	Transmittance
S	Siemens (Conductivity unit)
I	Current
V	Potential difference
R	Resistance
ρel	Resistivity
l	Length
A	Cross section area
σ	Conductivity
H	Thickness of film
L	Gap between fingers
W	Overlap distance between the electrodes
Nr	Number of fingers of interdigitated electrodes
$\sigma_{\circ}$	Zero kelvin conductivity
E_a	Activation energy
K_B	Boltzmann constant
T	Temperature
RMS	Root mean square
AFM	Atomic force microscopy
K	Spring Constant
IDE	Interdigitated Electrode
DC	Direct current
J	Current density
E	Electrical field

List of Figures

List of Tables

Chapter One
Introduction
and
Literature Review

1.1: Background

Metal Phthalocyanines (MPcs) are π-electron conjugated macrocyclic compounds, exhibiting outstanding performance in the field of chemical and bio sensors[1,2], liquid crystals [3,4], field effect transistors[5,6], electrochromic devices [7], and memory applications[8,9]. The structure of MPcs strongly affects their properties, such as specific surface area, electron transfer properties and thermal stability, therefore affecting their performance in device applications [10]. The major advantages of MPcs over other organic analogous are [11,12] : (i) Their tunable structure with high flexibility in having large variety of substitution on the periphery of the molecule's rim, as well as their ability to coordinate almost every metallic element in the centre of their macrocycle; (ii) an exceptional thermal and chemical stability compared with most of molecular materials; (iii) an excellent process-ability, resulting in the construction of a large variety of thin films by different deposition methods.

Although the MPc-based devices have been studied for long time, there are still some specific restrictions which need to be overcome; these include, (i) the improvement of the reproducibility of the organic thin film devices due to the difficult control of the crystallite orientation of the polycrystalline film of MPc, (ii) the improvement of the selectivity and sensitivity of the MPc thin film sensors, (iii) more homogenous films that are required for the manufacturing of semiconducting devices to avoid pin-holes and thus short circuit problems, (iv) the improvement of charge carrier mobility of the organic thin film diodes and transistors, which is determined by several key factors such as the type, orientation and structure of the MPcs, as well as the film thickness and the nature of interface between the organic film and the electrodes, (v) miniature, portable, robust, energy saving and low cost devices need to be fabricated

in order to satisfy the rapid development of nanodevices together with several other kinds of particular applications [12].

1.2: History of Phthalocyanine

Phthalocyanines (Pcs) represent without doubt the most important chromophoric system developed during the 20^{th} century. Historically, the most important event was probably their accidental discovery around 1928 by a dye manufacturing company in Scotland. The first synthesis of phthalocyanine was reported in 1907 [13] when Braun and Tcherniac engaged in a study of the chemistry of o-cyanobenzamide. When this compound was heated, a trace amount of a blue substance was obtained which undoubtedly was metal-free phthalocyanine [14].

The structure of this metal-free, unsubstituted phthalocyanine was determined only about a quarter of a century later by the comprehensive studies of Dent and Linstead [15] and the X-ray diffraction analyses of Robertson [16], while examining both metal-free phthalocyanines (Figure 1.a) and metallophthalocyanines (Figure 1.b). In 1927, de Diesbach and coworkers [17], reported that when 1,2-dibromobenzene was treated with copper(I) cyanide in boiling quinoline for eight hour, a blue product was obtained. This was almost certainly the first preparation of copper phthalocyanine (CuPc) [17].

The molecular formula was determined by elemental analysis and the compound was remarkably stable against alkali, concentrated acids and heat, but they were unable to suggest the structure. In 1928, in the manufacture of phthalimide by Scottish Dyes from the reaction of phthalic anhydride with ammonia in a reactor, the formation of a blue impurity was observed in certain production batches. This contaminant was isolated as a

dark-blue, insoluble crystalline substance. Ultimately, the compound proved to be iron [17].

Phthalocyanine (ZnPc), the source of the zinc will be the wall of the reactor. An independent synthesis involving passing ammonia gas through molten phthalic anhydride in the presence of iron filings confirmed the findings.

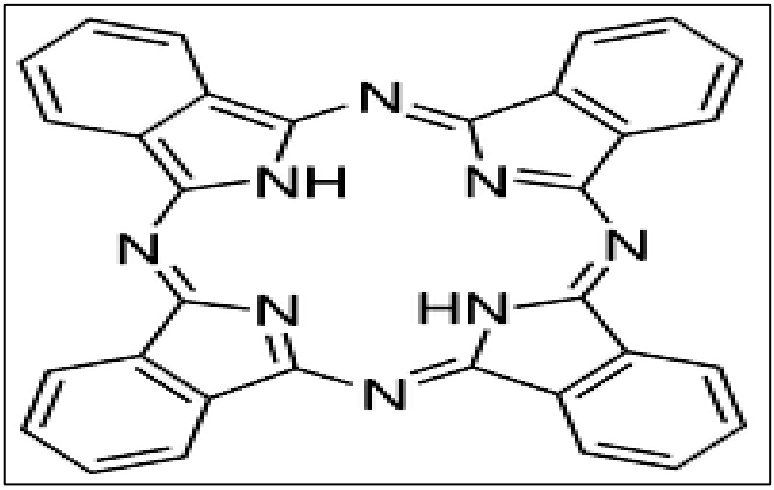

Fig.1.1.a- Metal-Free Phthalocyanine.

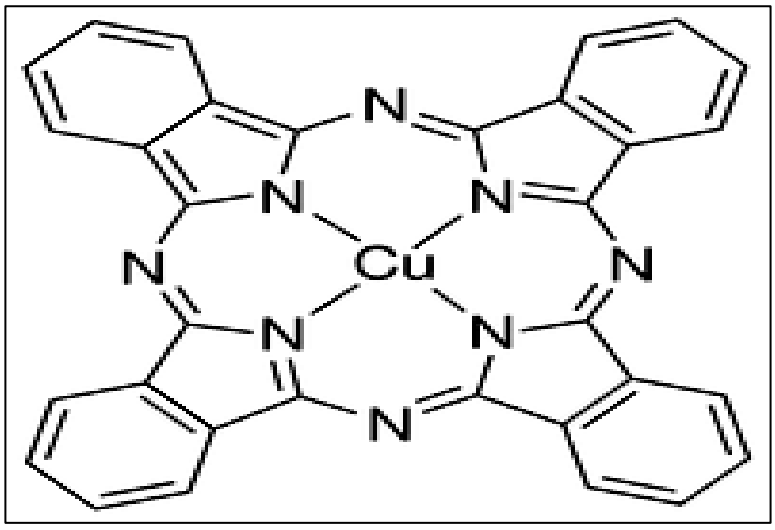

Fig.1.1.b -Metal Phthalocyanine.

The metal-free phthalocyanine (H_2Pc) has the general formula $C_{32}H_{18}N_8$ or $(C_8H_4N_2)4H_2$. It consists of four isoindole units linked by aza nitrogen atoms with two hydrogen atoms linked at the center. The phthalocyanine polymers have become one of the most studies of all organic functional materials and have recently attracted considerable interest due to their high thermal and chemical stability [18]. Phthalocyanines, known as tetrabenzo [19,20], tetraazaporphyrin, have thermally and chemically stable structures owing to their conjugated 18 π-electron systems [21,22].

Due to their stable structures with having high extinction coefficients ($\varepsilon max > 1.0 \_ 10^5\ M^{-1}cm^{-1}$) and long absorption wavelength maxima (600 nm > λmax > 900 nm), they have promising applications in many fields from chemical sensors to solar cells, from nonlinear optics to photodynamic therapy [23,24,25]. However, the tendency of unsubstituted phthalocyanines to self-assemble causes limitations in determining their superior properties. It is well known that the aggregation tendency of phthalocyanines has a negative effect on their optical properties in addition to causing low solubility. Therefore, in addition to increasing their solubility, control of their aggregation is of primary importance in phthalocyanine chemistry. Phthalocyanines generally form H-type aggregates in solution. This is due to the regularity of push and pull forces in H-aggregation. Because of the 18-π electrons conjugated by π–π and Van der Waals interactions, the molecules overlap strongly and tend to form columnar stacks. Besides, concentration, temperature, nature of the substituents, nature of the solvent and additives, and the metal ion in the center are effective factors on aggregation [26], J-type aggregates are less common in phthalocyanine complexes than H-type aggregates and usually occur by metal– ligand interaction [27], It is well known that the

substitution of bulky groups in the peripheral/nonperipheral positions of phthalocyanines increases their solubility in common organic solvents. Phthalocyanines containing 1-(4-hydroxyphenyl) propane-1-one groups previously synthesized by Gunsel and Epokur et al., have been found to have very high solubility in many organic solvents such as $CHCl_3$, CH_2Cl_2, THF, toluene, DMF, and DMSO [28,29]. Aggregation orientation of Pc depends on temperature, the character of the solvent, the position, the kind, number, and size of the substituent, the central metal ion, and the concentration of dye. Depending on the geometry of the aggregated structures, stacked arrangements have been called to as J-and H-aggregate type [30]. J-and H aggregate type means that the stacked structure may aggregate in a head to tail arrangement way to form a polymeric (J-aggregate type) or a parallel arrangement to form an oligomeric (H-aggregate type) (see Fig1.2) [31].

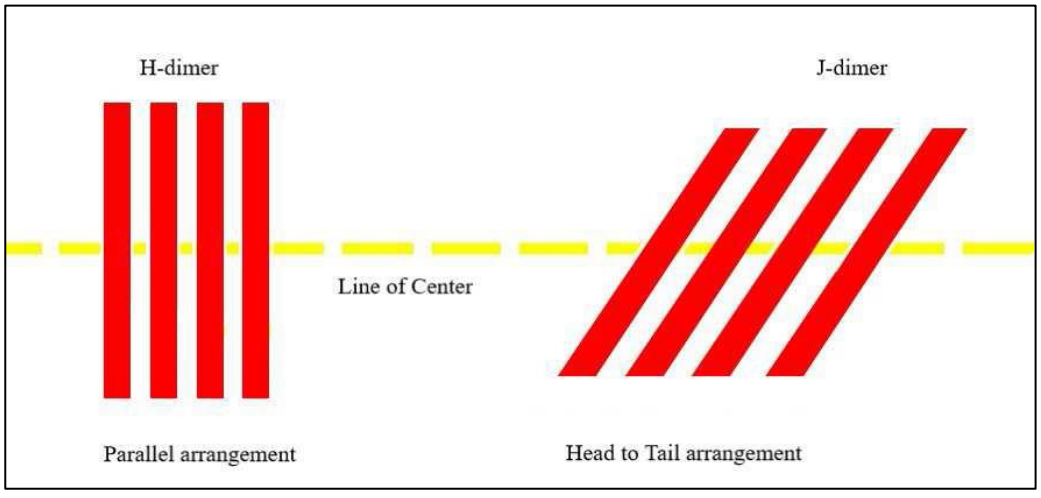

Figure1.2. The direction of transition dipole moments for H- and J-dimer[31].

1.3: Molecular Structure of Phthalocyanine

The single basic structural unit of a phthalocyanine molecule is given in Figure (1-1). The un-substituted form of phthalocyanine usually designated chemically as 5, 10, 15, 20 tetraazatetrabenzoporphyrin or tetrabenzoporphyrazin [32]. The molecule is planar, consisting of four isoindole molecules linked together at the corners of the pyrrole ring by four nitrogen atoms as shown in Figure (1-3). The space within the four central nitrogen atoms is occupied either by hydrogen atoms in metal free phthalocyanine or by a metal atom in metal substituted Pcs. Distinguishing feature of the organic semiconductors is its conjugate bonding. The most common polymorph of Pc belongs to the $P2_{l/a}$ space group with two planar centre symmetric molecules in a unit cell. The base centered arrangement of the two molecules and the crystal axes in the unit cell is given in Figure (1-5) [33]. The regularly spaced molecular units make the conduction mechanisms complex. The intermolecular binding is weak, but the electrons within a molecule are tightly bound. The electrons associated with the conjugated bonds are not localized on a particular atom, but they are associated with the entire molecule.

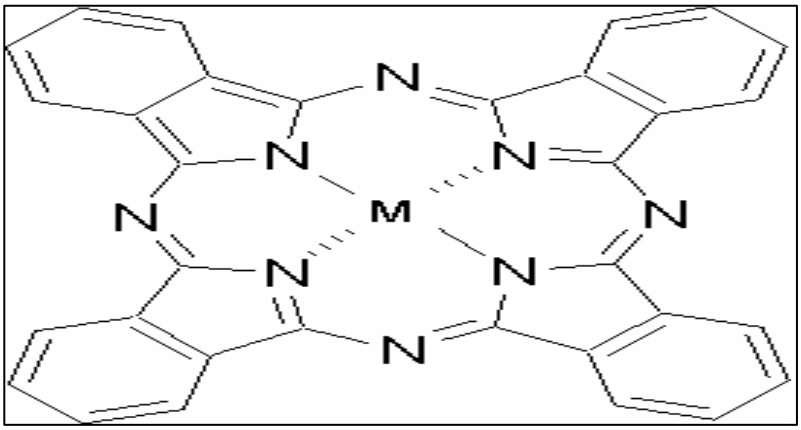

Fig.1.3. Basic structural unit of a metal phthalocyanine Molecule[33].

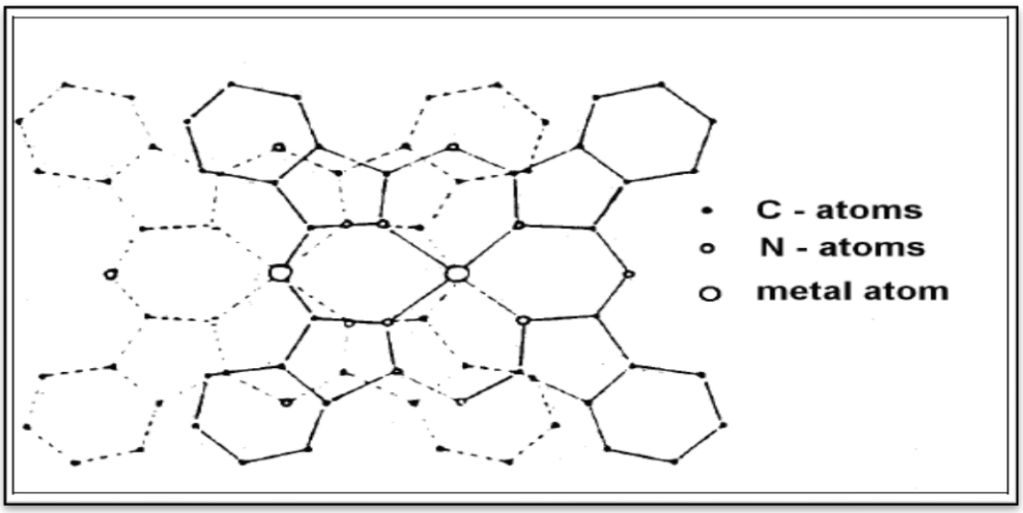

Fig.1.4. Normal projections of two molecules of metal Substituted Phthalocyanine [33].

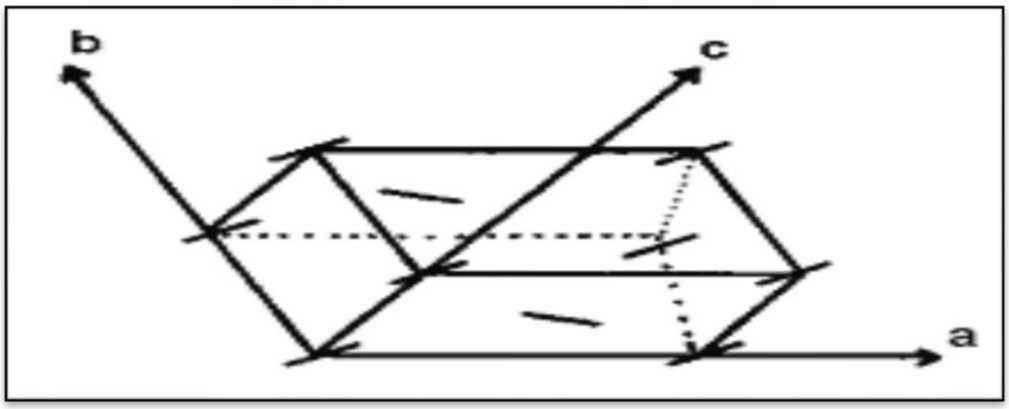

Fig.1.5. Unit cell of a base centered phthalocyanine molecule [33].

The atoms of the molecules at either ends of the b-axis do not fall in a plane exactly over another set when the projection normal to the molecular plane is taken for a metal phthalocyanine (MPc) [33] as shown in Figure (1-4). The replacement of the central hydrogen molecule by a metal ion does not alter the crystal structure of the material. Even though there is no significant effect on the crystal structure due to the metal substitution; the electrical conductivity is considerably affected by the substitution. Bao et al. [34] found that among the wide range of organic semiconductors

considered, metal phthalocyanines (Pc) are one of the most promising candidates to be used in the fabrication of organic devices.

1.4: Organic Semiconductors

Semiconductors can be broadly classified into two main groups as inorganic and organic semiconductors [35]. Though inorganic semiconductors like germanium and silicon are used extensively in electronic industry, now it is expected that organic semiconductors will replace inorganic semiconductors in the near future. Aromatic hydrocarbons such as anthracene and phthalocyanine are found to possess semiconducting properties [35].

The basic property of semiconductors is its electrical conductivity, which depends on the mobility and concentration of charge carriers [36]. The electrical conductivity, carrier concentrations and mobility of organic semiconductors are low in comparison with those of inorganic semiconductors. A comparison of the organic semiconductor with those of a conventional semiconductor (Germanium) is given in Table 1.1 [35,36] .

Table 1.1: Comparison of the electrical properties of the inorganic semiconductor [35] germanium and organic semiconductor [36]

Properties	Inorganic	Organic
Mobility (cm^2/ v. sec)	>3900	>0.02
Carrier concentration (cm^{-3})	>2.5x 10^{13}	>8 x 10^7
Trap density (cm^{-3})	_	10^{12}-10^{14}
Resistivity (Ohm . cm)	>43	10^{14}
Band gap (eV)	>0.67	>3.02

Semiconductors in general are characterized by covalent bonding between ions of the crystal. Electrons can be excited optically, thermally or any other way, promoting free electrons into the conduction band and leaving holes in the valence band [35].

Under an applied electric field, the free charge carriers are transported causing conduction. Electronic charge transport in organic molecules does not require perfect single crystals. A regular arrangement of atoms, ions or molecules over a distance of only a few lattice spacing of the structural units is necessary for the electronic charge transport and is usually a sufficient condition for electrical conductivity of the organic system[36]. Organic semiconductors have attracted much attention due to their successful application in optical and electronic devices with encouraging performances [37].

The organic semiconductors, the electrical properties are sensitive to the impurity content and doping [37,38]. Furthermore, the molecules interact by relatively weak Van der Waals or London type forces so that the intermolecular separations are larger compared with separations between atoms or ions of inorganic lattice. Consequently, there is only a weak overlap of molecular orbitals and the intermolecular electron exchange is small[38]. The electrons within a molecule are tightly bound, if there is an intermolecular overlap of electron wave. Their electrical and electronic behavior is of considerable significance in biological processes. Phthalocyanines are thermally stable and can be sublimed to form thin films without decomposition. Therefore, in contrast to many other organic materials, the preparation of phthalocyanine thin films by vacuum sublimation is feasible [39].

The success in the research and development of organic electronic devices has given us the confidence that organic semiconductors are really useful in conventional electronics applications, where only inorganic materials, such as silicon, germanium and compound semiconductors have been used in the last 50 years [39].Thin films of organic materials are currently widely tested for exploitation in devices such as light-emitting devices [38,39], optical recording [40], field-effect transistors (FETs) [41,42], solar cells [43,44] and sensors [45,46].

The body of knowledge accumulated over the years has triggered improvements in performance to the point where these organic-based devices start competing with their inorganic counterparts. Organic semiconductors are advantageous for the fabrication of electronic devices because of the ease of processing at low temperature, architectural flexibility, material variety, and environmental safety. Organic devices are expected to be ultimately incorporated, for instance, into all-plastic integrated circuits for low-end and low cost electronics and all-plastic light-emitting displays, where each pixel consists of an organic LED driven by an organic FET [41].

A large number of organic materials has been described, which show electrical conductivity in the semiconducting range. But, due to the extremely low intrinsic conductivity, most organic semiconductors should really be designated as insulators [42]. The use of the name semiconductor is based on the extrinsic semiconducting properties of organic systems. The capacity to transport charge is generated by light, injected by electrodes, or provided by chemical dopants. The physicochemical characteristics of organic semiconductors depend on their molecular structure and on the presence of amounts of impurities [42].

1.5: Metallo-Phthalocyanines (MPc)

Elements from groups I_A to V_B can all combine with phthalocyanine ring and more than 70 different metallophthalocyanines (MPc) are known [47]. Many of them have been studied over the past few years. Apart from their uses as dyes or pigments.

The electrons within a molecule are tightly bound, if there is an intermolecular overlap of electron wave. Their electronic behavior is of considerable significance in biological processes. Phthalocyanines are thermally stable and can be sublimed to form thin films without decomposition. Therefore, in contrast to many other organic materials, the preparation of phthalocyanine thin films by vacuum sublimation is feasible.

The phthalocyanine family has been regarded as potentially attractive gas-sensing and solar cell materials [48] because:

1. They are thermally stable to 770 K and therefore can be used for extended period of elevated temperatures.
2. Many of them are easily vacuum sublimed, giving stable films.
3. Functional groups can substitute on either the benzonoide ring or on the central metal atom – thus creating new materials differing in properties from those of the parent substance.

Metal phthalocyanine became one of the promising organic semiconductors due to the possibility of applications in electro-optic devices; photo conducting agents, photovoltaic cell elements, nonlinear optics, electro catalysis, and other photo electronic devices [49].

The versatility, architectural flexibility and ease of processing make them eligible candidates for use not only in electronic industry but also in photonic technology. These compounds have a longer storage life and high read out times for use in optical storage systems. The potential uses of

phthalocyanines include sensing elements in chemical sensors, electro-chromic display devices, photodynamic reagents, electro-catalysts for fuel cells, photovoltaic cell elements, dyes, colour photocopying, conducting polymers [50].

1.6: Emerging Material

Following this discovery, the colour manufacturing industry was quick to recognize the unique properties of the compound and to exploit their commercial potential.

Phthalocyanine has emerged as one of the most extensively studied classes of compounds, because of their intense, bright colours, their high stability and their unique molecular structure [51,52].

Phthalocyanines are two-dimensional 18 π-electron aromatic porphyrin synthetic analogues, consisting of four isoindole subunits linked together through nitrogen atoms. Phthalocyanines and their metallo derivatives (MPcs) have recently attracted an increasing interest not only for the preparation of dyes and pigments but also as building blocks for the construction of new molecular materials for electronics and optoelectronics. These arise from their electronic delocalization, which makes them valuable in different fields of science and technology [53] .

The chemical flexibility of this class of compounds allows the preparation of a large variety of related structures and, consequently, the tailoring of the physical, electronic, and optical properties, as well as the improvement of process ability. Therefore, peripheral substitution of phthalocyanines with bulky groups or hydrocarbon chains enhances their solubility and permits the deposition onto substrate, using spin-coating or LB deposition techniques [54].

The possibility of incorporating a broad range of metal atoms into the Pc cavity offers additional features to optimize the physical responses. On the other hand, their thermal and environmental stability are important characteristics that make them promising candidates to be incorporated into devices. To achieve this goal, an important point must be addressed which is the control of the supra molecular arrangement of these macrocycles in the solid state [55].

Liquid crystalline (LC) discotic mesophase materials can self-organise their molecules from organic solution into columnar stacks and develop potential solution processed molecular electronic materials. The columnar aggregates of discotic phthalocyanine molecules with effective overlap of π-orbitals along the stacking direction and low reformation energy [56] provide efficient anisotropic electronic transport networks along the molecular columns in the liquid crystalline mesophases with hole mobilities in the order of $10^{-1}\ cm^2$ / Vs [57]. Disk-like molecules, comprising a flat rigid aromatic core and flexible peripheral substituents, self-organize into one-dimensional supra molecular columns providing efficient anisotropic electronic transport channels [53] .

Such self- assembled columns in organic discotic molecules can adopt two types of characteristic orientations on surfaces: (i) homogeneous alignment, where the edge-on orientation of molecules and the columns parallel to the substrate surface is observed and (ii) homeotropic alignment, where the molecules are aligned face-on to the substrate and the columnar axes perpendicularly arranged with respect to the substrate surface [58] . Usually, homeotropic alignment can be generated by thermal annealing, that is slow cooling of the isotropic melt confined between two substrates [8] .

In the last few decades, phthalocyanines have been extensively studied as targets for optical switching and limiting devices [59] , organic field effect transistors [6] , sensors [60,61], light emitting devices [62], molecular solar cells [63], data storage media [64], photosensitizers [66] , and electronic nose for cancer detection [63] . There are significant number of studies that were concerned with insoluble unsubstituted-phthalocyanines and their application employing their unique ability to evaporate without decomposition [62]. However, peripherally substituted soluble metallophthalocyanines facilitate films fabrication and their investigation using wet-deposition techniques.

1.7: Literature Review

Phthalocyanine in general and metallophthalocyanine in particular have gained special interest recently as these materials have the potential for several possible applications ranging from photovoltaic to chemical and bio detections. This literature study provides an extensive analysis of the literature as related works and gives a comprehensive understanding to the reader about materials under investigation.

S Ambily and co-workers (1999) [67] have prepared copper phthalocyanine thin films using thermal evaporation and studied the electrical properties of the prepared devices. They found that activation energy is a clear function of annealing temperature as it decreases when temperature increases. This could be due to the reduction in trap sites because of annealing. The activation energy for metal phthalocyanine in general depends on the conduction mechanisms and charge carrier. In the study of *Araghi et al. (2019)* [68], where Arrhenius plot has been investigated as a function of temperature.

The conduction mechanism was found to be hopping, while increasing the substrate temperature caused a deviate from the typical hopping mechanism to three different regions and so activation energies would be lower values. However, additives to phthalocyanine have proved to change all the electrical properties especially carbon materials that applied as diodes and rectifiers [69]. In this prospect, *Akanksha Sharma et al. (2017)* [70] have identified the traps characteristics in polycrystalline organic thin films CuPc using two and three terminal devices and observed that the trap density can be controlled by varying growth conditions and CuPc thin films at low substrate temperature are proved to have larger concentration of traps. Charge carriers trapped by interface states at grain boundaries cannot hop to HOMO or LUMO unless they get sufficient energy to be released because trapped charges at the grain-boundary interfaces lead to the formation of a potential barrier for charge transport process. Polycrystalline thin films grown under favorable growth conditions to achieve anisotropic morphology with fewer grain boundaries seem to be providing a percolative passage for the carrier transport. In addition, *Chandra Sekhar et al.(2021)* [71] have found that metal phthalocyanine is clearly affected by the modifiers as the activation energies were obviously reduced by incorporating additives as active layer between top electrode and the phthalocyanine. In this study, the conduction mechanism has proved to be space charge limited conduction with exponential trap distribution.

The optical properties of phthalocyanine are related directly to the absorption bands in the UV-Visible spectra. The Q band of metal phthalocyanine is in the range between (600-700) nm, while B band is located at lower wavelength ~ around 300 nm [72]. *Nada K. Abbas et al. (2019*) [73] have prepared copper phthalocyanine thin films using spin coating technique. They found that, by using Tauc relation, *B* and Q bands

indicate the presence of two energy gaps. Also, the absorption intensity at both regions has been variably with the annealing temperature and the film annealed at 100 ◦C has the lowest optical energy gap due to phase transitions and nanostructure after annealing, the stability in the peak positions in absorption and transmission spectra in the absorbing region exhibited the stability of the structure of CuPc. The refractive index is generally independent on the film thickness. Copper and magnesium phthalocyanine thin films prepared using Langmuir technique have shown different behavior of energy gap. The functional groups on the rim of the molecule are meant to have more impact on the energy gap than the central atom and the values of energy gap calculated using Tauc plot were found to be lower than that calculated using electron binding energy. In fact the water presence in the thin films prepared by Langmuir technique can significantly affect the optical energy gap. These results observed by *Stachowiak et al. (2021)* [74].

Various-thick CuPc layers were respectively deposited on 50-nm-thick pentacene layer for studying the thickness effect of the CuPc layer on the ethanol gas sensors [75]. In this work, the performances of the resulting organic thin-film transistor-structured ethanol gas sensors were improved with an increase of the thickness of CuPc layer until 5 nm indicating that the optimal CuPc thickness was 5 nm. Furthermore, by measuring the performances of the ethanol gas sensors under NO_2, O_2,, and N_2 gases, their sensitivity was much smaller than that of the ethanol gas. These experimental results verified that the ethanol gas sensors possessed high selectivity performances. Consequently, high-performance, high-stability and high-selectivity ethanol gas sensors could be achieved by stacking CuPc layer on pentacene layer as double sensing layers. Nonetheless, the

substitutions in the preferably position of phthalocyanine rims have found to be of significant effect.

These foundations were confirmed by *Ahmet T. Bilgiçli et al. (2021)* [23], where octasubstituted phthalocyanine derivatives [ZnPc(3), CuPc (4), and CoPc(5)] have been prepared as thin films to apply as bio sensor.

Typical organic semiconductors, based on metal phthalocyanine have been extensively studies for the development of gas sensors based on their high sensitivities, fast response time and room temperature operation [76]. Phthalocyanine complexes have been recognized to exhibit substantial changes in optical, electrical and magnetic properties on interaction with wide range of reducing and oxidizing agents [75][78]. These characteristics can be employed for several kinds of chemical detection applications. The crystalline structure of phthalocyanines is such that they can easily accommodate dopant molecules in channels adjacent to the phthalocyanine stacks. When dopant molecule such as NO_2 is adsorbed onto phthalocyanine surface, charge transfer interaction takes place, which results in very large increase in surface conduction [79]. The process is somehow similar to the doping of intrinsic silicon to produce p-type semiconductor. In addition, phthalocyanine thin films conductivity has been shown to be sensitive to low concentrations of various gases [80]. Both the sensitivity and the reversibility of the Pc-based detectors are, in most cases, acceptable [81]. Much work has been carried out in order to understand the influence of the morphology, the temperature, the central metal and the peripheral substituents on the sensing ability of the phthalocyanine thin films. The most promising candidates as far as applications are concerned are based on double-decker phthalocyanines [1]. Efforts are being made to transform the present laboratory devices into real-world sensors especially with the development of phthalocyanine-

based electronic noses [1]. Many groups of researchers have been engaged in the synthesis of novel phthalocyanines for sensing applications to detect different types of agents such as halogens[79].

1.8: Aims and Objectives

The principal aim of this work is the preparation and characterization of metal phthalocyanine thin films deposited on glass slide, interdigitated electrodes.

In order to achieve the above goal, the following objectives will be addressed:

- Study the optical properties of the prepared devices including the optical energy gap.
- Study the structural and morphological properties of zinc phthalocyanine and copper phthalocyanine thin films.
- Examine the DC conductivity performance of the PCs materials.
- Investigate the temperature dependence conductivity of the semi-conductive phthalocyanine .
- Calculate the activation energy using Arrhenius plot.
- Study the interaction of PCs with some organic gases using homemade sensing system.

Chapter Two

Theoretical Part

2.1: Introduction

This chapter cover the general description of the theoretical part of the; structural, optical, and electrical measurements and gives a satisfactory review including all the relations, scientific explanations and the equations which are used in this dissertation.

2.2 : Spin Coating

Spin coating has been used for several decades for the application of thin films. In this process, a small drop of the coating material is loaded onto the centre of a substrate, which is then spun at a controlled high speed. In the spin coating process, the substrate spins around an axis which should be perpendicular to the coating area. As a result, the coating material spreads towards, and eventually off, the edge of the substrate leaving a thin film of coating on the surface. Final film thickness and other properties will depend on the nature of the coating (viscosity, drying rate, percent solids, surface tension, etc.) and the parameters chosen for the spin process such as the rotation speed as shown in Figure 2.1 [82].

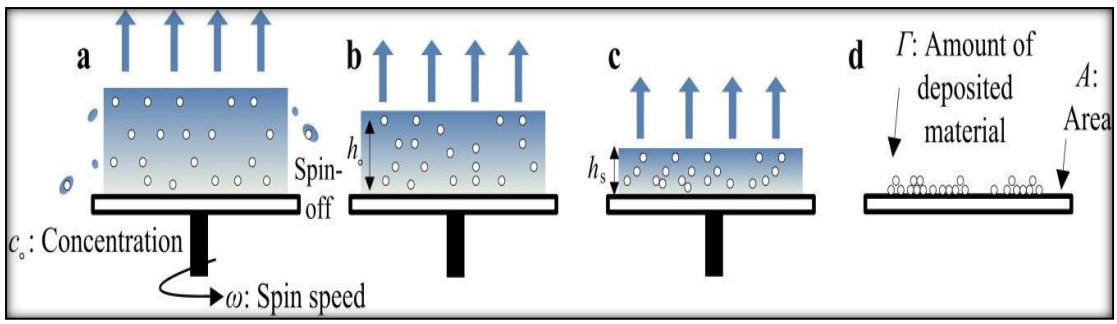

Figure 2.1: Schematic figure of spin-coating indicating the dominant process at the beginning of spin-coating (spin-off) and later after the equilibrium liquid film thickness.[82]

2.3: Excitation Theory

In many chemical compounds such as pure crystals and semiconductors, there exist some energy levels occupied by electrons, as well as some unoccupied energy levels. Excitation by photon causes an electron to transfer to one of these unoccupied levels. This electronic state resulted from excitation is called an excitation [83]**.** Before this electron goes back to its original state, according to Kasha's theory, a transition occurs between electronic and vibrational energy levels. The greater the overlap between vibrational energy levels, the quicker the molecule can undergo a transition from higher to lower level. The emission occurs with a different wavelength than the excitation wavelength[84]**.** Due to strong van der-Waals forces between dye molecules, the self-assembly is often common at the liquid solid interface. Compared to dispersed monomers, this aggregation makes some changes in the absorption bands, which are observed as some shifts in spectra. In this case, the shifts are reported as H- and J-bands, which are related to hypsochromic and bathochromic shifts, respectively. According to the exciton theory, these shifts are explained in terms of transition moments of the dye molecule [85].

As seen in Fig.2.2, the dye molecules composing H- and J-dimer types are generally arranged in two various arrangements (parallel or head to tail) and their two-dimensional crystals are formed [86]**.** The relation between monomers arrangement and spectral shift based on this theory presented in Figure 2.2. The interaction between dye molecules usually leads to the splitting of energy levels in the dimer species**.**

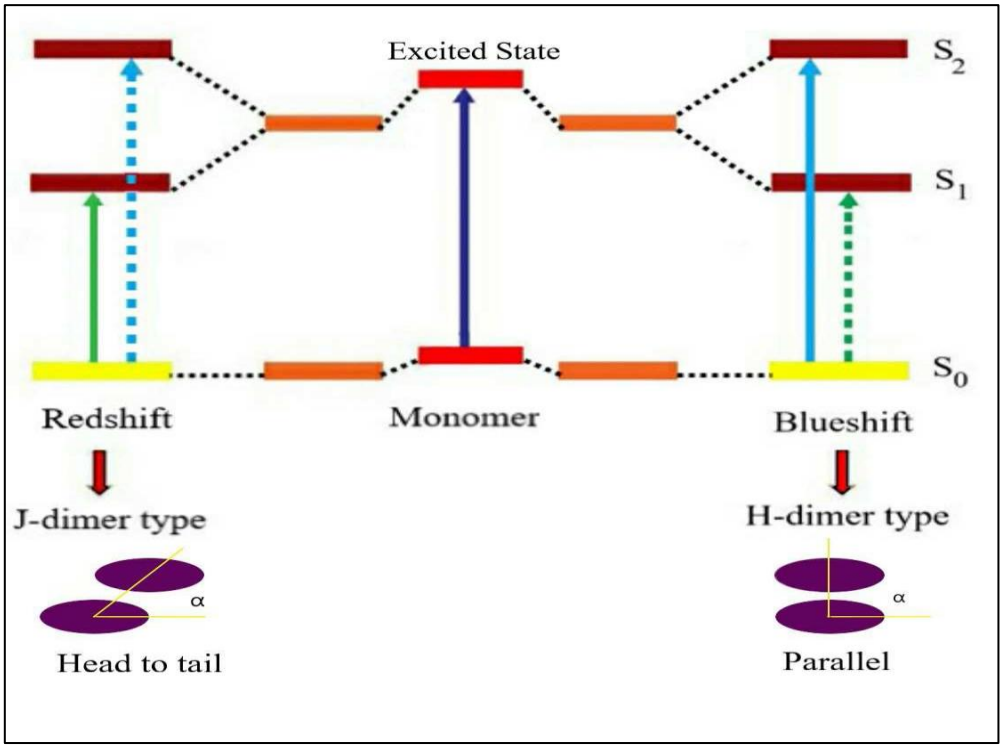

Figure 2.2: Presentation of the relation between the monomers arrangement and spectral shift based on the exciton theory[86].

2.4 : Optical Properties

The optical properties of a semiconductor are related to intrinsic effect. Based on the intrinsic location of the top of the valence band (V.B.) and bottom of the conduction band (C.B.) in the band structure, the electron-hole pair generation occurs directly or indirectly.

The ZnPc and CuPc thin film is a wide direct band gap compound semiconductor. It is highly transparent in the visible range which depends on the deposition technique and thickness[87],[88]. In the molecular scale valence and conduction bands become higher occupied molecular orbital (HOMO) and lower un-occupied molecular orbital (LUMO). Figure (2.3) represents the possible electronic transition. Many molecules absorb ultraviolet or visible light. The fundamental absorption is the most important absorption process which involves the transition of electrons

from the valence to the conduction band, which manifests itself by a rapid rise in absorption and this can be used to determine the energy gap of the semiconductor[89].

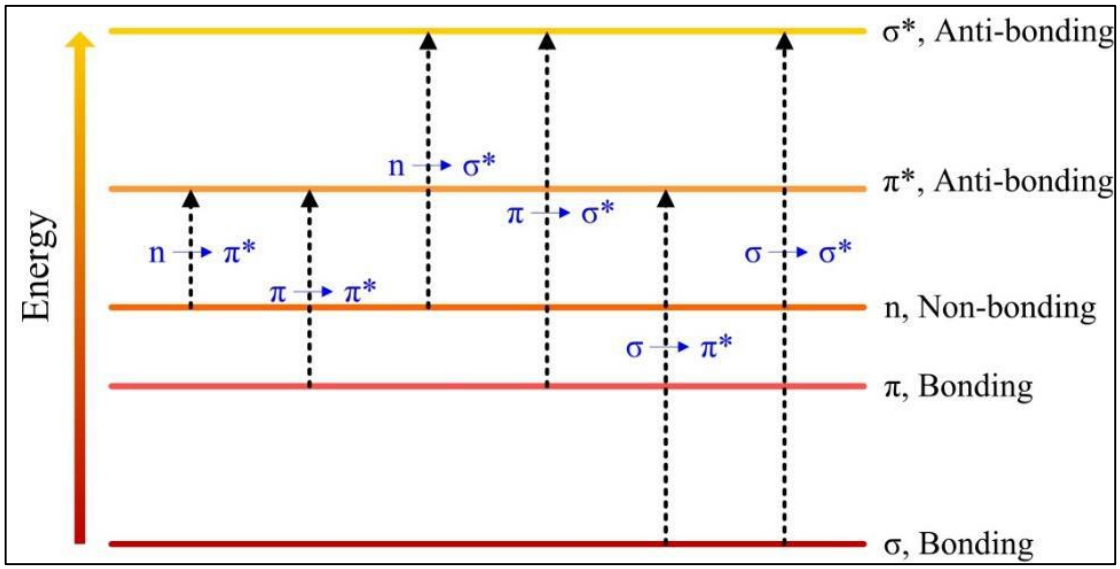

Figure 2.3: Possible electronic transition between intermolecular orbitals[89].

The semiconductor absorbs photon from the incident beam, the absorption depends on the photon energy (hv), where (h) is Plank's constant, (v) is the incident photon frequency, the absorption is associated with the electronic transition between the HOMO and LUMO in the material starting at the absorption edge which corresponds to minimum energy difference (Eg) between the lowest minimum of the HOMO and the highest maximum of the LUMO [90]. If the photon energy (hv) is equal or more than energy gap (E_g) then, the photon can interact with a valence electron, elevate the electron into the LUMO and create an electron–hole pair. The maximum wavelength (λ_{max}) of the incident photon which creates the electron–hole pair is defined as[91]:

$$\lambda_{max} = \frac{hc}{E_g} = \frac{1.24}{E_g\ (eV)} \quad (2\text{-}1)$$

The intensity of the photon flux decreases exponentially with distance through the semiconductor according to Beer's law[92]:

$$I_T = I_0 e^{-\alpha t} \quad (2\text{-}2)$$

Where (Io,IT) are the incident and the transmitted photon intensity respectively and (α) is the absorption coefficient. Which is defined as the relative number of the photons absorbed per unit distance of semiconductor, and (t) is the thickness of the film[93]**.**

$$\alpha = 2.303 \frac{A_b}{t} \quad (2\text{-}3)$$

Where (A_b) is the absorption.

The absorption of radiation that leads to electronic transitions between the valence and conduction bands is split into direct and indirect transitions. These transitions are described by the Tauc equation[94]**.**

$$(\alpha h\nu) = B(h\nu - E_g)^r \quad (2\text{-}4)$$

Where ($h\nu$)is the incident photon energy, (r) is constant which takes the values (1/2, 3/2, 2, and 3) depending on the material and the type of the optical transition whether it is direct or indirect, where (r) equal to (1/2, 2, 3/2 or 3) for direct allowed, indirect allowed, direct forbidden and indirect forbidden transitions, respectively[95]**.**

The optical constants are very important parameters because they describe the optical behavior of the materials. The absorption coefficient of

the material is a very strong function of the photon energy and band gap energy. As it is possible to know the nature of electronic transfers from knowing the value of the absorption coefficient, if the value of the absorption coefficient is high ($\alpha>10^4$), then this means a possibility of direct electronic transmission[96].

Optical constants included refractive index (n), and extinction coefficient (k). and real part (εr) and imaginary part (εi) of dielectric constant.

The complex refractive index (nc) is defined as[89]**.**

$$n_c = n - iK \qquad (2\text{-}5)$$

And it is related to the velocity of propagation (ϑ), and light velocity (c) by:

$$\vartheta = \frac{c}{n_c} \qquad (2\text{-}6)$$

The refractive index value can be calculated from the formula**.**

$$n = \frac{1}{Ts} + \sqrt{\frac{1}{Ts} - 1} \qquad (2\text{-}7)$$

Where (Re) is the reflectance, which is calculated by using equation [97].

$$Re = 1 - T_r - A_b \qquad (2\text{-}8)$$

Where (T_r) is the transmittance, (A_b) is the absorption.

The extinction coefficient, which is related to the exponential decay of the wave as it passes through the medium, is defined as[92] :

$$k_0 = \frac{\alpha\lambda}{4\pi} \qquad (2\text{-}9)$$

Where (λ) is the wavelength of the incident radiation.

2.5: UV-Visible Absorption Theory

UV-Vis absorption spectroscopy is the measurement of light absorption by a sample in the ultraviolet-visible spectral region of the electromagnetic spectrum. This absorption or attenuation can occur when light passes through a translucent liquid sample, or when light is reflected from a sample surface. The difference in the incident light and the transmitted light is used to determine the actual absorbance. When an atom or molecule absorbs energy, electrons are promoted from their ground state to an excited state. Molecules can only absorb radiant energy in definite units, or quanta, which correspond to the energy difference between the ground and excited states [82].

2.6: Electrical Properties

Studies on organic semiconducting thin films have become increasingly significant for electronic applications. These materials are chemically and thermally quite stable and therefore, efforts have been made to utilize thin films of these materials as molecular modules in a number of electronic and optoelectronic devices [98 ,65] .

Among these organic materials are the metal free phthalocyanines (H_2Pcs) and metal substituted phthalocyanines (MPcs) such as FePc, MgPc, PbPc, ZnPc, CuPc, and CoPc. These materials are generally p-type

semiconductors and can be simply deposited resulting in pure and homogeneous thin films [99].

The semiconductor materials are insulator material at (0K) temperature, but they can be conductor materials when the temperature increases to the limit values that converted to increase in conducted electron density. Therefore, the material can be classified according to the values of its electrical conductivity into three types; Conductor ($\sigma = 10^3 - 10^8$) S/m, Semiconductor ($\sigma = 10^3 - 10^{-8}$) S/m, and Insulator ($\sigma = 10^{-8} - 10^{-18}$) S/m [100].

The electrical properties measurement of semiconductor thin films allow the determination of the impurity levels present in the materials these parameters are critical to their utilization in various electronic and optoelectronic applications. The electrical properties depend upon the nature of semiconductor, if they are pure or doped and crystalline or amorphous [101]:

According to Ohm's law the current (I) (in amperes) in a sample is proportional directly to the potential difference (V) (in Volts) across two points on this sample [102]:

$$R = \frac{V}{I} \qquad (2\text{-}10)$$

Where (R) is the sample resistance measured in Ohms.

Electrical resistivity (also known as resistivity, specific electrical resistance, or volume resistivity) is an intrinsic property that quantifies how strongly a given material opposes the flow of electric current. A low resistivity indicates a material that readily allows the movement of electric charge. Resistivity is commonly represented by the Greek letter ρ. (rho).

The (SI) unit system of the electrical resistivity is the Ohm multiplies by meter (Ω·m) although other units like (Ω·cm) are also in use [97].

Consider that the current passes through a peace of material with length (*l*) (m) and a cross section area (*A*) (m^2). The electrical resistivity (ρ) can be defined as [90]:

$$\rho = \frac{RA}{L} \tag{2-11}$$

Electrical conductivity or specific conductance is the reciprocal of electrical resistivity and measures a material's ability to conduct an electric current. It is commonly represented by the Greek letter (σ) (sigma), (especially in electrical engineering) or (γ) (gamma) is which also occasionally used. Its (SI) unit is Siemens per meter (S/m) [88].

Where conductivity (σ), is the inverse of the resistivity (ρ) [88]:

$$\sigma = \frac{1}{\rho} \tag{2-12}$$

The interdigitated electrode geometry is used to determine the resistances based on equation below [88].

$$\sigma = \frac{L}{RHWN_r} \tag{2-13}$$

Where (*H*) is the film thickness, (*L*) is the gap between fingers, (*W*) is the overlap distance between the electrodes, (*Nr*) is the number of fingers of interdigitated electrodes and (*R*) is the films resistance.

The temperature dependence electrical conductivity of the materials can be analyzed by the Arrhenius equation[103]:

$$\sigma = \sigma_0 \exp\left[\frac{E_a}{K_B T}\right] \quad (2\text{-}14)$$

Where (σ_0) is constant, (Ea) is the activation energy, (K_B) is Boltzmann constant equal (1.38×10^{-23}) J/K and (T) temperature in Kelvin. From above equation, we can write the activation energy equation as:

$$E_a = \frac{T \times \ln \sigma}{1000} \times K_B \times 1000 \left(\frac{J}{K}\right) \quad (2\text{-}15)$$

2.7: Atomic Force Microscopy

The atomic force microscope (AFM) was invented in 1986 by Binning et al. [106]. AFM, like all other scanning probe microscopes, utilizes a sharp probe moving over the surface of a sample in a raster scan. In the case of AFM, the probe is a tip on the end of a cantilever, which bends in response to the force between the tip and the sample. Unlike traditional microscopes, scanned-probe systems do not use lenses, so the size of the probe determines the resolution limit. In AFM the cantilever is treated as a Hookean spring, and hence a simple relationship may be assumed between the deflection of the lever, *x*, and the force *(F*) acting on the tip [105]:

$$F = -kx \quad (2.16)$$

The constant of proportionality *k* is the spring constant, which, is strongly dependent on the physical dimensions of the cantilever (width-*w*, length-*l*, thickness-*t*) and the elasticity of material[106]**.**

In this work tapping mode has been used for measuring the topography of thin films surfaces, which allows a higher resolution and does not destroy the organic layers.

2.7.1: Distance between Sample Surface and Tip

Three different primary imaging modes are possible according to the distance (d) between sample surface and the tip, contact mode ($d < 0.5$ *nm*), non-contact mode ($0.5\ nm < d < 10$), and tapping mode ($d \sim 0.5\text{-}2$ *nm*), as shown in Figure 2.4, which illustrates the relation between force and distance. In contact mode, the tip scans the sample surface by being pushed against the surface. Contact mode is suitable for hard surfaces where the tip cannot damage the surface [107].

In non-contact mode, the separation of the tip from sample surface is large, that the interaction between tip and sample surface is small and mostly in the range of the damped forces in ambient conditions. Therefore, non-contact mode is appropriate for measurement mostly under vacuum, and even sub-molecular resolution could be achieved [108].

In tapping mode, the cantilever oscillates and the tip taps the surface slightly during scanning. Thus the surface is less damaged than in the case of contact mode while the lateral forces are eliminated. The feedback loop maintains a constant oscillation amplitude by maintaining a constant tip-sample interaction during scan [109].

Tapping mode tends to be more applicable to general imaging in air, particularly for soft-surfaces, as the resolution is similar to or even better than contact mode, while the forces applied to the sample are lower. In fact, the only disadvantage of tapping mode is that the scan speed is slightly slower than in contact mode and the AFM operation is a bit more complex, but these disadvantages are outweighed by the advantages.

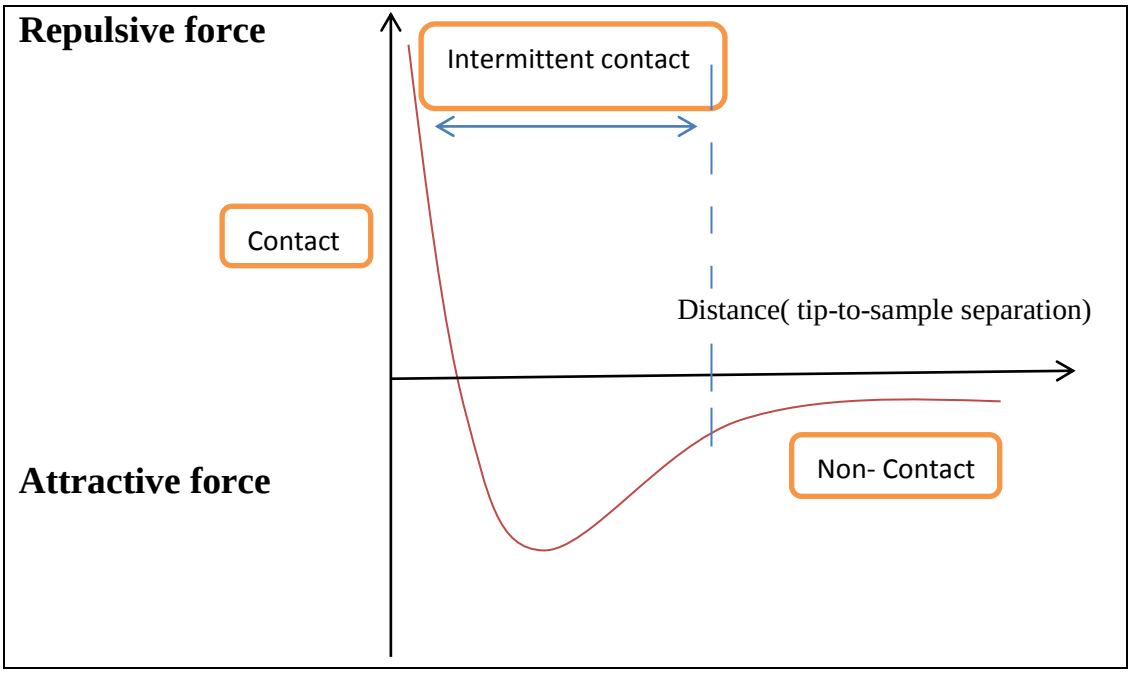

Figure 2.4: Van der Waals force against distance.

Chapter Three

Experimental Part

3.1:Introduction

This chapter is employed to represent the methodologies used in this work during the measurements as well as the materials that utilized to prepare solutions and thin films. Figure (3.1) shows the experimental procedure as a block diagram for the main steps that followed in this work.

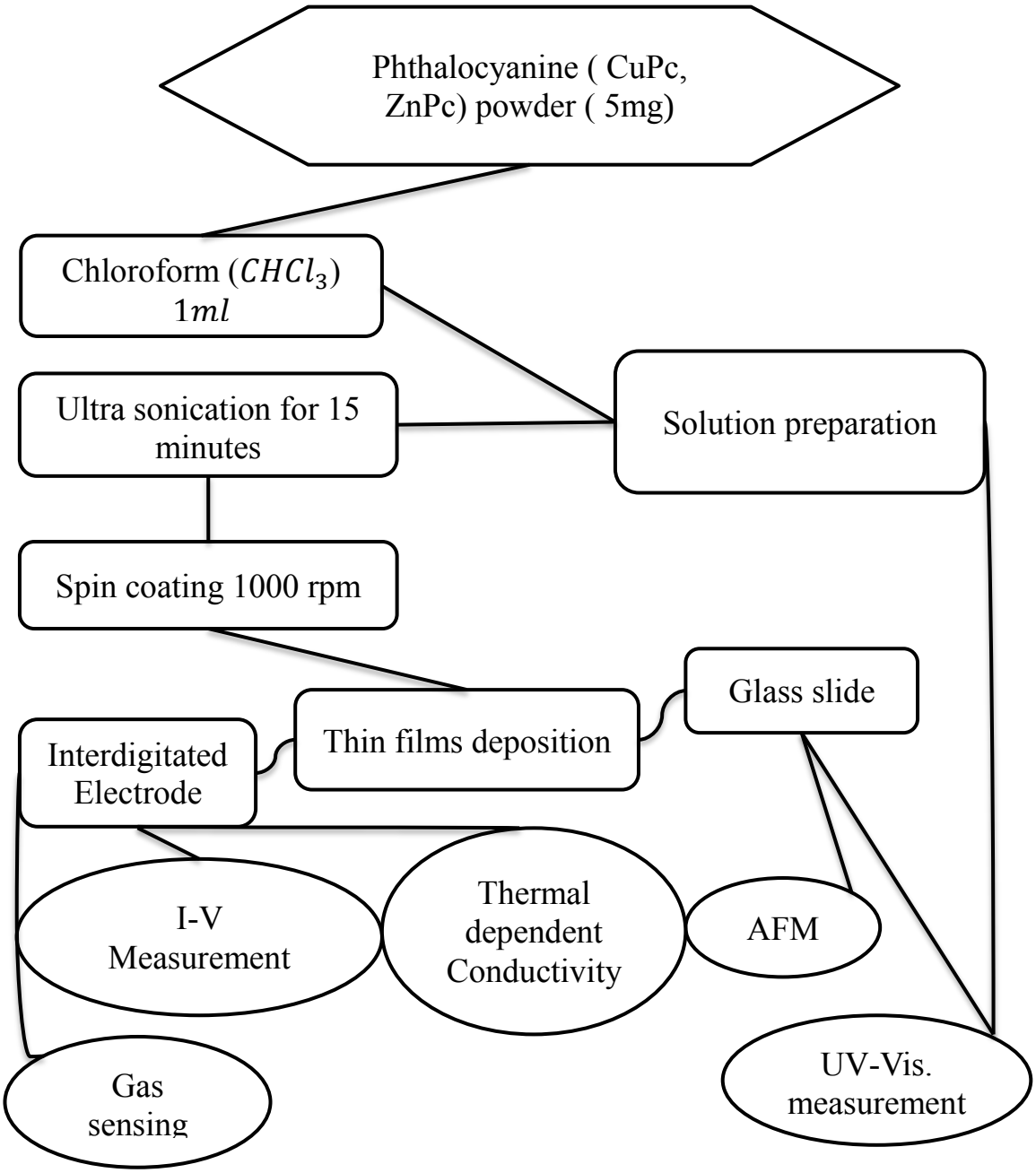

Figure 3.1: Schematic diagram of the experimental work

3.2: Materials

All the chemical reagents used in this work have been purchased from commercial supplier and used as it is without any purification and were listed below;

- Zinc phthalocyanine ($C_{96}\ H_{144}N_8O_8Zn$).
- Copper phthalocyanine ($C_{96}\ H_{144}N_8O_8Cu$).
- Chloroform ($CHCl_3$) solvent.
- Glass Slide.
- Gold , interdigitated electrode

3.3: Substrates

The cleaning procedure of glass substrate could be summarized as follows:

- Slides were cleaned by using detergent with water to remove any oil or dust that might be attached to the surface of the substrate.
- Slides were then placed in a clean beaker containing distilled water and then immersed in ultrasonic unit for 15 minutes .

3.4: Preparation of Samples

The procedure for the CuPc and ZnPc thin films can be described as follows; A approximately (5 mg) of zinc and copper phthalocyanine powder were dissolved in (1 ml) Chloroform solvent. Solutions were then ultrasonicated 15 minutes. After that, the prepared solutions have been deposited on glass slides and interdigitated electrodes by using spin coating technique at 1000 rpm. Homogeneous thin films were achieved for further characterization.

3.5: Methodology

Zinc 2,3,9,10,16,17,23,24 - octkis (octyloxy) - 29H ,31H - Phthalocyanine (ZnPc) with purity ~96 % and copper(II) 2,9,16,23- tetra-tert butyl-29H,31H - phthalocyanine (CuPc) with purity ~95 % have been purchased from sigma Aldrich. Chloroform was used to dissolve the initials. The concentration has been kept to 5mg/ml. Thin films of ZnPc and CuPc were deposited by spin coating technique onto the glass substrates ($1 \times 25 \times 75mm^3$) at room temperature and Gold- interdigitated electrods (IDE). Glass substrates were used to carry out the UV-Visible absorption spectra which were recorded on Shimadzu 1800 UV-visible spectrophotometer. On the other hand, sensing measurements were performed on films deposited onto interdigitated electrodes and carried out using home made sensing equipment. All substrates have been ultrasonically cleaned with chloroform and deionized water.

Interdigitated electrods (IDE) were prepared on 1cm by 1cm glass slide using sputtering technique of type GSL-1100X-SPC16-3. Gold was deposited using stainless steel mask in the argon ambient. DC electrical measurements for films were performed using semiconductor characterization system Keithly (2400). Morphological measurements were carried out by using Atomic Force Microscopy (AFM).

3.6: UV-Vis Absorption

UV-Visible refers to absorption spectroscopy in the ultra-violet and visible spectral region . In this region of the electromagnetic spectrum , molecules undego electronic transition. When sample molecules are exposed to light having an energy, that matches a possible electronic transition within the molecule, some of the light energy will be absorbed as the electron is promoted to a higher energy orbital. An optical spectrometer

records the wavelengths at which absorption occurs, together with the degree of absorption at each wavelength . The resulting spectrum is presented as a graph of absorbance versus wavelength. The main components of the UV-Vis. Spectrometers are a light source, double beam (reference and sample beam), a monochromatic, a detector and a recording device. The source is usually a tungsten filament lamp for visible abd deuterium discharge lamp for UV measurements. The light coming out of the source is split into two beams – the reference and the sample beam as shown in the Fig. 3.2.The sample and reference cells are rectangular quartz \ glass containers: they contain the solution (to be tested) and pure solvent, respectively. The spectrometer records the ratio between the reference and sample beam intensities. The recorder plots the absorbance (A) against the wavelength in nanometers (nm).

UV–Vis. Absorption analyses were performed by Shimadzu 1800 UV – Vis. Spectrophotometer in dual beam mode in the range (190-1100) nm using chloroform solution as a dispersing medium [109].

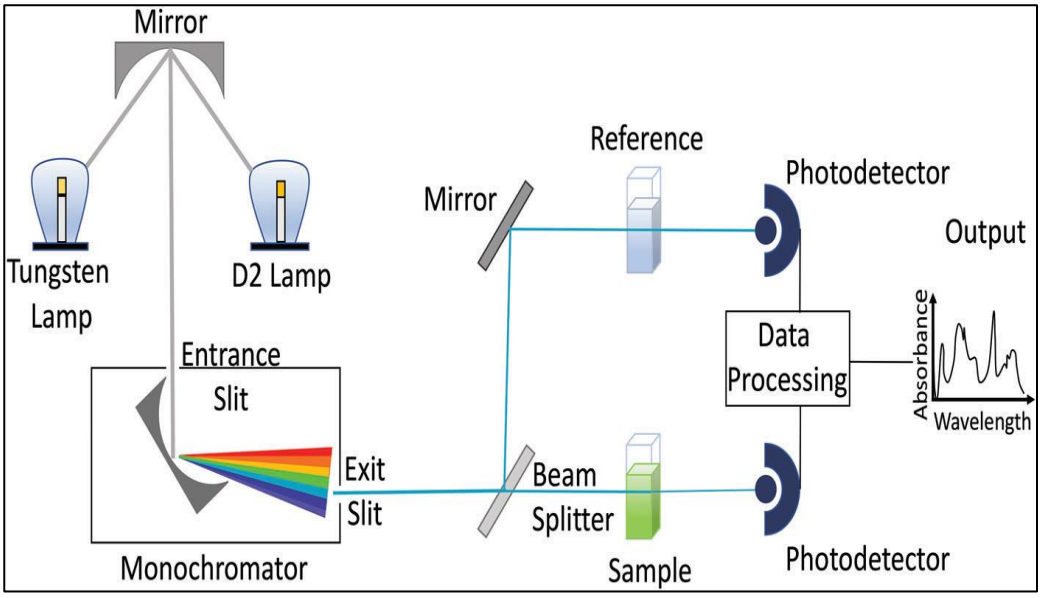

Figure. 3.2. Block Diagram of Double Beam UV-Vis. Spectrophotometer [109].

3.7: Electrical Measurements

According to Ohm's law the current *I (in amperes)* in a sample is proportional directly to the potential difference *V (in volts)* across two points on this sample that defined as mentioned in equation(2-10) [110].

Consider that the current passes through a peace of material with length *l (m)* and across section area *A* (m^2) as in Figure 3.3. The electrical resistivity ρ can be defined as mentioned in equation (2-11):
Therefore, we can write Ohm's low in the following expression

$$J = \sigma E$$

where J: is the current density (I/A) (in ampere/cm^2) and E is the magnitude of the electric field (V/L) (in volt/m).

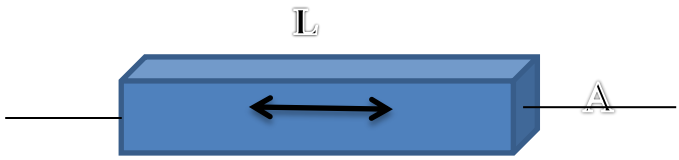

Figure 3.3. A piece of resistive material with electrical contacts on the ends.

In the planar structure (Figure 3. 4), the interdigitated electrode geometry is used to determine the conductivity as mentioned in equation (2-13).

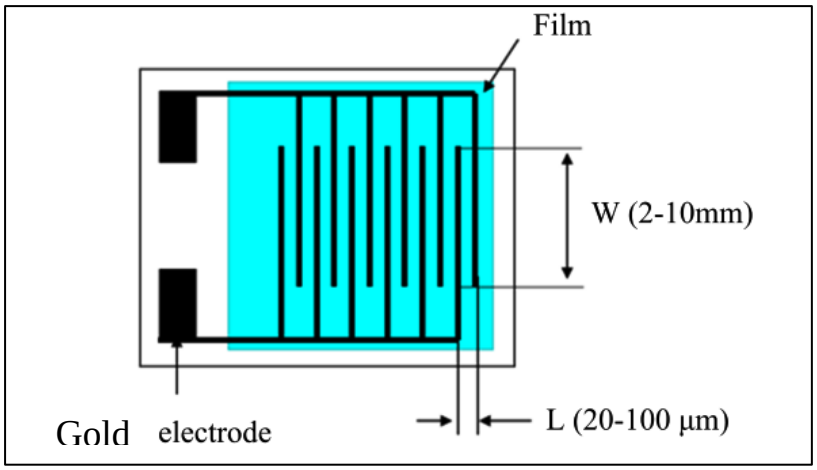

Figure 3.4. Schematic illustration of device structure used in this study, interdigitated electrodes

3.8: DC Conductivity Measurement

The Model 4200 Kiethely Semiconductor Characterization System (4200-SCS) has been used for the DC electrical characterization of MPc thin films utilizing interdigitated electrodes. The system is specified to work at the 1 pA-1 A current range with the maximum voltage of (21-210) V, and 200 mV-200 V voltage range with the maximum current of (10.5-105) mA. This system can automatically perform IV measurement of semiconductor devices.

3.9:Interdigitated Electrodes and Sputtering Technique

Interdigitated (IDEs) Gold electrodes have been prepared by using Gold target sputtering instrumentation. The dimensions of the IDEs ,(W) which is the overlapping distance between the fingers (4) mm, (N) is the number of fingers (10) and (L) is the space between electrodes (0.5) mm. Figure (3.5) represents the IDE prepared in this work.

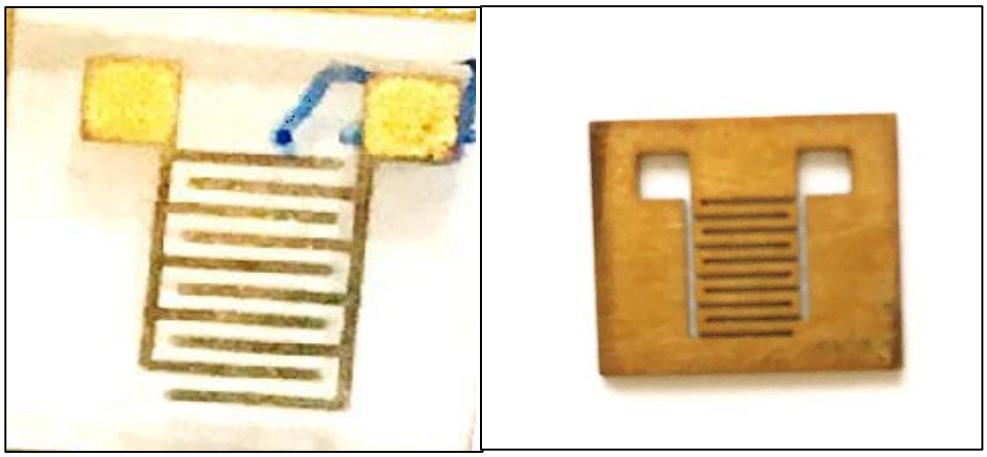

Figure.3.5. The mask and IDE prepared in this work.

3.10: Gas Sensor Measurements

Gas sensor measurements were carried out under room temperature by homemade gas chamber with inlet and outlet knobs. The inlet of gas chamber was connected to the concentration measuring flowmeter for measuring the exact volume percentage of the gas inserted inside the chamber.

Sensing film with gold interdigitated electrodes protruded outside was placed inside the chamber. The outer ends of the wires were connected to the digital Multimeter for measuring the electrical resistance of film. This digital was connected to computer. The complete system of gas sensor measurement arrangement is shown in Figure.3.6.

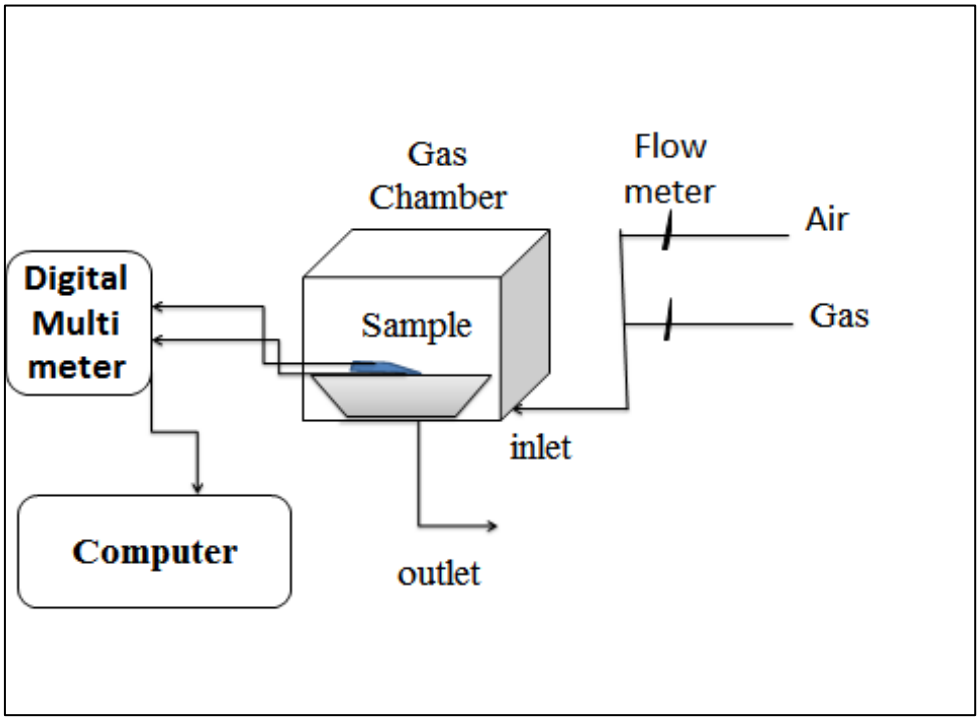

Figure.3.6. Blok diagram of Gas sensor.

Chapter Four

Results and Discussion

4.1: Introduction

This chapter includes results that obtained from each parts of experimental work and followed by the discussion of these results. Experimental results include structural, optical and electrical properties of the ZnPc and CuPc thin films , and gas sensing for the prepared thin films.

4.2:Optical Properties

4.2.1: UV-Visible Absorption Spectra

The UV-Vis spectrum observed for phthalocyanines originates from molecular orbitals within the aromatic 18 π electron system and from overlapping orbitals on the central metal atom [111]. A close examination of this band shows the characteristic splitting (Davydov splitting) present in all phthalocyanine derivatives [112]. The high-energy peak of the Q-band has been assigned to the first π–π* transition on the phthalocyanine macrocycle [111]. The low-energy peak of the Q-band has been previously explained as a second π–π* transition [111,113]. In the high-energy region of the B (Soret) band near 300 nm, the main suggestion of the large differences occurring in the absorption spectra of the phthalocyanines in this region indicate the presence of a d – band associated with the central metal atom. It is though that π-d transitions are involved since strong absorption occurs near 320 nm, the V peak, in CuPc and the other metal phthalocyanine derivatives [114]. This is because CuPc has partially occupied d-bands. The absorption bands in the region of (210–275) nm, the S-band, may be due to d–π* transition [111,113]. Which implies a broader d-band. UV–Vis absorption spectra of the copper and zinc phthalocysnines solution in chloroform is shown in figure (4.1). Absorption peaks at UV and visible light regions are due to B and Q

bands, respectively. The absorptions of Q-band have two peaks at approximately 615 nm and 695nm and the relative intensity of absorption at 615nm was smaller than that at 695nm, these two peaks are due to the monomer and aggregate of CuPc, ZnPc, respectively [115]. In the Q band, an intense absorption peak at 695 nm is due to the transition between the bonding and antibonding (π-π^*) at the dimer part of the phthalocyanine molecule. Copper atom of the phthalocyanine molecule is associated with the d-band . Therefore, within the UV region of the spectrum, a strong absorption peak at 335 nm, is attributed to partially occupy $d - \pi*$ transitions. The variations in absorbance with B band are greater than the variations in Q band. In case of Zn phthalocyanine, in the Q-band the electronic transition occurs from HOMO, which has an electronic density mainly located on the phthalocyanine molecule, to the LUMO, which has a small electronic density on Zn–N bond. The B-band electronic transition occurs between HOMO-4/LUMO orbitals. The electrostatic potential surface and contours of ZnPc , where the $+\delta$ and $-\delta$ charges are residing on Zn and on N-atoms, respectively. The electrostatic potential surfaces can give us an idea about how the ZnPc molecules are stacking in the nanostructure system. The most probable aggregation in the system is the H-aggregation due to high energy shift in the absorption spectrum. The absorbance spectra of ZnPc CuPc, in case of thin film (100 nm thickness) was recorded and compared as shown in Figure (4.2). The figure shows that both of two spectra have two band in the visible region which is Q-band at the range about (523-775) nm , and by comparison to the results of the ZnPc, CuPc solution. It produces a little red shift. In addition, the peak that assigned to aggregations of dimer and trimmer molecules in the thin films became more intense in comparison to monomer peak which was higher in the solution. That could be explained by the fact that, in the solid face,

phthalocyanine tends to form more aggregation of dimer and trimmer chain of molecules instead being monomers.

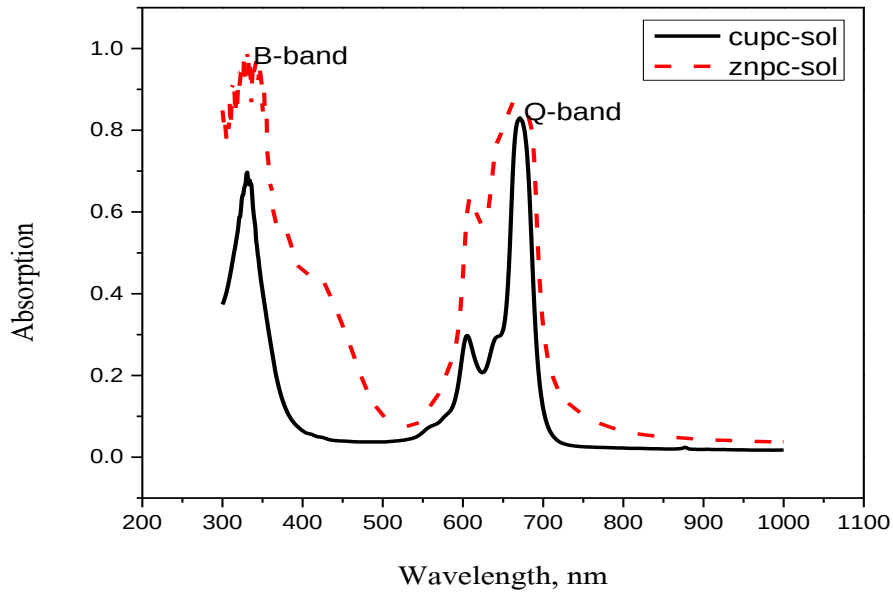

Figure 4.1. Absorption spectra of CuPc and ZnPc solution.

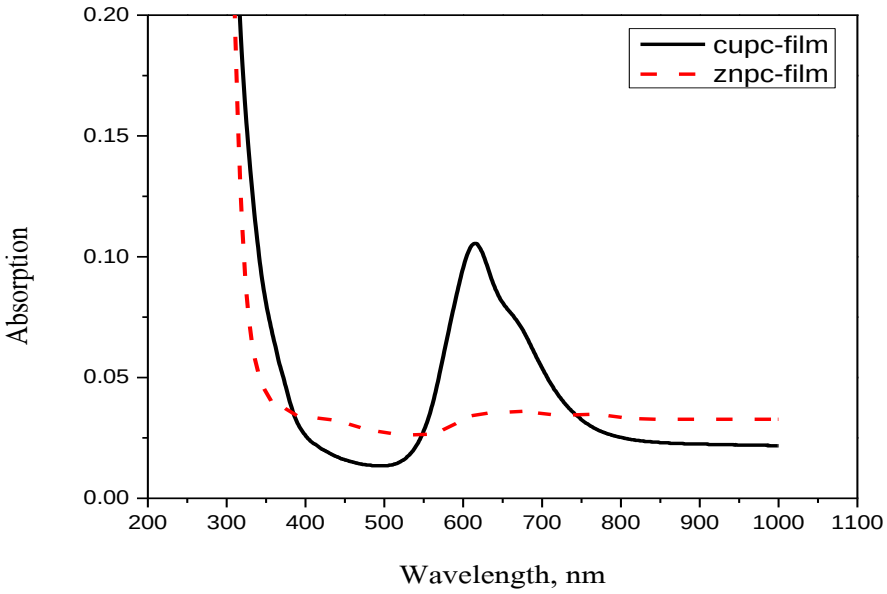

Figure4.2.Absorption spectra of CuPc and ZnPc thin films deposited on glass substrate using spin coating technique.

4.2.2: Transmittance Spectra

The best transmittance is at room temperature and that is conformable to the results of absorption spectra, also there is two bands; Q and B. The Q is in the region of (628-695) nm and B band at the wavelength of 340 nm as shown in Figure 4.3. The transmittance spectra for CuPc thin films, are shown in figure 4.4, which shows that the maximum transmittance value of CuPc is at around 600 nm, while at ZnPc, the maximum transmittance value is at around 650 nm, and these finding is quite consistent with the absorption spectra and reported similarly elsewhere [116].

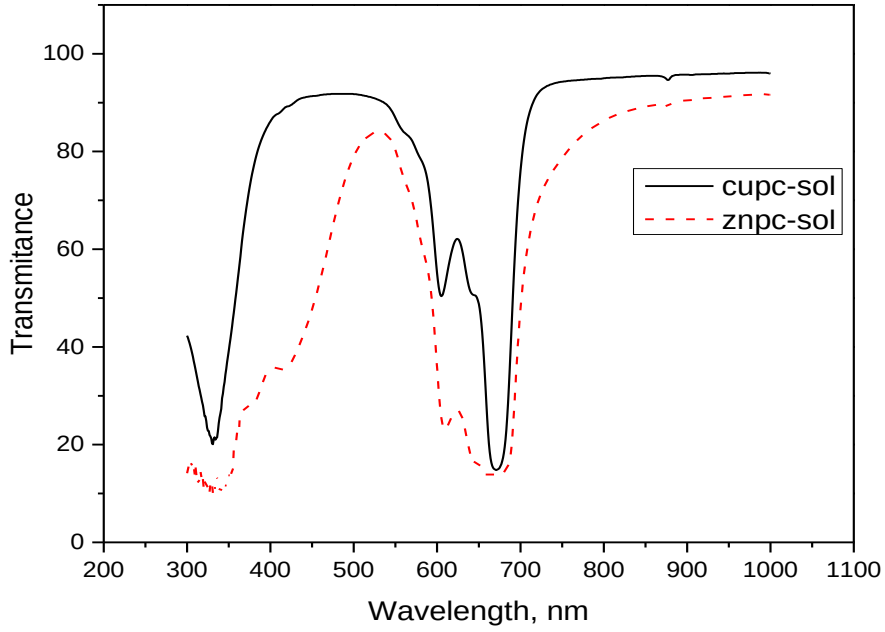

Figure 4.3. Percent transmittance spectra of CuPc and ZnPc solution.

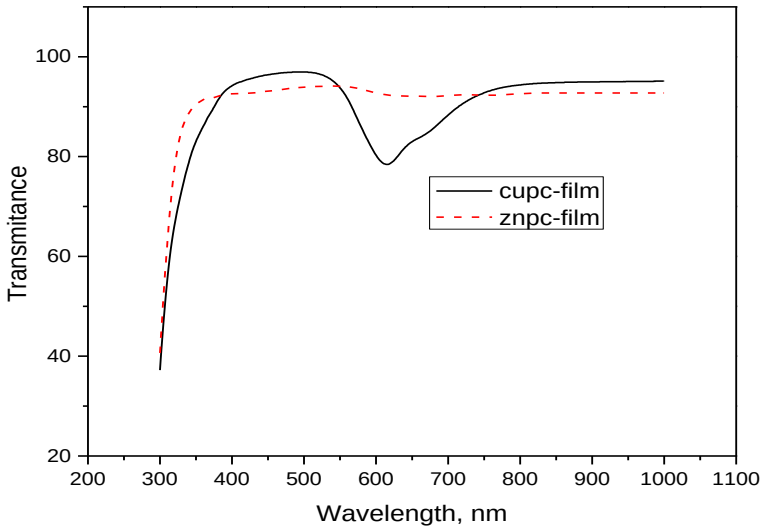

Figure 4.4. Percent transmittance of CuPc and ZnPc thin films deposited on glass substrate using spin coating technique.

4.2.3: Refractive Index

From the transmittance values, the refractive index *(n)* is calculated using equation (2-7) :

$$\text{And , } T_s = 10^{-A} \times 100 \qquad (4\text{-}1)$$

Where Ts; transmittance , A; absorbance.

In figure(4.5), solid line shows the variation of refractive index at wavelength range(550-750) nm, the behavior of refractive index changes the preparation conditions and method used in preparation. from this figure, it is observed slightly that the increased refractive index in CuPc upon λ equals to , 745nm to 618nm, and then started to decrease until λ equals to 538 nm.

Refractive index number is greater than one, and its value is directly proportional to the density of matter and depends on the temperature [83].

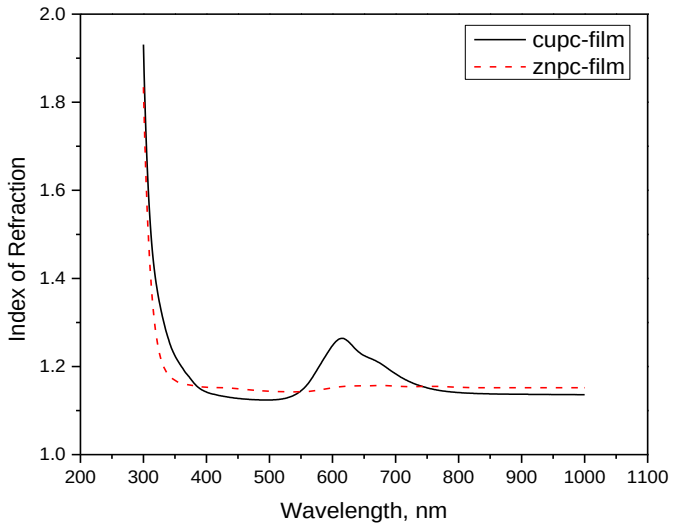

Figure 4.5. Index of refraction of CuPc and ZnPc thin films deposited on glass substrate using spin coating technique.

4.2.4: Optical Energy Gap

The absorption coefficient (α) is determined from the region of high absorption using equation (2-3) .

The absorption coefficient helps to conclude the types of electronic transitions. When the values of absorption coefficient are higher than ($\alpha > 10^4\ cm^{-1}$) at high photonic energies, direct electronic transitions are expected and the electron momentum energy is conservation, but when the values of the absorption coefficient are lower than ($\alpha < 10^4\ cm^{-1}$) at low photonic energies, indirect electronic transitions are expected, in which the momentum of electron and photon is conservation with the help of a phonon [117] [118].

The maximum wavelength (λm) of the incident photon which creates the electron–hole pair using equation (2-1). The optical energy gap values (Eg) for CuPc and ZnPc, thin films have been determined by using equation (2-4).

For an allowed direct transition, the transition occurs from the top of the valence band to the bottom of the conduction band. When graphing the relation between each of the $(\alpha h\upsilon)^2$ with photon energy of incident radiation, through which it is possible to calculate the value of allowed direct energy gap, and best graph obtained that can be the extension of the straight line that intersects the (hυ) - axis to determine the value of energy gap for allowed direct transition of the ZnPC, CuPC thin films, as shown in the figure (4.6), and the values of energy gaps are 3.87 eV, 3.93 eV respectively. Similar findings have also been reported elsewhere [119].

figure(4.6) shows a linear change at high energy range which does not appear with the other curves, which indicates the occurrence of the allowed direct electronic transition in the prepared films. There are variation between energy gap values and its impact by mechanism a formation thin films and conditions accompanying the preparation process. Energy gap value and type depends on crystal structure of material and how atoms distribution in crystalline lattice and the levels energy structure, this mean that any change in structure properties and the parameterized another , can be caused by the change occurring of energy gap and transitions type which occurring in thin films[119,120].

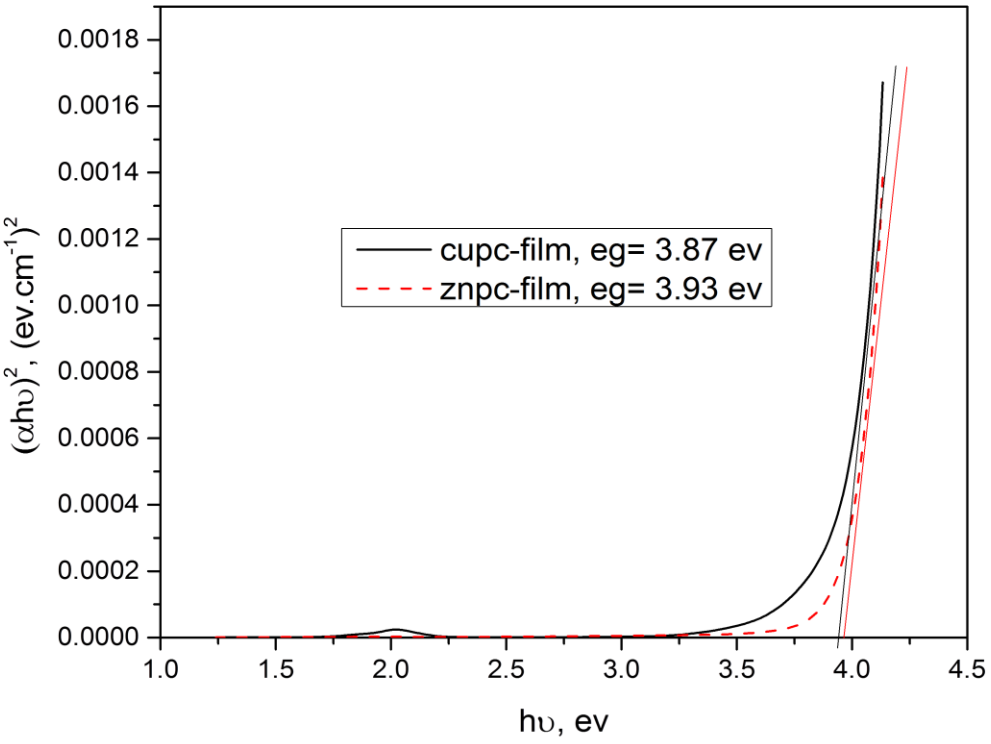

Figure 4.6. Tauc plot and optical energy gap calculations of CuPc and ZnPc thin films deposited on glass slides using spin coating technique.

4.3: Electrical Characterization

4.3.1: I-V Measurements

The I-V curves have been measured for prepared devices using Kiethly semiconductor characterization system. Figure (4.7 and 4.8) show the current vs voltage characteristics of CuPc and ZnPc thin films deposited onto gold interdigitated electrodes. The voltage is swapped from -5 to 5 volt to carry out the experiments

CuPc has shown Ohmic behavior as expected for interdigitated electrodes since the voltage is applied laterally through the device and the resistivity is calculated using equation 3.4, and found to be 0.2 kΩ.cm. Similar results are also published in the literature [73], for thermally evaporated CuPc films. However, in the ZnPc device, the change in the curve is exponential exhibiting diode behavior. The observed exponential dependence of the forward current in the lower voltage range may be due to the formation of a depletion region between ZnPc layer and Gold- interdigitated electrodes substrate.

A linear trend characteristic of ohmic behavior in the case of CuPc, which observed as mentioned in the beginning of the paragraph is similar to the finding that was reported by Rajesh and Menon [122]. It is known that the conductivity and driving mechanism depend on the nature of the metal contacts [121]. Here, the resistivity was calculated from a linear adjustment of the *I-V* curve using the model developed by Olthuis et al.[121] and found to be 79 kΩ.cm. The difference between ZnPc and CuPc behavior , attributed to Zinc`s atomic radius is 0.137 nm while copper`s is 0.128 nm. Hence the atomic size of zinc is greater than that of copper, this result causes of the effective molecular change of Cu that will be more, due to lesser d electrons.

Hence, lesser screening effect leads to more effective nuclear change, making smaller covalent radius than zinc [73].

The interpretation of this exhibiting behavior is suggested to be:

Firstly , depletion region in the ZnPc as a result of the bigger atomic radius of the atom may cause a deviation of Zn from the cavity of phthalocyanine molecule and hence create a depletion region.

Secondly, the bigger size of the atom causes some defect to the molecule, this led to random orientation alignment on the film surface and as a result of this disorder, the depletion region has been created between the metal electrode and the active layer.

Thirdly, the work function for gold electrodes is estimated as 5.3 eV [123], and from UV- visible measurements, and energy gap of ZnPc and CuPc are obtained estimated as 3.9 eV, 3.8 eV, respectively. From these results, it is likely that electron transition to CuPc is more easily than ZnPc.

The ratio of the forward current to the reverse current at a certain applied voltage is defined as the rectification factor RR. It is evident that the junction exhibits strong rectifying characteristics showing diode-like behavior [124]. As seen from the figure , there is potential barrier in depletion region that the estimated 3 V. The forward current (mA) arises from majority charge carriers, while reverse current arises from minority charge carriers and they are extremely small current (μA).

Graphing the I-V Curve for forward bias, the diode forward voltage (V_F) increases to the right along the horizontal axis, and the forward current (I_F) increases upward along the vertical axis. After potential barrier, the relation (I,V) represents exponential, the resistance of the forward is not constant over the entire curve. it is called dynamic resistance ($r`_d$), below the threshold of the curve the resistance which is the greatest because the current increases

very little for a given change in voltage ($r`_d = \frac{\Delta V_F}{\Delta I_F}$). The resistance begins to decrease in the region of the threshold of the curve and becomes that smallest above the threshold where there is a large change in current for a given change in voltage. When a reverse- bias voltage is applied across a sample, there is only an extremely small reverse current(I_R) through the p type-metal junction, as V_R gradually increases , there is a very small reverse current [125].

To examine the reversibility of the devices, cyclic voltammetry measurements have been carried out and presented in the figure (4.9 and 4.10).

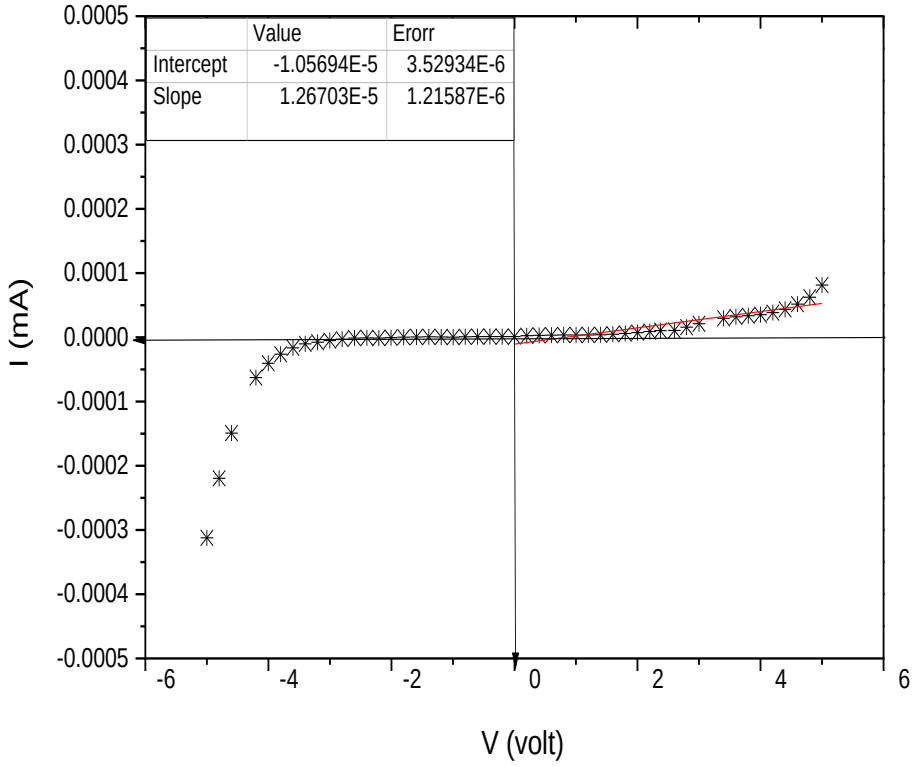

Figure 4.7. Current–voltage characteristics of CuPc thin films.

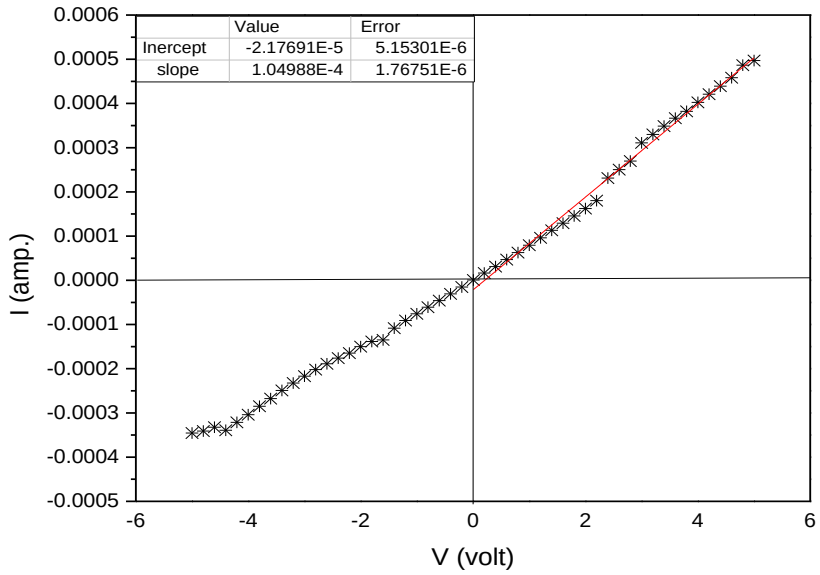

Figure 4.8. Current–voltage characteristics of ZnPc thin films.

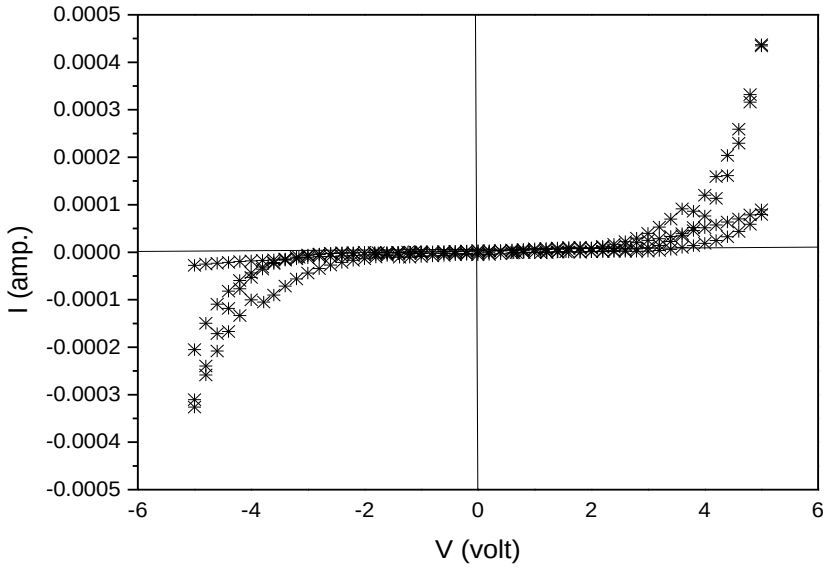

Figure 4.9. Two cycle of current vs voltage of ZnPc thin films on interdigitated electrode.

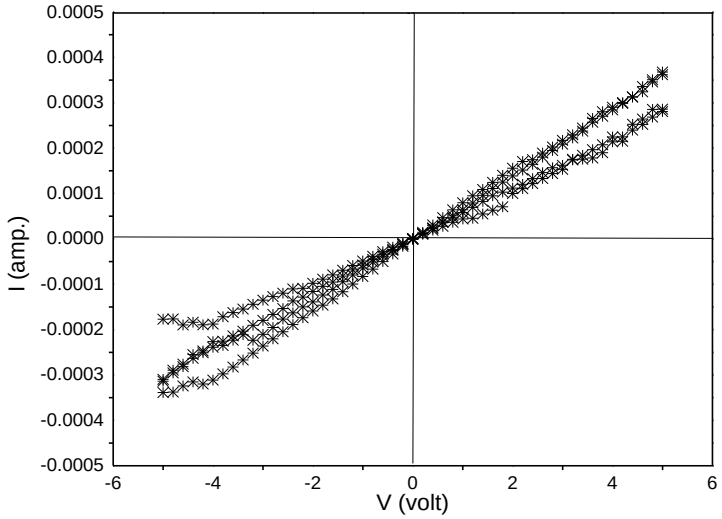

Figure 4.10. Two cycle of current vs voltage of cuPc thin films on interdigitated electrode.

4.3.2: Thermal Dependence Conductivity

The electrical conductivity of CuPc and ZnPc thin films are performed to determine the thermal activation energy. Measurements are carried out in the temperature range 313 to 483 K for the specimens and plotted in the figures 4.11 and 4.12.

The inset to figures 4.11 and 4.12 have shown the temperature dependence of the conductivity calculated utilizing equation (2-15).

A graph of $\ln \sigma$ vs. 1000/T for CuPc and ZnPc films of 100 nm thickness deposited on Gold- interdigitated electrodes show the existence of three regions. However, region II is neglected as it is caused by the recombination of charge carriers. Region I and region III correspond to two activation energies. The values of the activation energies of CuPc for region I , Ea = 0.076 eV and region III , Ea= 0.407 eV , while in the case of ZnPc, the activation energies are found to be 0.029 and 0.056 eV for region I and region

III respectively. The activation energy have been summarized in table (4.1).There are two semiconductor distinct liner parts, which correspond to two activation energies, E_1 corresponds to extrinsic region and represents transition process for carriers within localized states in the energy gap and this suggests the existence of high density of localized states in the energy gap, and E_2 corresponds to intrinsic region and represents the carriers transport across the grain boundaries by thermal excitation. The change in the slope and hence the activation energy is interpreted as a change from extrinsic to intrinsic conduction[126,127].

The conduction mechanism is explained in terms of hopping through a band of localized states at lower temperatures and by free conduction at higher temperature. These findings have also been concluded previously in the literature [128].

Table 4.1: Activation Energy of Prepared Films

Film	Activation energy E_1(eV)	Activation energy E_2(eV)
CuPc	0.076	0.407
ZnPc	0.029	0.056

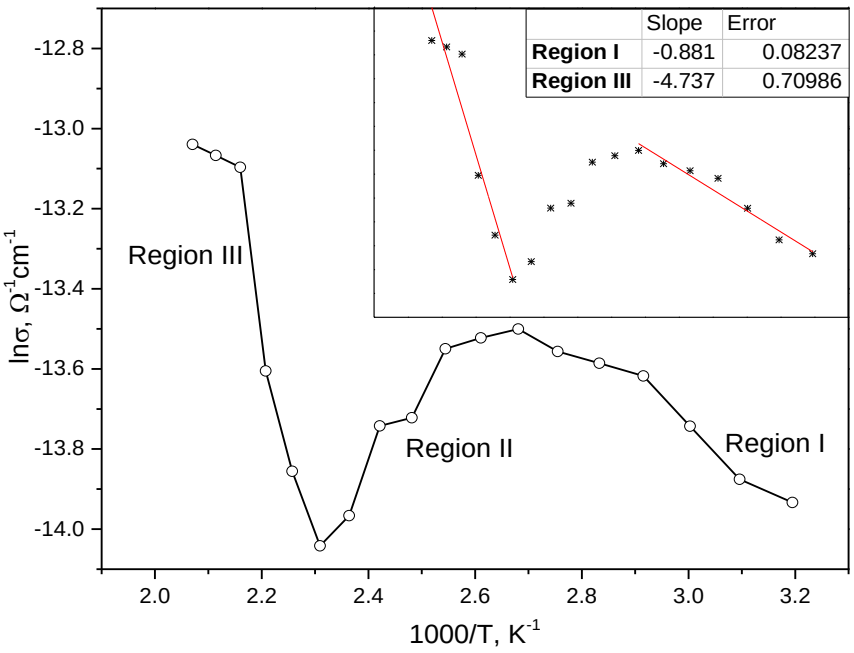

Figure 4.11. Lnσ as a function of 10^3/T for CuPc Thin Films. The inset shows the fitting analysis of activation energy regions.

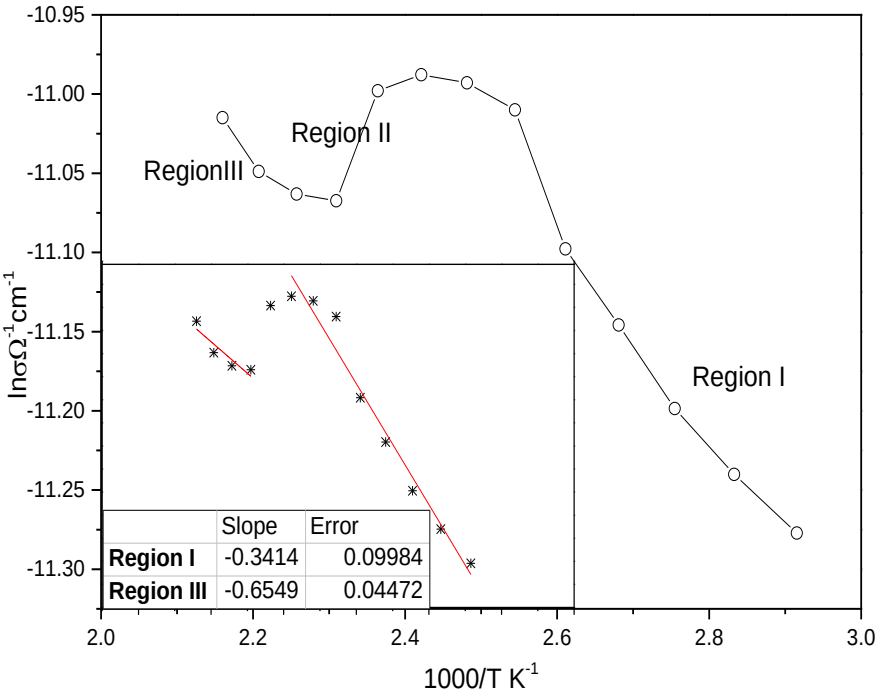

Figure 4.12. Lnσ as a function of 10^3/T for ZnPc Thin Films. The inset shows the fitting analysis of activation energy regions.

4.5: Morphology

AFM measurements in tapping mode are performed on all samples in this study. Figures (4.13,4.14.) shows the typical aggregation of phthalocyanine thin films. Phthalocyanine and almost all organic dyes tend to make very dense aggregations in the solid state. These aggregates are represented as a conplanar association of rings which develop from monomer to dimer and higher order complexes. They are driven by π-π interaction and van der Waals forces[129].

The results of (AFM) of the CuPc and ZnPc films which prepared by spin coating have showed a uniform granular surface morphology, as in figures (4.13,4.14). Where it can be noted that the roughness of ZnPc is higher than CuPc and this result is consistent with the interpretation of electrical characterization.

One of the most important factors commonly used in the description of morphology of surface layer is the surface roughness represented by the RMS parameter. Basing on the recorded AFM images we determined the RMS parameter for the CuPc and ZnPc thin films deposited on glass substrate that is summarised in Figures. 4.13,4.14. The smallest RMS value of 2.6 nm is calculated from the image for CuPc thin films deposited on the substrate at room temperature. Almost a similar RMS value, equal to 4.8 nm is reported by Berger et al.[129].

Figure (4.13-a, and b) reports AFM 2D and 3D images of the film morphology on scan size 1μm × 1μm. The surface of the film appears very aggregated and the RMS roughness and maximum height are concluded in table (4.2).

Table 4.2 : Parameters of Surface.

Parameters	CuPc nm	ZnPc nm
Root - mean- square	2.668	7.994
Maximum height	19.27	44.81

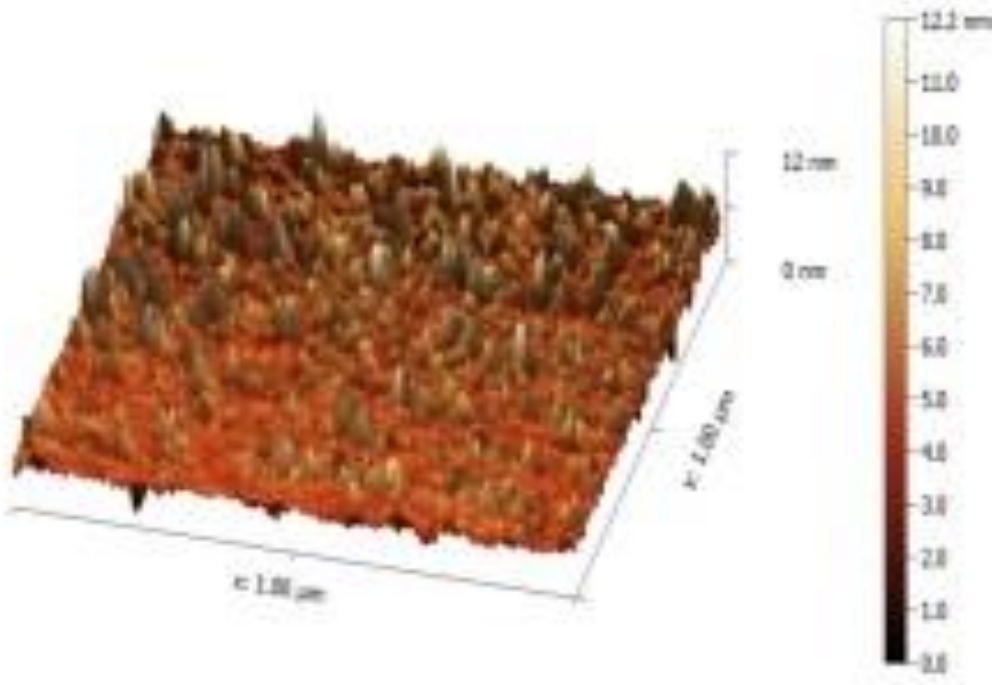

(a)

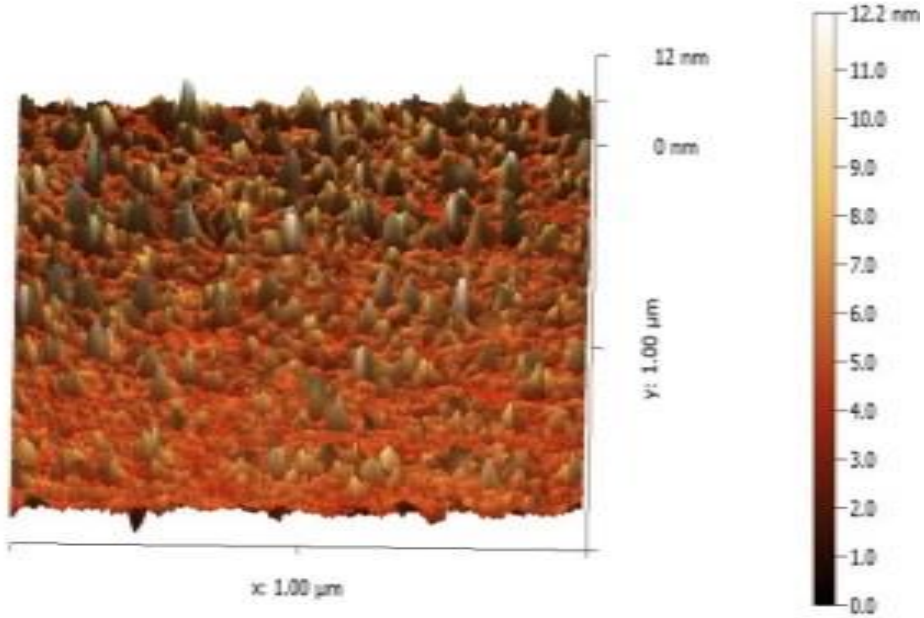

(b)

Figure 4.13. Atomic force microscope(AFM)images of ZnPc films, (a)3D,(b)2D.

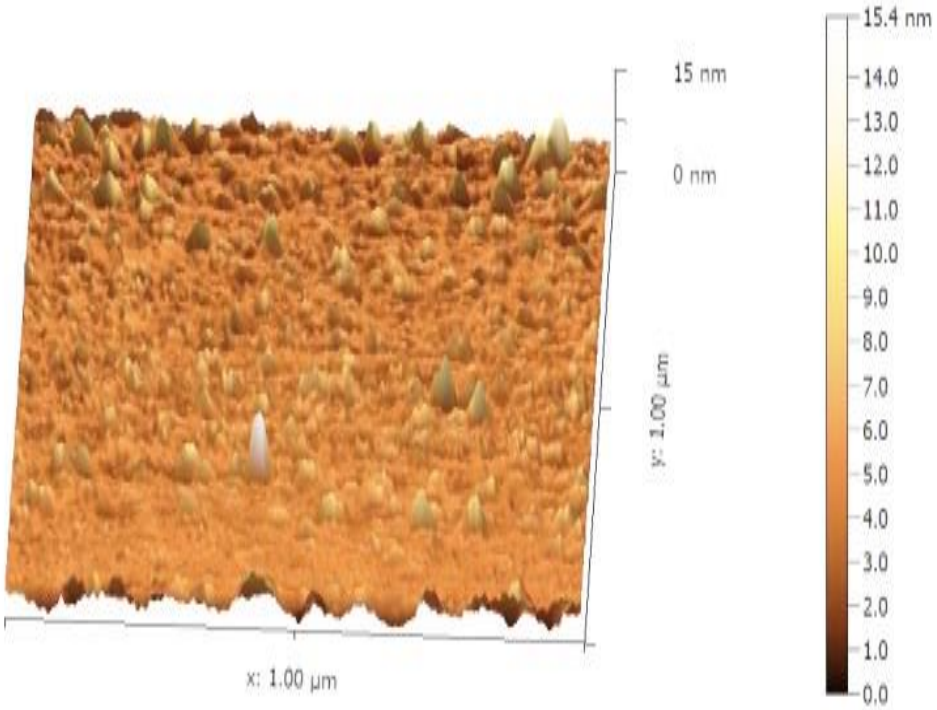

(a)

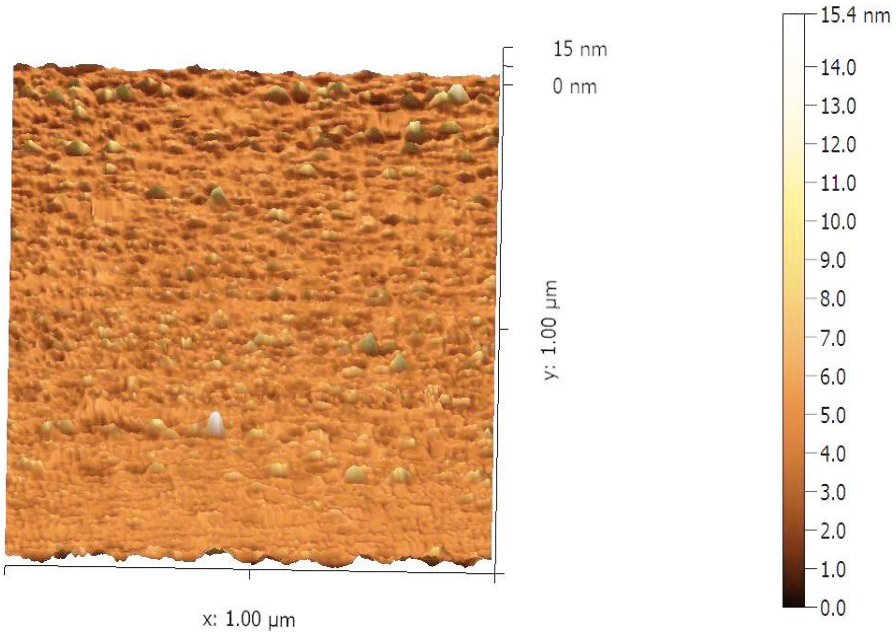

(b)

Figure 4.14. Atomic force microscope(AFM)images of CuPc films, (a)3D,(b)2D.

4.4 :Gas Sensor

In present work, the sensitivity of CuPc and ZnPc devices are studied during exposure to 100 ppm concentration of chloroform, dimethyleformamide and nitrogen dioxide odorents at room temoerature. The samples are fixed in a special per- evaluated chamber. After that gas is separately introduced to the chamber.

The change in resistance ratio $\frac{R_g}{R_a}$ (where R_g is the resistance in the present of gas and R_a is the resistance in zero grade air) on exposure to contaminate air at room temperature for 10 s. ZnPc have shown no obvious behavior towareds contaminations as exhibited in the time dependence Figure.(4.15). Zn atom is a littile bigger than the cavity of phthalocyanine, which results in a deviation in the position from the plane of the molecule. Consequently, hindering of orientation takes place and the adsorption of odorant will be random and not reversible. On the other hand, CuPc thin film has shown quite reasonable performance towards gases and presented in Figure.4.16. From this Figure, the response of CuPc film to NO_2 gas is oposite to other gases which makes it selective to this particular gas [79].

The reason for the decrease in resistance of the devices can be understood in terms of a change in the surface conductivity of thin films. Such effects can be interpreted within the framework of the band theory. If we consider the adsorbed gases to produce appropriate donor or acceptor levels within the band gap of the organic materials at the film surface. CuPc and ZnPc are a p - type organic semiconductor, upon exposure to the oxidizing gases such as NO_2 , the hole concentration near the surface will be enhanced through a doping mechanism, resulting in the increase of electrical conductivity[130].

In the case of chloroform and DMF odorants, film resistance decreased rapidly and no reversibility occurred. The recovery rate of the film resistance is slower and did not recover to the original value before exposure. The present recovery characteristic is less than that in a previous work operated at the same temperature [131].These results confirm that the sensitivity of phthalocyanine as gas sensor depends on different factors such as ambient condition, method of device fabrication, sensing temperature and the type of central metallic element.

The response and recovery times have been calculated as 90% of the highst R value and 90% due the lowest R value and found to be 20 sec and 142.6 sec respectively. Figure. 4.17 represent clearly the calculations of both response and recovery times.

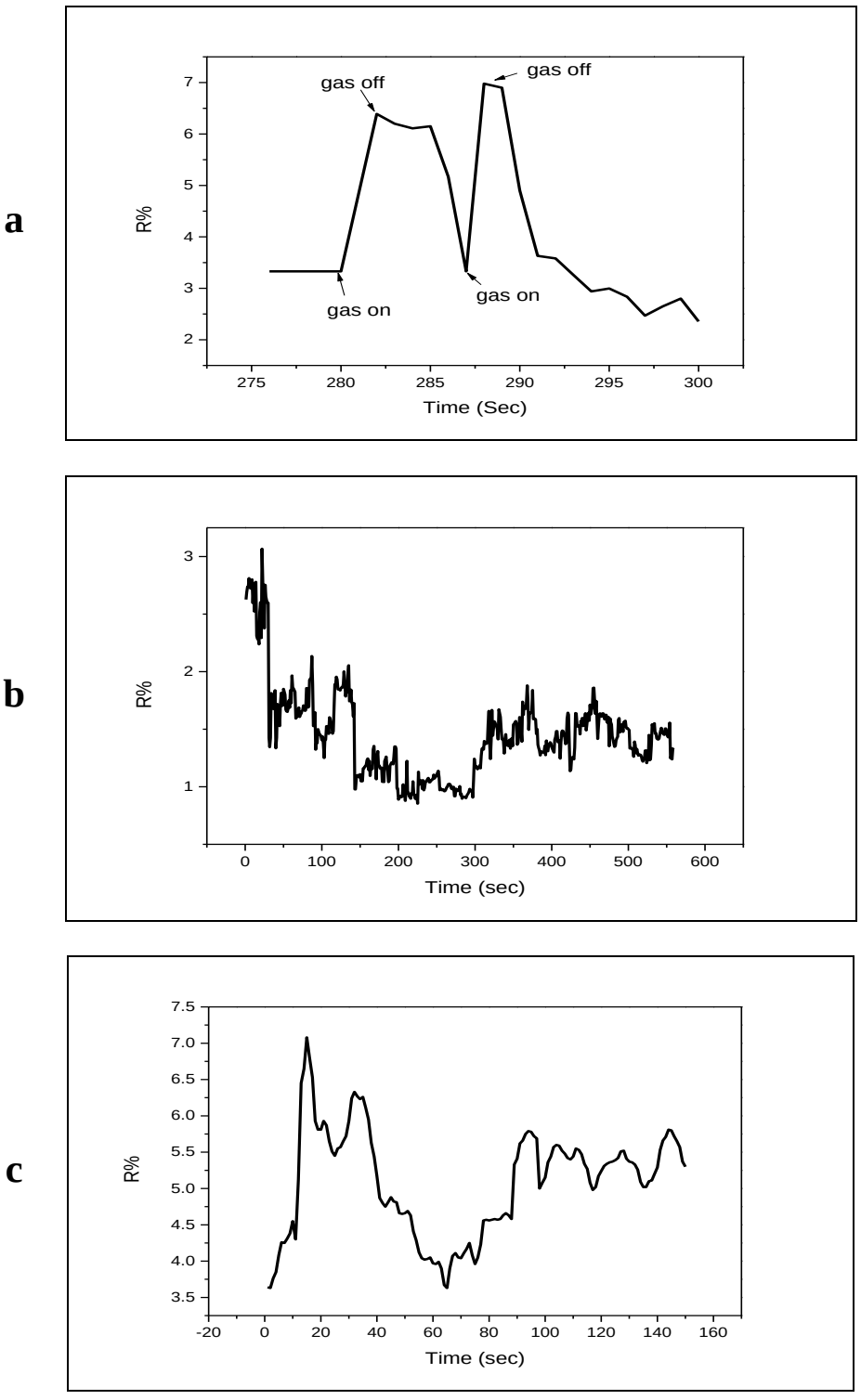

Figure 4.15. Response vs. time of ZnPc deposited on interdigitated electrodes at room temperature for NO_2(a), Chloroform(b), and DMF(c) vapors at 100 ppm.

a

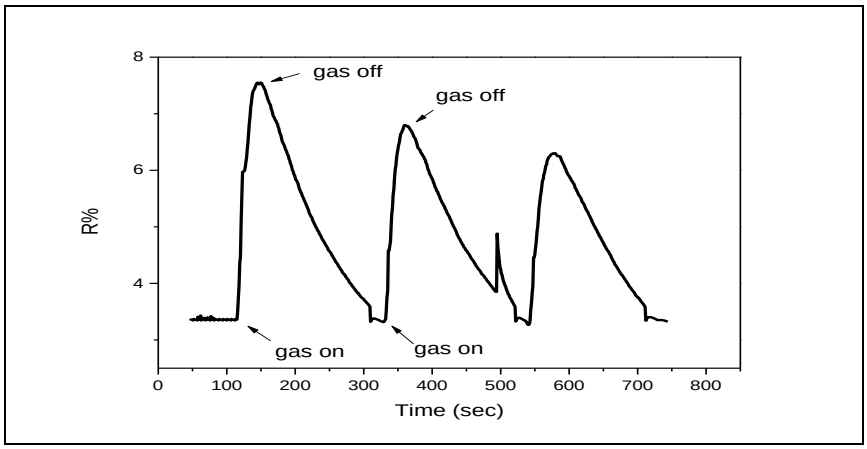

b

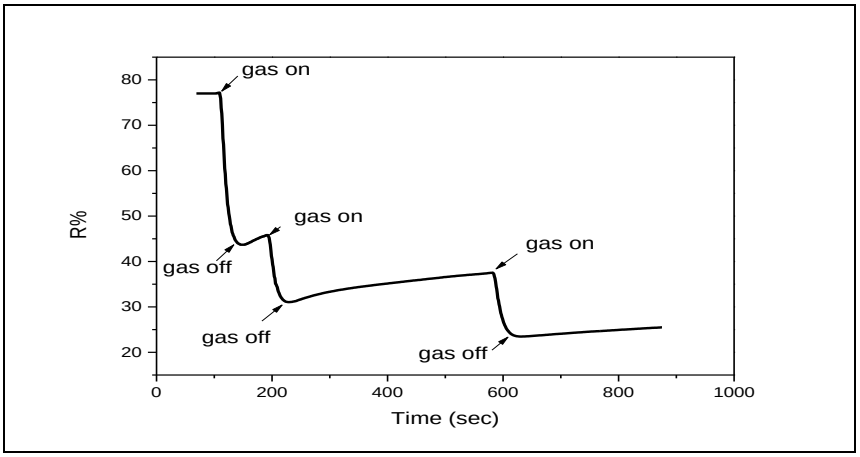

c

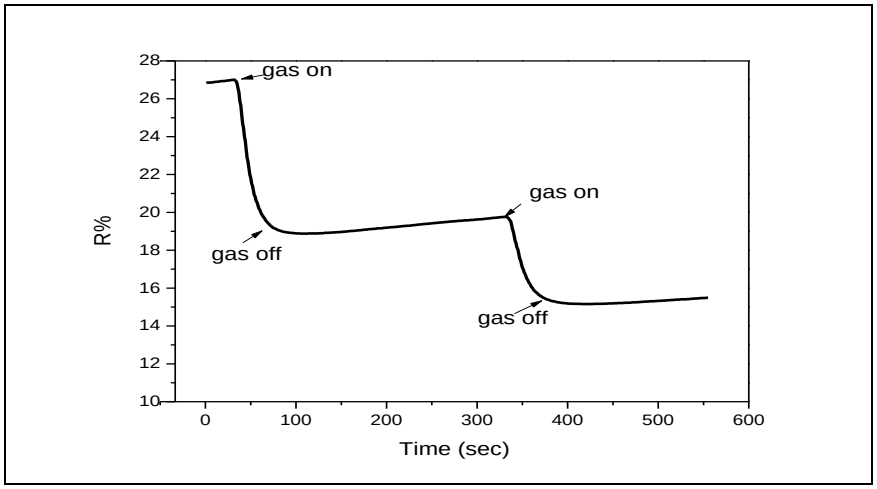

Figure 4.16. Response vs. time of CuPc deposited on interdigitated electrodes at room temperature for NO_2(a), Chloroform(b), and DMF(c) vapors at 100 ppm.

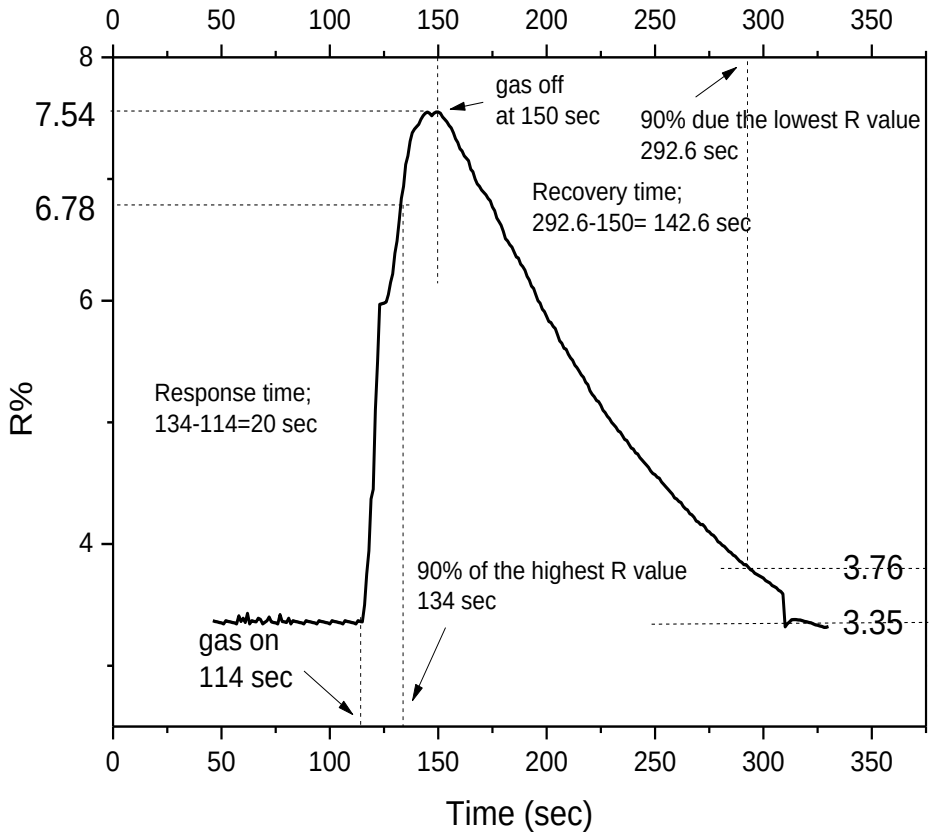

Figure 4.17. Response and recovery times of copper phthalocyanine film upon exposure to NO_2.

Chapter Five

Conclusions and Future Work

5.1: Conclusions

Copper and zinc captivated phthalocyanines solutions in chloroform are deposited onto glass slides and interdigitated electrodes using spin coating technique at 1000 rpm. Optical , electrical and sensing properties have been investigated through this project and could be concluded as follows:

1. Thin films absorption spectra has red shifted in comparison to solution spectra indicating that phthalocyanine tends to make aggregation of dimer and trimmer in the solid phase while only monomers are existent in the solution phase.

2. Using Tauc ʾs equation, energy gap calculation how that the copper and zinc phthalocyanine films having band gaps of 3.87 eV and 3.93 eV respectively and the transition of charge carriers is direct transition.

3. Activation energies for prepared samples are calculated using Arrhenius equation from the temperature dependence conductivity curve. It is found that, there are two regions in the curve indicating two conduction mechanisms for the charge hopping from lower to higher energy levels. The activation energies are found to be, E_{a1}= 0.076 eV and E_{a2}= 0.407 eV for copper phthalocyanine, while: E_{a1}= 0.029 eV and E_{a2}= 0.056 eV for zinc phthalocyanine.

4. Morphology of the films surfaces has been investigated and shows that zinc phthalocyanine has rougher films than copper phthalocyanine as zinc atom is bigger than copper resulting in the increasing of random alignment.

5. Using homemade sensing system, several odorants are exposed to the film devices. ZnPc has shown no obvious behavior towards gases, while CuPc is

selective to NO_2 gas and the response and recovery times are found to be 20 sec and 142.6 sec, respectively.

5.2: Future Works

A further investigation can be suggested to develop this work as follows:

1. Other kinds of phthalocyanines can be examined for the comparison such as lead and cobalt phthalocyanines.

2. Carbon nanotubes or graphene oxide can be introduced to the solution before depositing to enhance the electrical properties.

3. Sandwich device structure can be synthesized to study the normal conductivity rather than lateral conductivity which studied in the current project.

4. Exposing the sensor device to more gases to investigate the response and recovery times towards different gases.

5. Applying some theoretical calculations to investigate the values of sensitivity and selectivity.

References

References

[1] T. Basova et al., “Investigation of gas-sensing properties of copper phthalocyanine films,” Mater. Sci. Eng. C, vol. 29, no. 3, pp. 814–818, 2009.

[2] T. Basova, I. Jushina, A. G. Gürek, V. Ahsen, and A. K. Ray, “Use of the electrochromic behaviour of lanthanide phthalocyanine films for nicotinamide adenine dinucleotide detection,” J. R. Soc. Interface, vol. 5, no. 24, pp. 801–806, 2008.

[3] D. Atilla et al., “The synthesis and characterization of novel mesomorphic octa-and tetra-alkylthio-substituted lead phthalocyanines and their films,” Dye. Pigment., vol. 88, no. 3, pp. 280–289, 2011.

[4] N. Kılınç et al., “Electrical properties of mesomorphic phthalocyanine-carbon nanotube composites,” Sens. Lett., vol. 6, no. 4, pp. 607–612, 2008.

[5] H. U. Khan, M. E. Roberts, W. Knoll, and Z. Bao, “Pentacene based organic thin film transistors as the transducer for biochemical sensing in aqueous media,” Chem. Mater., vol. 23, no. 7, pp. 1946–1953, 2011.

[6] S. Liu, W. M. Wang, A. L. Briseno, S. C. B. Mannsfeld, and Z. Bao, “Controlled deposition of crystalline organic semiconductors for field-effect-transistor applications,” Adv. Mater., vol. 21, no. 12, pp. 1217–1232, 2009.

[7] P. R. Somani and S. Radhakrishnan, “Electrochromic materials and devices: present and future,” Mater. Chem. Phys., vol. 77, no. 1, pp. 117–133, 2003.

[8] S. Tuncel et al., “Liquid crystalline octasubstituted lead (II) phthalocyanines: effects of alkoxy and alkylthio substituents on film alignment and electrical properties,” New J. Chem., vol. 36, no. 8, pp.

1665–1672, 2012.

[9] B. Mukherjee, A. K. Ray, A. K. Sharma, M. J. Cook, and I. Chambrier, “A simply constructed lead phthalocyanine memory diode,” J. Appl. Phys., vol. 103, no. 7, p. 74507, 2008.

[10] H. Li et al., “Modification of multi-walled carbon nanotubes with cobalt phthalocyanine: effects of the templates on the assemblies,” J. Mater. Chem., vol. 21, no. 4, pp. 1181–1186, 2011.

[11] J. Brunet, A. Pauly, C. Varenne, and B. Lauron, “On-board phthalocyanine gas sensor microsystem dedicated to the monitoring of oxidizing gases level in passenger compartments,” Sensors Actuators B Chem., vol. 130, no. 2, pp. 908–916, 2008.

[12] N. L. Tran, F. I. Bohrer, W. C. Trogler, and A. C. Kummel, “A density functional theory study of the correlation between analyte basicity, ZnPc adsorption strength, and sensor response,” J. Chem. Phys., vol. 130, no. 20, 2009, doi: 10.1063/1.3134743.

[13] A. v Braun and J. Tcherniac, “Über die produkte der einwirkung von acetanhydrid auf phthalamid,” Berichte der Dtsch. Chem. Gesellschaft, vol. 40, no. 2, pp. 2709–2714, 1907.

[14] S. H. Nowfal, H. A. Banimuslem, N. A. Al-Isawi, and H. M. A. Ghanimi, “Zinc and Aluminum Phthalocyanine Modified Carbon Nanotubes; Preparation and Characterizations,” NeuroQuantology, vol. 19, no. 9, pp. 132–141, 2021, doi: 10.14704/nq.2021.19.9.NQ21146.

[15] C. E. Dent and R. P. Linstead, “215. phthalocyanines. part iv. copper phthalocyanines,” J. Chem. Soc., pp. 1027–1031, 1934.

[16] J. M. Robertson and X. An, “ray study of the structure of the phthalocyanines. P h I. The metal-free, nickel, copper, and platinum compounds, I. Chem.” Soc, 1935.

References

[17] H. De Diesbach and E. Von der Weid, “Quelques sels complexes des o-dinitriles avec le cuivre et la pyridine,” Helv. Chim. Acta, vol. 10, no. 1, pp. 886–888, 1927.

[18] M. M. El-Nahass, Z. El-Gohary, and H. S. Soliman, “Structural and optical studies of thermally evaporated CoPc thin films,” Opt. Laser Technol., vol. 35, no. 7, pp. 523–531, 2003.

[19] M. Sönmez, İ. Berber, and E. Akbaş, “Synthesis, antibacterial and antifungal activity of some new pyridazinone metal complexes,” Eur. J. Med. Chem., vol. 41, no. 1, pp. 101–105, 2006.

[20] M. Aydın, E. H. Alıcı, A. T. Bilgiçli, M. N. Yarasir, and G. Arabaci, “Synthesis, characterization, aggregation, fluorescence and antioxidant properties of bearing (4-(methylthio) phenylthio) tetra substituted phthalocyanines,” Inorganica Chim. Acta, vol. 464, pp. 1–10, 2017.

[21] X. Li et al., “Phthalocyanines as medicinal photosensitizers: Developments in the last five years,” Coord. Chem. Rev., vol. 379, pp. 147–160, 2019.

[22] G. De La Torre, P. Vázquez, F. Agullo-Lopez, and T. Torres, “Role of structural factors in the nonlinear optical properties of phthalocyanines and related compounds,” Chem. Rev., vol. 104, no. 9, pp. 3723–3750, 2004.

[23] M. N. Y. E. H. Alici, A. T. Bilgiçli, A. Günsel, G. Arabaci and 3224. Dalton Trans. 2021, 50, “α-Substituted phthalocyanines based on metal-induced H-or J-type aggregation for silver and palladium ions: synthesis, fluorescence, and antimicrobial and antioxidant properties,” Dalt. Trans., vol. 50, no. 9, pp. 3224–3239, 2021.

[24] M. Urbani, M.-E. Ragoussi, M. K. Nazeeruddin, and T. Torres, “Phthalocyanines for dye-sensitized solar cells,” Coord. Chem. Rev., vol.

381, pp. 1–64, 2019.

[25] B. Yıldız et al., “Non-aggregating zinc phthalocyanine sensitizer with bulky diphenylphenoxy donor groups and pyrazole-3-carboxylic acid anchoring group for coadsorbent-free dye-sensitized solar cells,” Sol. Energy, vol. 226, pp. 173–179, 2021.

[26] E. J. Osburn, L.-K. Chau, S.-Y. Chen, N. Collins, D. F. O’brien, and N. R. Armstrong, “Novel amphiphilic phthalocyanines: formation of Langmuir− Blodgett and cast thin films,” Langmuir, vol. 12, no. 20, pp. 4784–4796, 1996.

[27] F. Bächle, C. Maichle-Mössmer, and T. Ziegler, “Helical Self-Assembly of Optically Active Glycoconjugated Phthalocyanine J-Aggregates,” Chempluschem, vol. 84, no. 8, pp. 1081–1093, 2019.

[28] A. Günsel, E. Güzel, A. T. Bilgiçli, G. Y. Atmaca, A. Erdoğmuş, and M. N. Yarasir, “Synthesis and investigation of photophysicochemical properties of novel ketone-substituted gallium (III) and indium (III) phthalocyanines with high singlet oxygen yield for photodynamic therapy,” J. Lumin., vol. 192, pp. 888–892, 2017.

[29] C. Epokur et al., “Novel type ketone-substituted metallophthalocyanines: synthesis, spectral, structural, computational and anticancer studies,” RSC Adv., vol. 7, no. 89, pp. 56296–56305, 2017.

[30] S. Moradian, H. Dezhampanah, J. B. Ghasemi, and H. Behnejad, “Spectrophotometric-chemometrics study of the effect of solvent composition and temperature on the spectral shape and shift of copper and nickel phthalocyanines in different aqueous-nonaqueous mixed solvents,” Spectrochim. Acta Part A Mol. Biomol. Spectrosc., vol. 227, p. 117621, 2020.

[31] J. K. F. van Staden, “Application of phthalocyanines in flow-and

sequential-injection analysis and microfluidics systems: A review," Talanta, vol. 139, pp. 75–88, 2015.

[32] M. J. Stillman, T. Nyokong, C. C. Leznoff, and A. B. P. Lever, "Phthalocyanines: properties and applications," by CC Leznoff ABP Lever, VCH, New York, vol. 1, p. 133, 1989.

[33] C. Hamann, "On the trap distribution in thin films of copper phthalocyanine," Phys. status solidi, vol. 26, no. 1, pp. 311–318, 1968.

[34] J. Puigdollers et al., "Copper phthalocyanine thin-film transistors with polymeric gate dielectric," J. Non. Cryst. Solids, vol. 352, no. 9–20, pp. 1778–1782, 2006.

[35] S. R. Forrest, "The path to ubiquitous and low-cost organic electronic appliances on plastic," Nature, vol. 428, no. 6986, pp. 911–918, 2004.

[36] A. Altindal, Z. Z. Öztürk, S. Dabak, and Ö. Bekaroğlu, "Halogen sensing using thin films of crosswise-substituted phthalocyanines," Sensors Actuators B Chem., vol. 77, no. 1–2, pp. 389–394, 2001.

[37] W. Wacławek and M. Ząbkowska-Wacławek, "The influence of iodine on the electrical properties of lead phthalocyanine," Thin Solid Films, vol. 146, no. 1, pp. 1–6, 1987.

[38] H. Meier, "Organic semiconductors". Verlag Chemie, 1974.

[39] Y. Qiu, Y. Gao, P. Wei, and L. Wang, "Organic light-emitting diodes with improved hole-electron balance by using copper phthalocyanine/aromatic diamine multiple quantum wells," Appl. Phys. Lett., vol. 80, no. 15, pp. 2628–2630, 2002.

[40] D. Hohnholz, S. Steinbrecher, and M. Hanack, "Applications of phthalocyanines in organic light emitting devices," J. Mol. Struct., vol. 521, no. 1–3, pp. 231–237, 2000.

[41] S. Zhou, A. Patty, and S. Chen, "Advances in Energy Science and

Equipment Engineering II," in Proceedings of the 2 nd International Conference on Energy Equipment Science and Engineering (ICEESE 2016), pp. 12–14,2017.

[42] J.-Z. Zhang and I. Galbraith, "Erratum:'Intraband absorption for InAs⁄GaAs quantum dot infrared photodetectors'[Appl. Phys. Lett. 84, 1934 (2004)]," Appl. Phys. Lett., vol. 85, no. 21, p. 5105, 2004.

[43] Z. Bao, A. J. Lovinger, and A. Dodabalapur, "Organic field-effect transistors with high mobility based on copper phthalocyanine," Appl. Phys. Lett., vol. 69, no. 20, pp. 3066–3068, 1996.

[44] K. Petritsch et al., "Dye-based donor/acceptor solar cells," Sol. energy Mater. Sol. cells, vol. 61, no. 1, pp. 63–72, 2000.

[45] A. Schütze, N. Pieper, and J. Zacheja, "Quantitative ozone measurement using a phthalocyanine thin-film sensor and dynamic signal evaluation," Sensors Actuators B Chem., vol. 23, no. 2–3, pp. 215–217, 1995.

[46] T. Miyata, S. Kawaguchi, M. Ishii, and T. Minami, "High sensitivity chlorine gas sensors using Cu–phthalocyanine thin films," Thin Solid Films, vol. 425, no. 1–2, pp. 255–259, 2003.

[47] G. Guillaud, J. Simon, and J. P. Germain, "Metallophthalocyanines: Gas sensors, resistors and field effect transistors," Coord. Chem. Rev., vol. 178, pp. 1433–1484, 1998.

[48] M. ZąBkowska-Wacławek, P. Talik, and W. Wacławek, "On the Compensation Behaviour of Copper Phthalocyanine Films in NOx Ambient," Phys. status solidi, vol. 121, no. 2, pp. 489–494, 1990.

[49] R. HAMAD, "Production and characterization of the metal oxide-organo metalic composites by hydrothermal method/Hidrotermal metod ile metal oksit-organo metalik kompozitlerin üretilmesi ve karakterizasyonu," 2017.

References

[50] F. H. Moser, “A. L. Thomas, The Phthalocyanines.” CRC Press, Boca Raton, Florida," 1983.

[51] R. Christie, Colour chemistry. Royal society of chemistry, 2014.

[52] Z. Li, B. Li, J. Yang, and J. G. Hou, “Single-molecule chemistry of metal phthalocyanine on noble metal surfaces,” Acc. Chem. Res., vol. 43, no. 7, pp. 954–962, 2010.

[53] C. G. Claessens, U. W. E. Hahn, and T. Torres, “Phthalocyanines: From outstanding electronic properties to emerging applications,” Chem. Rec., vol. 8, no. 2, pp. 75–97, 2008.

[54] S. Kumar, “Chemistry of discotic liquid crystals: from monomers to polymers.” Taylor and Francis, 2014.

[55] J.-L. Brédas, D. Beljonne, V. Coropceanu, and J. Cornil, “Charge-transfer and energy-transfer processes in π-conjugated oligomers and polymers: a molecular picture,” Chem. Rev., vol. 104, no. 11, pp. 4971–5004, 2004.

[56] A. M. van de Craats and J. M. Warman, “The core-size effect on the mobility of charge in discotic liquid crystalline materials,” Adv. Mater., vol. 13, no. 2, pp. 130–133, 2001.

[57] G.de la Torre, C. G. Claessens,and T. Torres," Phthalocyanines: old dyes, new materials. Putting color in nanotechnology,"Chem. Commun.,no. 20,pp. 2000- 2015,2007.

[58] S. Kumar, Chemistry of discotic liquid crystals: from monomers to polymers. CRC press, 2016.

[59] G. Giancane et al., “Investigations and application in piezoelectric phenol sensor of Langmuir–Schäfer films of a copper phthalocyanine derivative functionalized with bulky substituents,” J. Colloid Interface Sci., vol. 377, no. 1, pp. 176–183, 2012.

References

[60] M. J. Jafari, M. E. Azim-Araghi, S. Barhemat, and S. Riyazi, “Effect of post-deposition annealing on surface morphology and gas sensing properties of palladium phthalocyanine thin films,” Surf. interface Anal., vol. 44, no. 5, pp. 601–608, 2012.

[61] Y. Chen, Q. Wang, J. Chen, D. Ma, D. Yan, and L. Wang, “Organic semiconductor heterojunction as charge generation layer in tandem organic light-emitting diodes for high power efficiency,” Org. Electron., vol. 13, no. 7, pp. 1121–1128, 2012.

[62] T. Torres et al., “Phthalocyanines and Subphthalocyanines for Solar Cell Applications,” in ECS Meeting Abstracts, no. 34, p. 1116,2008.

[63] K. Onlaor, B. Tunhoo, P. Keeratithiwakorn, T. Thiwawong, and J. Nukeaw, “Electrical bistable properties of copper phthalocyanine at different deposition rates,” Solid. State. Electron., vol. 72, pp. 60–66, 2012.

[64] J. F Zhao et al., “Gallium phthalocyanine photosensitizers: carboxylation enhances the cellular uptake and improves the photodynamic therapy of cancers,” Anti-Cancer Agents Med. Chem. (Formerly Curr. Med. Chem. Agents), vol. 12, no. 6, pp. 604–610, 2012.

[65] S. Karan, B. Mallik, "Thickness dependent surface electrical conductivity in copper (II)phthalocyanine thin films, Thin Solid Films". 520, 2343-2350,2012.

[66] T. Basova, P. Semyannikov, V. Plyashkevich, A. Hassan, and I. Igumenov, “Volatile phthalocyanines: vapor pressure and thermodynamics,” Crit. Rev. solid state Mater. Sci., vol. 34, no. 3–4, pp. 180–189, 2009.

[67] S. Ambily, and C. S. Menon, "The effect of growth parameters on the

electrical, optical and structural properties of copper phthalocyanine thin films". Thin Solid Films , **347**, 284–288,1999.

[68] M. E. A. Araghi, and M. Akbari, " Thermal and Temporal Properties of a Thin Layer of Bromo Indium Phthalocyanine Nanostructures". J. Electron. Mater. **48**, 7862–7867, 2019.

[69] C.S. Lopes, L. Merces, R. F. de Oliveira, D. H. S. de Camargo, and C. C. B. Bufon, " Rectification ratio and direction controlled by temperature in copper phthalocyanine ensemble molecular diodes." Nanoscale **12**, 10001–10009, 2020.

[70] V. Rani, A. Sharma, P. Kumar, B. Singh, and S. Ghosh, "Charge transport mechanism in copper phthalocyanine thin films with and without traps." RSC Adv. **7**, 54911–54919, 2017.

[71] K. C. Sekhar, M.R. Kiran, H. Ulla, R.G. Urs, and G.L. Shekar, " Exploring the temperature-dependent hole-transport in vanadyl-phthalocyanine thin films." Physica B: Condensed Matter, 608, 412895,2021.

[72] A. H. M. Jassim, and H.A. Banimuslem, " Metal Phthalocyanine Modified Multi Walled Carbon Nanotubes; DC-Conductivity and Optical Properties. in Nano Hybrids and Composites" vol. 29 22–36 ,Trans Tech Publ, 2020.

[73] N. K. Abbas, A.F. Abdulameer, R.M. Ali, and S.M. Alwash," The Effect of Heat Treatment on Optical Properties of Copper (II) Phthalocyanine Tetrasulfonic Acid Tetrasodium Salt (CuPcTs) Organic Thin Films." Silicon **11**, 843–855, 2019.

[74] A.Stachowiak, K.Kędzierski, B.Barszcz, K.Kotwica, and D.Wróbel, "Determination of phthalocyanines energy gaps based on spectroscopic

and electrochemical studies and DFT calculations." J. Mol. Liq. **341**, 116800, 2021.

[75] H.-Y.Lee, P.Chou, and C.T.Lee, " Investigation of Various Thick Copper Phthalocyanine Buffer Layers on Pentacene-Based Organic Thin-Film Transistors." J. Electron. Mater. **47**, 4818–4822, 2018.

[76] C. Bruker , Multimode 8 with Scan Asyst Instruction Manual 004-1033-000, Bruker, UK,2009,2010.2011

[77] F.I.Bohrer,A. Sharoni, C. Colesniuc, J. Park, I.K. Schuller, A.C.Kummel, and W.C. Trogler, " Gas sensing mechanism in chemiresistive cobalt and metal-free phthalocyanine thin films ," Journal of the American Chemical Society, 129-17, 5640-5646,2007.

[78] F. Aziz, K. Sulaiman, K.S. Karimov, M.R. Muhammad, M.H. Sayyad, B.Y. Majlis," Investigation of optical and humidity-sensing properties of vanadyl phthalocyanine-derivative thin films, Molecular Crystals and Liquid Crystals." 566 , 22-32,2012.

[79] N. Kilinç, S. Öztürk, D. Atilla, A.G. Gürek, V. Ahsen, Z.Z. Öztürk, " Electrical and NO2 sensing properties of liquid crystalline phthalocyanine thin films, Sensors and Actuators," B: Chemical. 173 , 203-210,2012.

[80] M.J. Jafari, M.E. Azim-Araghi, S. Barhemat, S. Riyazi," Effect of post-deposition annealing on surface morphology and gas sensing properties of palladium phthalocyanine thin films, Surf." Interface Anal. 44 , 601-608,2012.

References

[81] T. Basova, E. Kol'tsov, A.K. Ray, A.K. Hassan, A.G. Gurek, V. Ahsen," Liquid crystalline phthalocyanine spun films for organic vapour sensing, Sensors and Actuators, B: Chemical. 113 , 127-134,2006.

[82] H. A. Banimuslem, "Organic/Carbon Nanotubes Hybrid Thin Films for Chemical Detection," PhD Thesis 2015**.**

[83] J. O. Dimmock, "Introduction to the theory of exciton states in semiconductors," in Semiconductors and semimetals, vol. 3, Elsevier, pp. 259–319,1967.

[84] R. S. Knox, "Introduction to exciton physics," in Collective Excitations in Solids, Springer, pp. 183–245,1983.

[85] J. Bujdák, N. Iyi, and R. Sasai, "Spectral properties, formation of dye molecular aggregates, and reactions in rhodamine 6G/layered silicate dispersions," J. Phys. Chem. B, vol. 108, no. 14, pp. 4470–4477, 2004.

[86] Y. Deng, W. Yuan, Z. Jia, and G. Liu, "H-and J-aggregation of fluorene-based chromophores," J. Phys. Chem. B, vol. 118, no. 49, pp. 14536–14545, 2014.

[87] K. Ban et al., "Discotic liquid crystals of transition metal complexes 29: Part 28: Ref. 1. mesomorphism and charge transport properties of alkylthio-substituted phthalocyanine rare-earth metal sandwich complexes Elemental analysis data, recrystallization solvents, yield," J. Mater. Chem., vol. 11, no. 2, pp. 321–331, 2001.

[88] A. Barranco, A. Borras, A. R. Gonzalez-Elipe, and A. Palmero, "Perspectives on oblique angle deposition of thin films: From fundamentals to devices," Prog. Mater. Sci., vol. 76, pp. 59–153, 2016.

[89] K. Chopra, "Thin film device applications." Springer Science and Business Media, 2012.

References

[90] D. A. Neamen," Semiconductor physics and devices." 1992.

[91] A. Almohammedi, A. Ashour, and E. R. Shaaban, “The pivotal role of copper on the structural and optical parameters of ZnS thin films for optoelectronic applications,” Chinese J. Phys., vol. 71, pp. 235–247, 2021.

[92] R. J. Elliott and A. F. Gibson, An introduction to solid state physics and its applications. Barnes and Noble, 1974.

[93] A. H. Clark, “Optical properties of polycrystalline semiconductor films,” Polycryst. Amorph. Thin Film. Devices, pp. 135–142, 1980.

[94] S. H. Trier, “The Study of [Mg. sub. 1-x][Co. sub. x][Fe. sub. 2][O. sub. 4] Ferrite Physical Properties and its Applications.,” NeuroQuantology, vol. 18, no. 2, pp. 143–157, 2020.

[95] O. Stenzel, The physics of thin film optical spectra. Springer, 2015.

[96] M. Kamruzzaman, T. R. Luna, and J. Podder, “Elemental, structural and optical properties of Cd1-xCoxS thin films prepared by spray pyrolysis technique,” Innov. Syst. Des. Eng., vol. 2, no. 5, pp. 117–124, 2011.

[97] R. S. Alnayli and H. Alkazaali, “Study on the linear and nonlinear optical properties of silver nanoparticles colloids in DDDW obtained by means of laser ablation.”2015.

[98] T. Higuchi, T. Murayama, E. Itoh, and K. Miyairi, “Electrical properties of phthalocyanine based field effect transistors prepared on various gate oxides,” Thin Solid Films, vol. 499, no. 1–2, pp. 374–379, 2006.

[99] H. S. Soliman, A. A. M. Farag, N. M. Khosifan, and M. M. El-Nahass, “Electrical transport mechanisms and photovoltaic characterization of cobalt phthalocyanine on silicon heterojunctions,” Thin Solid Films, vol. 516, no. 23, pp. 8678–8683, 2008.

[100] C. C. Thong, D. C. L. Teo, and C. K. Ng, “Application of polyvinyl

alcohol (PVA) in cement-based composite materials: A review of its engineering properties and microstructure behavior," Constr. Build. Mater., vol. 107, pp. 172–180, 2016.

[101] T. Allen, S. Rutherford, S. Murray, S. Reipert, and M. Goldberg, "Field emission scanning electron microscopy and visualization of the cell interior," in Cell Biology, Elsevier, pp. 325–333,2006.

[102] D. Walsh and L. Solymar," Electrical properties of materials." Oxford University Press, 2010.

[103] G. Busch and H. Schade, Lectures on Solid State Physics: International Series in Natural Philosophy, vol. 79. Elsevier, 2013.

[104] H.-J. Butt, K. H. Downing, and P. K. Hansma, "Imaging the membrane protein bacteriorhodopsin with the atomic force microscope," Biophys. J., vol. 58, no. 6, pp. 1473–1480, 1990.

[105] I. S. Gilmore and J. C. Vickerman, Surface analysis: the principal techniques. John Wiley and Sons, 2009.

[106] A. Tsargorodska, Research and development in optical biosensors for determination of toxic environmental pollutants. Sheffield Hallam University (United Kingdom), 2007.

[107] I. Schmitz, M. Schreiner, G. Friedbacher, and M. Grasserbauer, "Tapping-mode AFM in comparison to contact-mode AFM as a tool for in situ investigations of surface reactions with reference to glass corrosion," Anal. Chem., vol. 69, no. 6, pp. 1012–1018, 1997.

[108] R. Pawlak, S. Kawai, S. Fremy, T. Glatzel, and E. Meyer, "High-resolution imaging of C60 molecules using tuning-fork-based non-contact atomic force microscopy," J. Phys. Condens. Matter, vol. 24, no. 8, p. 84005, 2012.

References

[109] F.S. Rocha, A.J. Gomes, C.N. Lunardi, S. Kaliaguine, and G.S. Patienece, Experimental methods in chemical engineering: Ultraviolet visible spectroscopy, The Canadian engineering Journal of chemical Engineering, 96(12), 2512-2517,2018.

[110] L. Solymar, D. Walsh, and R. R. A. Syms, Electrical properties of materials. Oxford university press, 2014.

[111] G. A. Kumar et al., "Optical absorption studies of free (H2Pc) and rare earth (RePc) phthalocyanine doped borate glasses," Phys. Chem. Glas., vol. 41, no. 2, pp. 89–93, 2000.

[112] K. J. Hamam and M. I. Alomari, "A study of the optical band gap of zinc phthalocyanine nanoparticles using UV–Vis spectroscopy and DFT function," Appl. Nanosci., vol. 7, no. 5, pp. 261–268, 2017.

[113] V. Mekla and C. Saributr, "Structural and optical studies of thermally evaporated NiPc thin films," in Advanced Materials and Structural Engineering: Proceedings of the International Conference on Advanced Materials and Engineering Structural Technology (ICAMEST 2015), April 25-26, 2015, Qingdao, China, 2016, p. 139.

[114] M. M. El-Nahass, K. F. Abd-El-Rahman, A. A. M. Farag, and A. A. A. Darwish, "Optical characterisation of thermally evaporated nickel phthalocyanine thin films," Int. J. Mod. Phys. B, vol. 18, no. 03, pp. 421–434, 2004.

[115] M. M. El-Nahass, A. A. Atta, H. E. A. El-Sayed, and E. F. M. El-Zaidia, "Structural and optical properties of thermal evaporated magnesium phthalocyanine (MgPc) thin films," Appl. Surf. Sci., vol. 254, no. 8, pp. 2458–2465, 2008.

References

[116] J. A. A. Engelbrecht and O. J. Lombard, “The influence of some optical parameters on IR spectroscopy of oxygen in silicon,” Infrared Phys., vol. 26, no. 2, pp. 75–81, 1986.

[117] R. J. Elliott and A. F. Gibson," An introduction to solid state physics and its applications", Barnes and Noble, 1974.

[118] M. Alias, “Optoelectronic study of a-Si-Ge-Al (As): H thin films.” Ph. D. thesis, College of Science, University of Baghdad, Baghdad, Iraq, 1998.

[119] M. M. El Nhass, H. S. Soliman, H. S. Metwally, A. M. Farid, A. A. M. Farag, and A. A. El Shazly, “Optical properties of evaporated iron phthalocyanine (FePc) thin films,” J. Opt., vol. 30, no. 3, pp. 121–129, 2001.

[120] J. I. Pankove, “Optical processes in semiconductors Prentice-Hall,” New Jersey, vol. 92, 1971.

[121] A. M. Saleh, A. O. Abu-Hilal, and R. D. Gould, “Investigation of electrical properties (ac and dc) of organic zinc phthalocyanine, ZnPc, semiconductor thin films,” Curr. Appl. Phys., vol. 3, no. 4, pp. 345–350, 2003.

[122] K. R. Rajesh and C. S. Menon, “Electrical and optical properties of vacuum deposited MnPc thin films,” Eur. Phys. J. B-Condensed Matter Complex Syst., vol. 47, no. 2, pp. 171–176, 2005.

[123] A. C. Varghese and C. S. Menon, “Electrical properties of nickel phthalocyanine thin films using gold and lead electrodes,” J. Mater. Sci. Mater. Electron., vol. 17, no. 2, pp. 149–153, 2006.

References

[124] A. A. Zanfolim, D. Volpati, C. A. Olivati, A. E. Job, and C. J. L. Constantino, "Structural and electric-optical properties of zinc phthalocyanine evaporated thin films: temperature and thickness effects," J. Phys. Chem. C, vol. 114, no. 28, pp. 12290–12299, 2010.

[125] M. Alnot, J. J. Ehrhardt, and J. A. Barnard, "A characterization of heterogeneous Pt surfaces by work function measurements and photoemission of adsorbed xenon," Surf. Sci., vol. 208, no. 3, pp. 285–305, 1989.

[126] S. Darwish, I. K. El Zawawi, and A. S. Riad, "Photovoltaic properties of ZnSe/metal-free phthalocyanine heterojunctions deposited on substrates of InP single crystals," Thin Solid Films, vol. 485, no. 1–2, pp. 182–187, 2005.

[127] R. Bube, Electronic properties of crystalline solids: an introduction to fundamentals. Elsevier, 2012.

[128] N. He, Y. Chen, J. Bai, J. Wang, W. J. Blau, and J. Zhu, "Preparation and optical limiting properties of multiwalled carbon nanotubes with π-conjugated metal-free phthalocyanine moieties," J. Phys. Chem. C, vol. 113, no. 30, pp. 13029–13035, 2009.

[129] O. Berger, W.-J. Fischer, B. Adolphi, S. Tierbach, V. Melev, and J. Schreiber, "Studies on phase transformations of Cu-phthalocyanine thin films," J. Mater. Sci. Mater. Electron., vol. 11, no. 4, pp. 331–346, 2000.

[130] C. J. Liu, J. J. Shih, and Y. H. Ju, "Surface morphology and gas sensing characteristics of nickel phthalocyanine thin films," Sensors Actuators B Chem., vol. 99, no. 2–3, pp. 344–349, 2004.

References

[131] Y.-L. Lee, C.-Y. Sheu, and R.-H. Hsiao, Gas sensing characteristics of copper phthalocyanine films: effects of film thickness and sensing temperature, Sensors Actuators B Chem. 99 , 281–287,2004.

وزارة التعليم العالي والبحث العلمي

جامـــــعة با بـل/ كلية العلوم

قسم الفيزياء

دراسة الخصـائص البصرية والكهربائية للأغشية الرقيقة المحضرة مـن بـعض الثالوسيانينات ومـشتقاتها

رسالة

مقدمة إلى مجلس كلية العلوم- جامعة بابل كجزء من متطلبات نيل درجة الماجستير في علوم الفيزياء

تقدم بها

أثير عباس شاطي زابي

بكالوريوس علوم فيزياء/ ٢٠٠٣

بإشراف

الاستاذ المساعد الدكتور

حكمت عدنان جواد بني مسلم

٢٠٢٢ م ١٤٤٤هـ

الخلاصة

تم في هذه الدراسة عرض كامل للدراسات السابقة والمبادئ النظرية الاساسية المرتبطة من خلال الفصل الاول والثاني من هذه الرسالة. الخلفية العلمية لاهم الاساسيات والتي أتبعت في هذا البحث أيضا تم عرضها .

الجزء العملي تضمن اذابة ثالوسيانين النحاس و ثالوسيانين الخارصين في محلول الكلوروفورم وبتركيز ٥mg/ml كما عرض المحلول للموجات فوق الصوتية لمدة ١٥ دقيقة . بعد ذلك ُرسبت الأغشية الرقيقة من المحلول باستخدام طريقة ال (spin coating) فوق اساس زجاجي وكذلك اساس من أقطاب كهربائية متداخلة من الذهب وبسرعة ١٠٠٠ دورة\ دقيقة .

تم قياس التعرجية السطحية للنماذج بواسطة مجهر القوة الذرية وتبين ان ثالوسيانين الخارصين يمتلك سطح اخشن من ثالوسيانين النحاس ويرجع السبب في ذلك الى ان حجم ذرة الخارصين اكبر قليلًا من حجم ذرة النحاس مما ادى الى اعاقة جزيئة ثالوسيانين الخارصين من الحركة بحرية على سطح الزجاج وهذا بدورهِ يؤدي الى ترتيب اكثر عشوائية وبالتالي خشونة اكبر.

الخواص البصرية وحسابات فجوة الطاقة تم دراستها بواسطة مطياف امتصاص الضوء المرئي والأشعة فوق البنفسجية . يشير الانحراف الى الطول الموجي الاعلى في طيف الامتصاص في حالة الغشاء الى ان مادة الثالوسيانين بشكل عام تميل الى تكوين تجمع ثنائي او ثلاثي الجزيئات مقارنةً بالمحلول الذي يكون فيهِ الجزيئات احادية. اظهرت حسابات فجوة الطاقة ان فجوة الطاقة الضوئية تساوي ٣.٩٣ الكترون- فولت و ٣.٨٧ الكترون - فولت لكل من ثالوسيانين النحاس والخارصين على التوالي . كما اشارة الحسابات الى ان ناقلات الشحنة تعاني انتقال مباشر من المستوي الارضي الى المستوي المتهيج الاقرب .

تم دراسة الخواص الكهربائية باستخدام جهاز ال Kiethly وخاصية اعتمادية التوصيلة على درجات الحرارة واظهرت النتائج ان أغشية الثالوسيانين تمتلك منطقتين للتوصيل وطاقات التنشيط والتي تبرز من ميكانيكيات التوصيل .عُرضت الأغشية المصنعة الى بعض الغازات السامة لقياس قابلية الاستشعار باستخدام جهاز معتمد عل المقاومة الكهربائية . اظهرت الفحوصات ان ثالوسيانين الخارصين لا يمتلك حساسية عالية وانتقائية لأي من الغازات المعرضة لهُ , بينما اظهر غشاء ثالوسيانين النحاس انتقائية عالية وحساسية عالية اتجاه غاز ثاني اوكسيد النتروجين .

J Nanostruct 12(3): 491-502, Summer 2022

RESEARCH PAPER

Optical Characterizations and Gas Detection Study of Metalo-Phthalocyanine Thin Film Species

*Atheer Abbas Shaty and Hikmat Adnan Banimuslem**

Depertment of Physics, Faculty of Science, University of Babylon, Babylon, Iraq

ARTICLE INFO

Article History:
Received 27 March 2022
Accepted 10 June 2022
Published 01 July 2022

Keywords:
Band gap
Copper phthalocyanine
Gas sensing
UV-Visible
Zinc phthalocyanine

ABSTRACT

Copper and zinc phthalocyanines (CuPc and ZnPc) were deposited onto glass slides and platinum-interdigitated electrodes using spin coating technique to investigate the optical properties and sensing capability towards some odorants. The optical properties have been studied using UV-Visible absorption spectroscopy. The red shift in the absorption band in case of thin films indicated that phthalocyanines tend to make aggregation of dimer and trimmer in comparison to solution where only monomers exist. Energy gap calculations, utilizing Tauc plot, show that the CuPc and ZnPc having band gaps of 3.87 ev and 3.93 ev respectively and the transition of charge carriers is direct transition. Detection of some gases has been carried out using resistive based sensor measurements. ZnPc has shown no obvious behavior towards chloroform, dimethylformamide and nitrogen dioxide gases, while CuPc was selective to nitrogen dioxide gas and shown very high sensitivity and reversibility. The response and recovery times of copper phthalocyanine thin film due 100 ppm nitrogen dioxide were 20 and 142.6 sec respectively.

How to cite this article
Shaty A A., Banimuslem H A. Optical Characterizations and Gas Detection Study of Metalo-Phthalocyanine Thin Film Species. J Nanostruct, 2022; 12(3):491-502. DOI: 10.22052/JNS.2022.03.002

INTRODUCTION

Phthalocyanines are aromatic organic compounds having semiconducting properties. Besides, they are chemically stable having dense colors suitable to be used as dyes and pigments in textile. In addition, phthalocyanine compounds may have the potential to be used in a variety of studies ranging from electronic devices to sensing applications [1-4] . Copper and zinc Phthalocyanines are currently regarded as optical materials because, it has a good light absorption in the (UV-Vis) region and also can absorb light on side of a blue green region in the spectrum [1,2]. Metal free Pc's contains two hydrogen atoms in the center of the molecule, but the various metal Pc's occure when the hydrogen atoms are replaced by a single metal atom [5]. A phthalocyanine molecule consists of a central cavity that can accommodate different metal ions, and a phthalocyanine containg one or two metal ions is called a metal phthalocyanine (MPc). Introduction of metal cantons (e.g. Zn ,Fe, Cu , etc) into the central cavity of Pc molecule influences its physical properties greatly. For example, when a metal cation is introduced to the Pc molecule, the macrocycle exists as dianion and can be oxidized or reduced to different oxidation states. Many metal atoms can fit exactly into the central cavity without destruction of the planar structure of the phthalocyanine, however, some metal ions are too large to be accommodated in the central cavity of the phthalocyanine, causing distortion

* *Corresponding Author Email: hikmatadnan@gmail.com*

of the planar structure of the macrocycle. The nature of the chemical bonding between the central metal ion and the four nitrogen atoms of the two groups is of interest [6]. Phthalocyanine has become distinguished in material science and nanotechnology because it is thermochemically stable when exposed to high electromagnetic radiation. Importantly, phthalocyanine is remarkably versatile because the two hydrogen atoms in the central cavity allow the incorporation of different alternatives and can be replaced with more than 70 metals. This mean that the structural allows adjusting the physical properties. This modification is possible in the periphery of the structure and in the axial locations. Possible structural adjustments can allow the creation of analogues phthalocyanine. Generally, the extension of the π-system, different number of isoindole units an exchange of isoindol uints with other heteroaromatic ring moieties lead to the construction of these phthalocyanine analogues [7]. The emerging functions of MPcs are mainly based on electron transfer reactions resulting from the π-conjugated ring system, interaction of the π- electrons with center metal atoms and the substituents in their structure [8,9]. In this work, CuPc and ZnPc thin films have been optically investigated and employed to utilize as gas sensing devices.

MATERIALS AND METHODS

Zinc 2,3,9,10,16,17,23,24-octkis(octyloxy) -29H,31H-phthalocyanine (ZnPc) with purity ~96 % and copper(II) 2,9,16,23-tetra-tert butyl-29H,31H-phthalocyanine (CuPc) with purity ~95 % have been purchased from sigma Aldrich. Chloroform was used to dissolve the initials. The concentration has been kept to 5mg/ml.

Thin films of ZnPc and CuPc were deposited by spin coating technique onto the glass substrates ($1^{*}25^{*}75\,mm^{3}$) at room temperature and platinum-interdigitated electrods (IDE). Glass substrates were used to carry out the UV-Visible absorption spectra which were recorded on Shimadzu 1800 UV-visible spectrophotometer. On the other hand, Sensing measurements were performed on films deposited onto interdigitated electrodes and carried out using home made sensing equipment. All substrates have been ultrasonically cleaned with chloroform and deionized water.

Interdigitated electrods (IDE) were prepared on 1cm by 1cm glass slide using sputtering technique of type GSL-1100X-SPC16-3. platinum was deposited using stainless steel mask in the argon ambient.

RESULTS AND DISCUSSION

UV-Visible Absorption Spectra. The UV-vis spectrum observed for phthalocyanines originates from molecular orbitals within the aromatic 18 π electron system and from overlapping orbitals on the central metal atom [10]. A close examination of this band shows the characteristic splitting (Davydov splitting) present in all phthalocyanine derivatives [11]. The high-energy peak of the Q-band has been assigned to the first π–π* transition on the phthalocyanine macrocycle [10] The low-energy peak of the Q-band has been previously explained as a second π–π* transition [10,12]. In the high-energy region of the B (Soret) band near 300 nm, the main suggestion of the large differences occurring in the absorption spectra of the phthalocyanines in this region indicate the presence of a d – band associated with the central metal atom. It is though that π-d transitions are involved since strong absorption occurs near 320 nm, the V peak, in CuPc and the other metal phthalocyanine derivatives [13]. This is because CuPc has partially occupied d-bands. The absorption bands in the region of 275–210 nm, the S-band, may be due to d–π* transition[10,12]. Which implies a broader d-band. UV–Vis absorption spectra of the copper, zinc phthalocysnines solution in chloroform are shown in Fig. 1. Absorption peaks at UV and visible light regions are due to B and Q bands, respectively. The absorptions of Q-band have two peaks at approximately 615nm and 695nm and the relative intensity of absorption at 615nm was smaller than that at 695nm, these two peaks are due to the monomer and aggregate of CuPc, ZnPc, respectively [13]. In the Q band, an intense absorption peak at 695nm is due to the transition between the bonding and antibonding (π-π*) at the dimer part of the phthalocyanine molecule. Copper atom of the phthalocyanine molecule is associated with the d-band . Therefore, within the UV region of the spectrum, a strong absorption peak at 335nm is attributed to partially occupy d – π^{*} transitions. The variations in absorbance with B band are greater than the variations in Q band. In case of Zn phthalocyanine, in the Q-band the electronic transition occurs from higher ocupied molecular orbital (HOMO), which

has an electronic density mainly located on the phthalocyanine molecule, to the lower unocupied molecular orbital (LUMO), which has a small electronic density on Zn–N bond. The B-band electronic transition occurs between HOMO-4/ LUMO orbitals . The electrostatic potential surface and contours of ZnPc , where the +δ and -δ charges are residing on Zn and on N-atoms, respectively. The electrostatic potential surfaces can give us an idea about how the ZnPc molecules are stacking in the nanostructure system. The most probable aggregation in the system is the H-aggregation due to high energy shift in the absorption spectrum.

The absorbance spectra for ZnPc CuPc, in case of thin film (100 nm thickness) was recored and compared as shown in Fig. 2. The Figure shows that both of two spectra have two band in the visible region which is Q-band at the range about 523-775nm , and by comparison to the results of the ZnPc,CuPc solution, It produces a little red shift. In addition, the peak that assigned to aggregations of dimer and trimmer molecules in the thin films became more intense in comparison to monomer peak which was higher in the solution. That could be explained by the fact that, in the solid case, phthalocyanine tend to form more aggregation of dimer and trimmer chain of molecules instead being monomers.

The best transmittance is at room temperature and that is conformable to the results of absorption spectra, also there is two bands; Q and B. The Q is in the region of 628-695nm and B band at the wavelength of 340nm as shown in Fig. 3. The transmittance spectra for CuPc thin films, having UV- exposure intensity are shown in Fig. 4, which shows that the maximum transmittance value of CuPc is at the range of 390- 540nm, while at ZnPc, the maximum transmittance value is at the range of 350- 555nm. The transmittance decrease clearly with UV- exposure intensity increasing for both B and Q band, where the increase of UV- irradiation led to increased absorbance and therefore cause a decrease in the value of transmittance [14]. From the transmittance values, the refractive index (n)

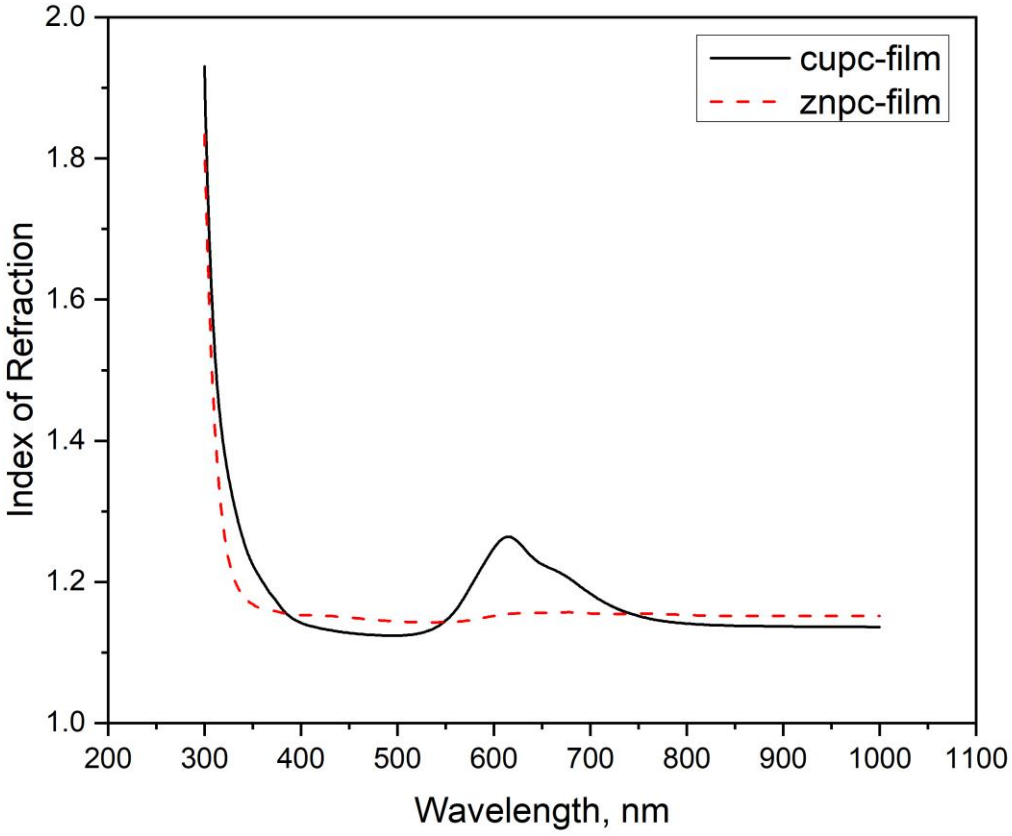

Fig. 1. Absorption spectra of CuPc and ZnPc solution in chloroform.

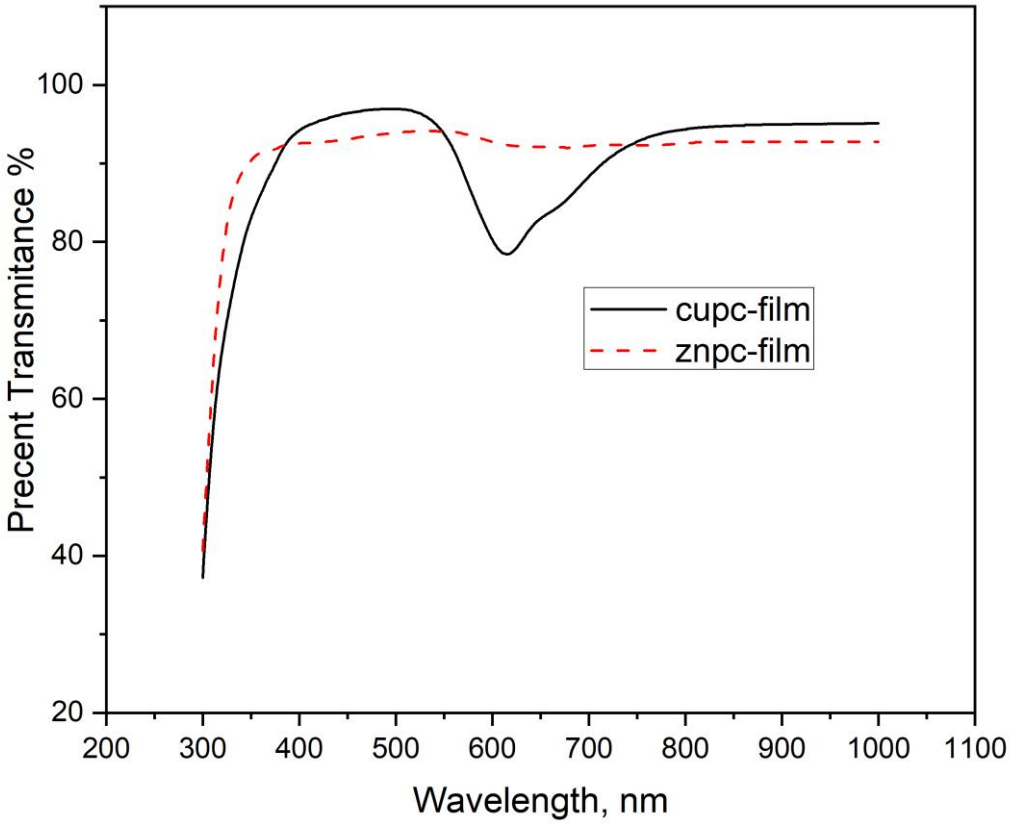

Fig.2. Absorption spectra of CuPc and ZnPc thin films deposited on glass substrate using spin coating technique.

were calculated using the following equations:

$$n = \frac{1}{Ts} + \sqrt{\frac{1}{Ts} - 1} \quad (1)$$

$$T_s = 10^{-A} \times 100 \quad (2)$$

Where Ts; transmittance , n; refractive index, A; absorobance.

In Fig. 5, solid line shows the variation of refractive index at wavelength range 550-750nm, the behavior of refractive index change of preparation conditions and method used in preparation. From this Figure, slightly increase in refractive index in CuPc upon λ of 745nm to 618nm, and then started to decrease until λ equals to 538nm. These finding are reported previously [14]. The absorption coefficient (α) were determined from the region of high absorption using the equation [15]:

$$\alpha = 2.303(A/t) \quad (3)$$

Where t is the thickness of thin films (nm). α is the absorption coefficient (1/ cm) .

The absorption coefficient helps to conclusion the types of electronic transitions. When the values of absorption coefficient are higher than ($\alpha > 10^3$ cm^{-1}) at high photonic energies, direct electronic transitions are expected and the electron momentum energy is conservation, but when the values of the absorption coefficient are lower than ($\alpha < 10^3$ cm^{-1}) at low photonic energies, indirect electronic transitions are expected, in which the momentum of electron and photon are conservation with the help of a phonon[16]. The maximum wavelength (lm) of the incident photon which creates the electron–hole pair is defined as [17].

$$h\nu = \frac{1240}{\lambda m} \quad (4)$$

The optical energy gap values (Eg) for CuPc ZnPc, thin films have been determined by using

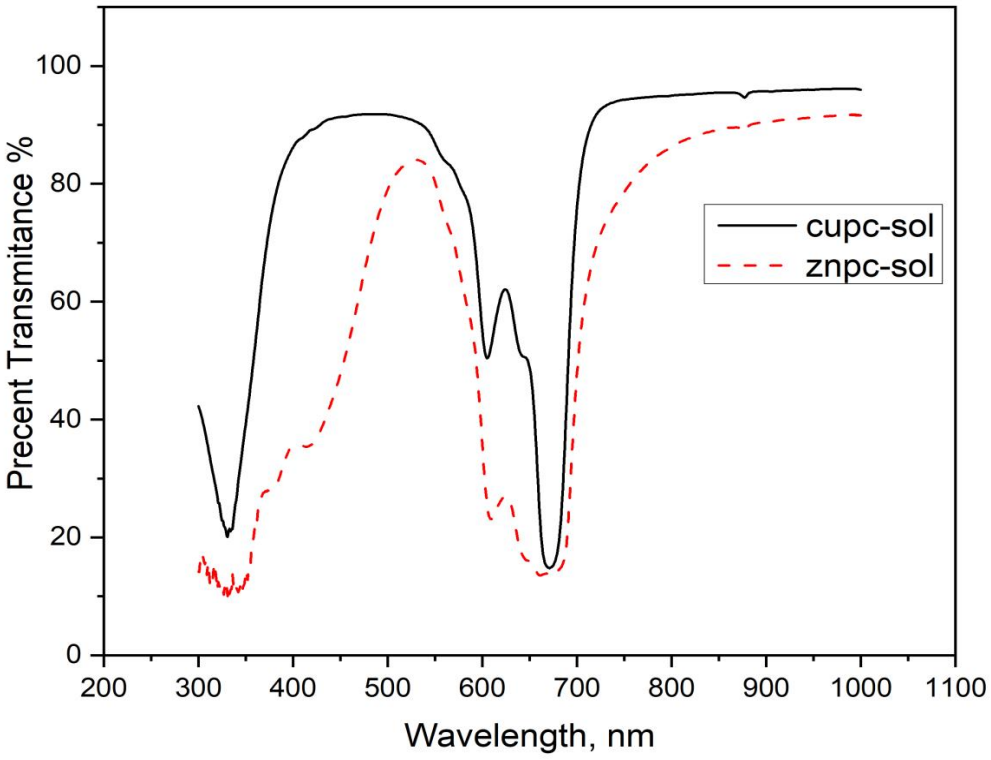

Fig. 3. Percent transmitance spectra of CuPc and ZnPc solution in chloroform.

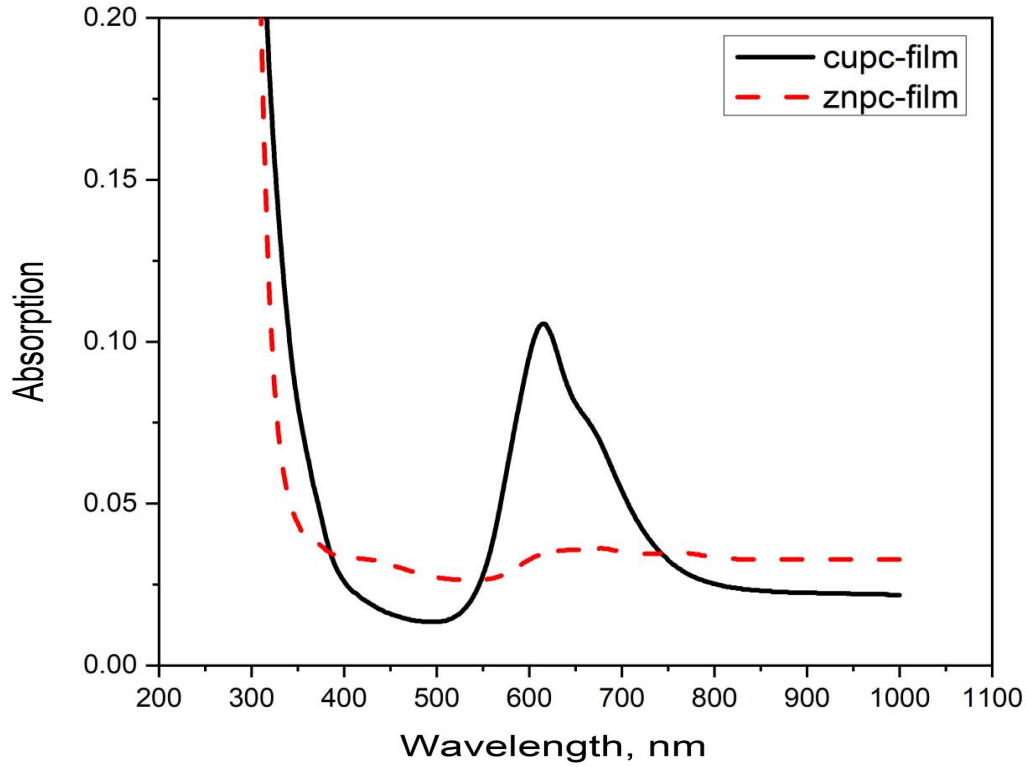

Fig. 4. Percent transmitance of CuPc and ZnPc thin films deposited on glass substrate using spin coating technique.

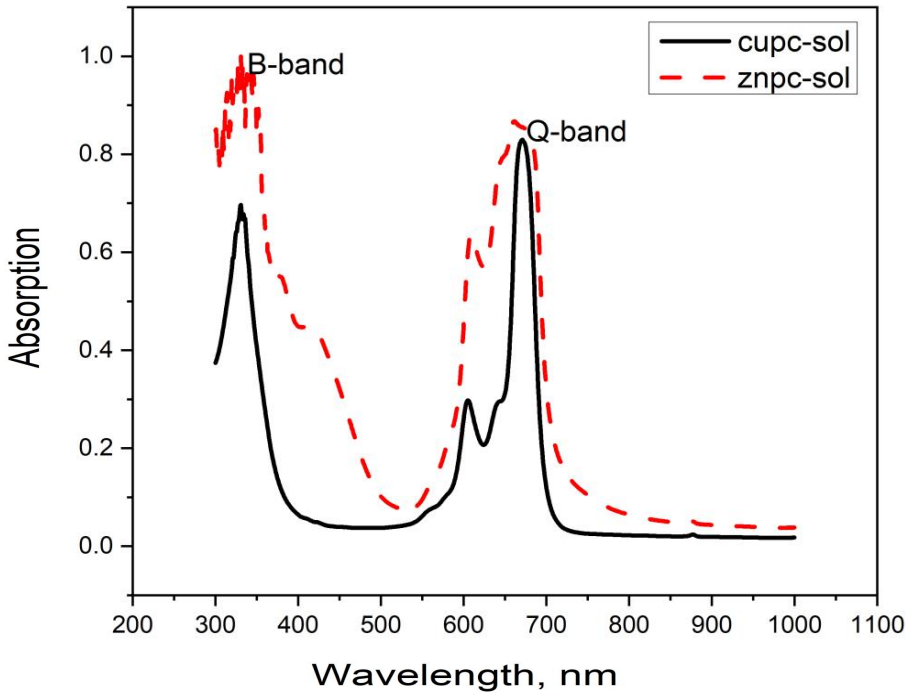

Fig. 5. Index of refraction of CuPc and ZnPc thin films deposited on glass substrate using spin coating technique.

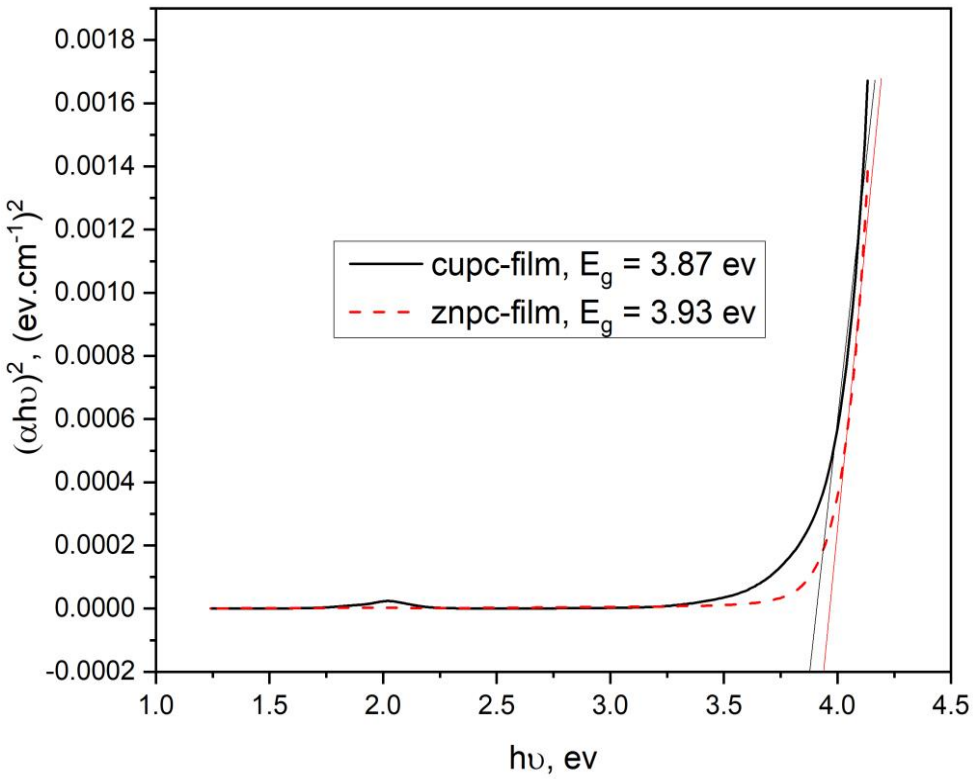

Fig. 6. Tauc plot and optical energy gap calculations of CuPc and ZnPc thin films deposited on glass slides using spin coating technique.

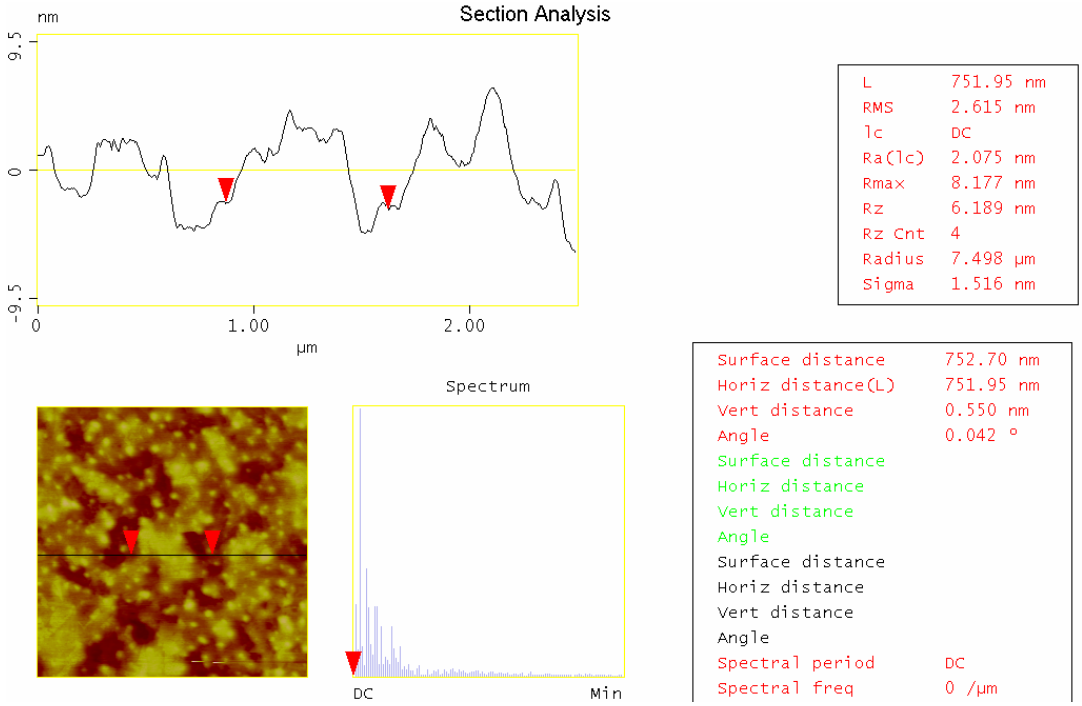

Fig. 7. AFM image and analysis of CuPc thin films deposited on silicon substrate using spin coating technique.

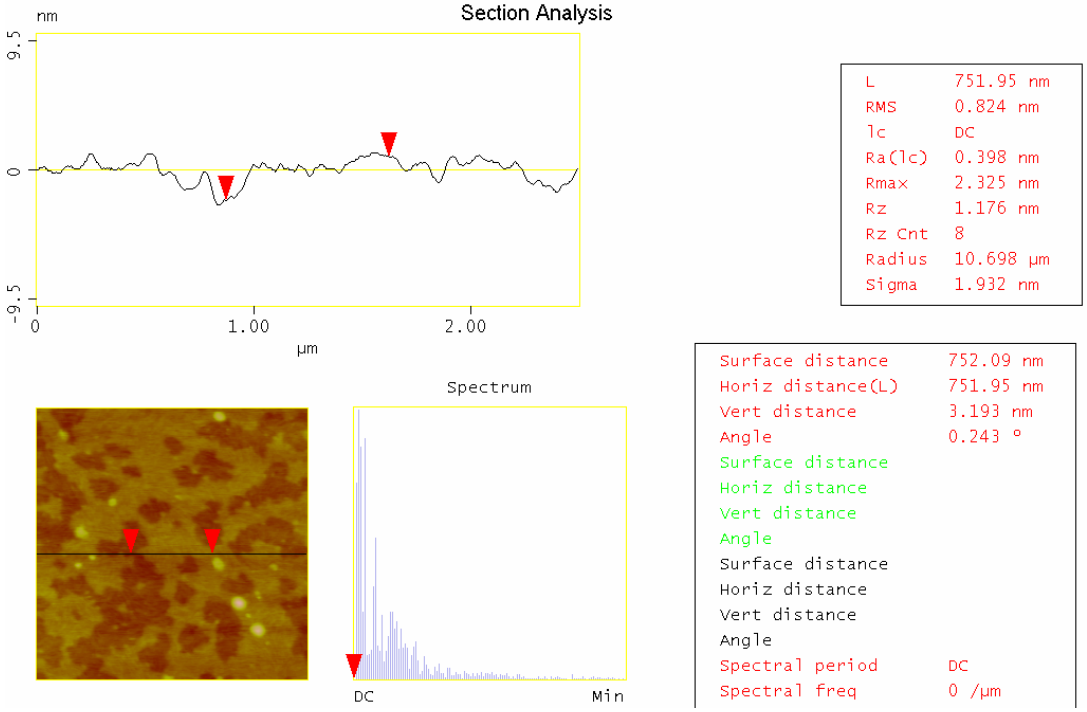

Fig. 8. AFM image and analysis of ZnPc thin films deposited on silicon substrate using spin coating technique.

Tauc equation [18]:

$$\alpha h\nu = B(h\nu - E_g)^2 \quad (5)$$

For an allowed direct transition, the transition occurs from the top of the valence band to the bottom of the conduction band. When graphing the relation between each of the $(\alpha h\nu)^2$ with photon energy of incident radiation, through which it is possible to calculate the value of

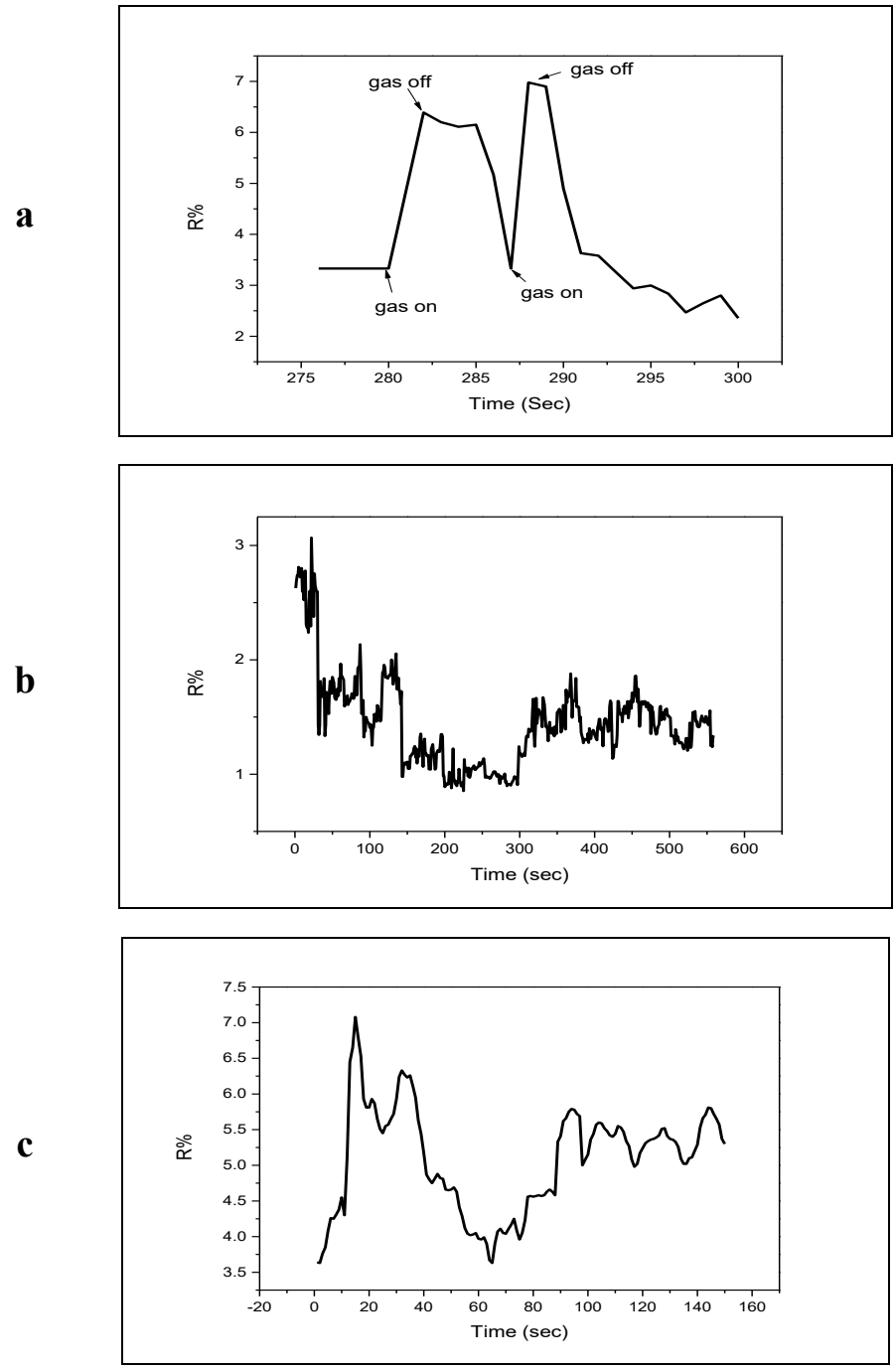

Fig. 9. Response vs. time of ZnPc deposited on interdigitated electrodes at room temperature for NO_2(a), Chloroform(b), and DMF(c) vapors at 100 ppm.

allowed direct energy gap, and best graph obtained that can be the extension of the straight line that intersects the hv- axis to determine the value of energy gap for allowed direct transition of the ZnPC, CuPC thin films, as shown in the Fig. 6, and the values of energy gaps was 3.87 eV,3.93eV respectively. Similar findings have also been reported elsewhere [18]. Fig. 6 shows a linear change at high energy range did not appear with the other curves, which indicates the occurrence

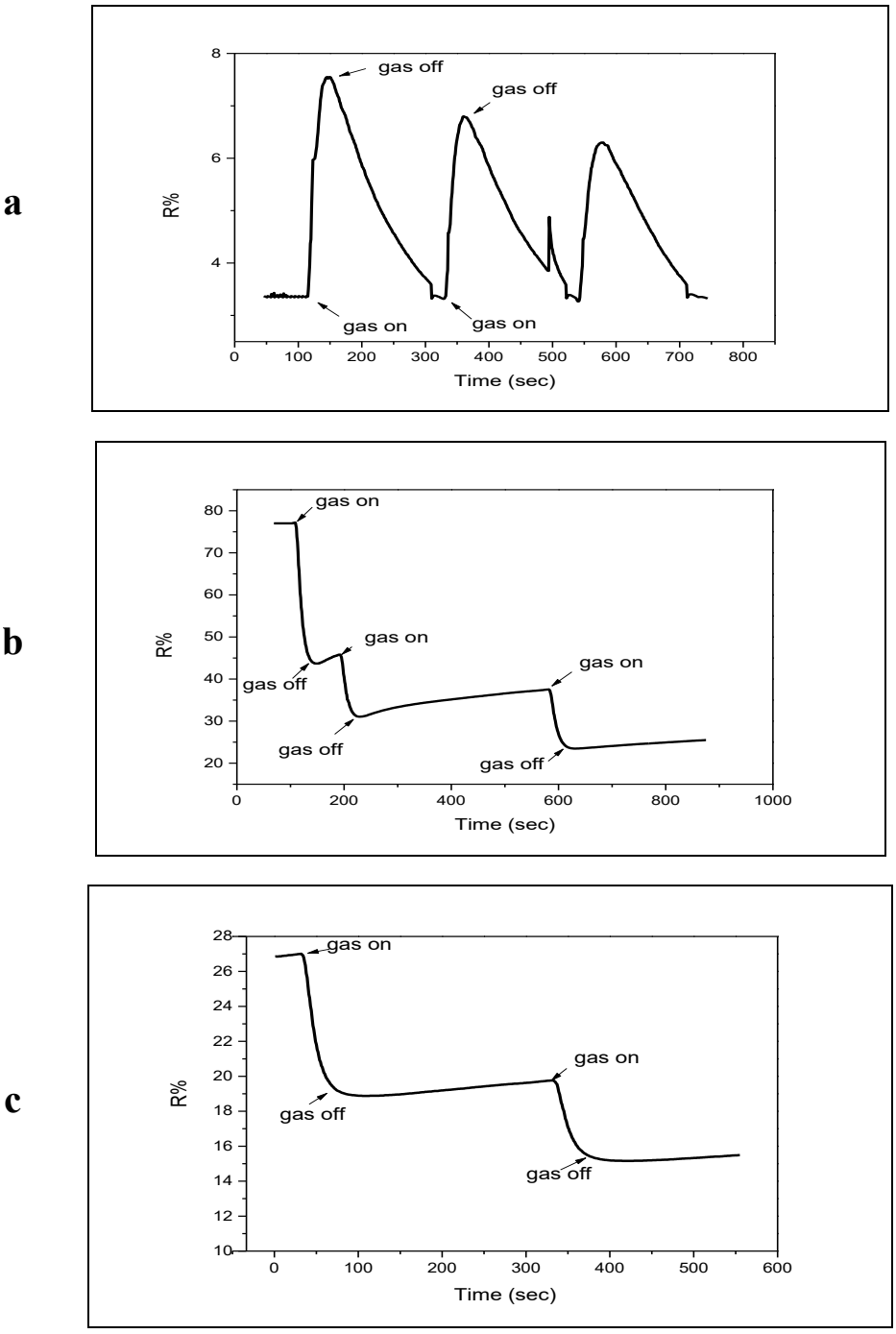

Fig. 10. Response vs. time of CuPc deposited on interdigitated electrodes at room temperature for NO_2(a), Chloroform(b), and DMF(c) vapors at 100ppm.

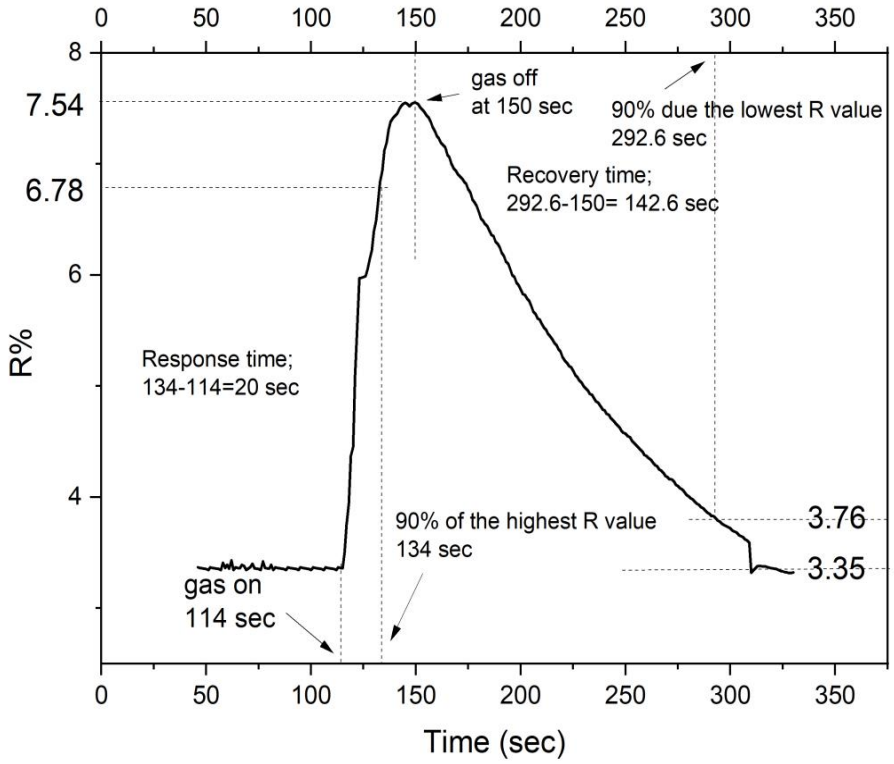

Fig. 11. Response and recovery times of copper phthalocyanine film upon exposure to NO_2.

of the allowed direct electronic transition in the prepared films. There are variation between energy gap values and it is impact by mechanism a formation thin films and conditions accompanying the preparation process. Energy gap value and type depends on crystal structure of material and how atoms distribution in crystalline lattice and the levels energy structure, this mean that any change in structure properties can being caused by the change occurring of energy gap and transitions type which occurring in thin films [19].

Figs. 7 and 8 show AFM images of CuPc and ZnPc films spun onto silicon substrates with the roughness analysis presented AFM measurements in tapping mode have been performed on all samples in this study. Typical fibre features of phthalocyanine has been obviously seen in the films, which is similar to the topology of phthalocyanine and almost all organic dyes which tend to make very dense aggregations in the solid state. These aggregates are represented as a coplanar association of rings developing from monomer to dimer and higher order complexes and are driven by π-π interaction and van der Waals forces [4].

In present work, the sensitivity of CuPc and ZnPc devices were studied during exposure to 100 ppm concentration of chloroform, dimethyleformamide and nitrogen dioxide odorents at room temoerature. The samples were fixed in a special per- evaluated chamber. After that gaswas separately introduced to the chamber. The change in resistance ratio R_g/R_a (where R_g is the resistance in the present of gas and R_a is the resistance in zero grade air) on exposure to contaminated air at room temperature for 10 s. ZnPc have shown no obvious behavior towareds contaminations as exhibited in the time dependence Fig. 9. Zn atom is a littile bigger than the cavity of phthalocyanine, results in a deviation in the position from the plane of the molecule. Consequently, hindering of orientation took place and the adsorption of odorant would be random and not reversible. On the other hand, CuPc thin film has shown quite reasonable performance towards gases and presented in Fig. 10. From this Figure, the response of CuPc film to NO_2 gas was oposite to other gases which makes it selective to this particular gas. The reason for the decrease in resistance of the devices can be understood in

terms of a change in the surface conductivity of thin films. Such effects can be interpreteds within the framework of the band theory. If we consider the adsorbed gases to produce appropriate donor or acceptor levels within the band gap of the organic materials at the film surface. CuPc and ZnPc are a p _ type organic semiconductor, upon exposure to the oxidizing gases such as , the hole concentration near the surface will be enhanced through a doping mechanism, resulting in the increase of electrical conductivity[20]. In the case of chloroform and DMF odorants,

film resistance decreased rapidly and no reversibility occureed. The recovery rate of the film resistance was slower and did not recover to the original value before exposure. The present recovery characteristic is less than that in a previous work operated at the same temperature [21]. These results confirm that the sensitivity of phthalocyanine as gas sensor depend on different factors such as ambient condition, method of device fabrication, sensing temperature and the type of central metalic element. The response and recovery times have been calculated as 90% of the highst R value and 90% due the lowest R value and found to be 20 sec and 142.6 sec respectively. Fig. 11 represent clearly the calculations of both response and recovery times.

CONCLUSION

Thin films of zinc and copper phthalocyanine have been prepared in the mean of spin coating mechanism. UV-Visible spectra have revealed that thin film has shown a little red shift in the position of Q band in comparison to solution spectra and formation of dimer and trimmer molecules instead of being monomers. The optical energy gaps were found to be 3.87 eV and 3.93 eV for copper and zinc phthalocyanine respectively. Films of copper phthalocyanine have been quite sensitive and selective to nitrogen dioxide gas while zinc phthalocyanine performed randomly upon exposure to contaminated ambient.

CONFLICT OF INTEREST

The authors declare that there is no conflict of interests regarding the publication of this manuscript.

REFERENCES

1. Inigo AR, Xavier FP, Goldsmith GJ. Copper phthalocyanine as an efficient dopant in development of solar cells. Mater Res Bull. 1997;32(5):539-546.
2. Sharma GD, Kumar R, Sharma SK, Roy MS. Charge generation and photovoltaic properties of hybrid solar cells based on ZnO and copper phthalocyanines (CuPc). Sol Energy Mater Sol Cells. 2006;90(7-8):933-943.
3. Gülmez AD, Polyakov MS, Volchek VV, Kostakoğlu ST, Esenpinar AA, Basova TV, et al. Tetrasubstituted copper phthalocyanines: Correlation between liquid crystalline properties, films alignment and sensing properties. Sensors and Actuators B: Chemical. 2017;241:364-375.
4. Banimuslem H, Hassan A, Basova T, Gülmez AD, Tuncel S, Durmuş M, et al. Copper phthalocyanine/single walled carbon nanotubes hybrid thin films for pentachlorophenol detection. Sensors and Actuators B: Chemical. 2014;190:990-998.
5. Varghese AC, Menon CS. Electrical Properties of Nickel Phthalocyanine Thin Films Using Gold and Lead Electrodes. Journal of Materials Science: Materials in Electronics. 2006;17(2):149-153.
6. Arslan O, BİLgİL A, Veske O. STANDART YAĞIŞ İNDİSİ YÖNTEMİ İLE KIZILIRMAK HAVZASI'NIN METEOROLOJİK KURAKLIK ANALİZİ. Ömer Halisdemir Üniversitesi Mühendislik Bilimleri Dergisi. 2016;5(2):188-194.
7. de la Torre G, Bottari G, Hahn U, Torres T. Functional Phthalocyanines: Synthesis, Nanostructuration, and Electro-Optical Applications. Functional Phthalocyanine Molecular Materials: Springer Berlin Heidelberg; 2009. p. 1-44.
8. Lütfi Uğur A, Erdoğmuş A, Koca A, Avcıata U. Synthesis, spectroscopic, electrochemical and spectroelectrochemical properties of metal free, manganese, and cobalt phthalocyanines bearing peripherally octakis-[4-(thiophen-3-yl)-phenoxy] substituents. Polyhedron. 2010;29(18):3310-3317.
9. Banimuslem H, Hassan A, Basova T, Durmus M, Tuncel S, Esenpınar AA, et al. Copper Phthalocyanine Functionalized Single-Walled Carbon Nanotubes: Thin Films for Optical Detection. Journal of Nanoscience and Nanotechnology. 2015;15(3):2157-2167.
10. Thomas J, Kumar GA, Unnikrishnan NV, Nampoori VPN, Vallabhan CPG. Optical studies of phthalocyanine molecules in PVA film. Mater Lett. 2000;44(5):275-278.
11. Hamam KJ, Alomari MI. A study of the optical band gap of zinc phthalocyanine nanoparticles using UV–Vis spectroscopy and DFT function. Applied Nanoscience. 2017;7(5):261-268.
12. El-Nahass MM, El-Gohary Z, Soliman HS. Structural and optical studies of thermally evaporated CoPc thin films. Optics & Laser Technology. 2003;35(7):523-531.
13. El-Nahass MM, Abd-El-Rahman KF, Farag AAM, Darwish AAA. OPTICAL CHARACTERISATION OF THERMALLY EVAPORATED NICKEL PHTHALOCYANINE THIN FILMS. Int J Mod Phys B. 2004;18(03):421-434.
14. Engelbrecht JAA, Lombard OJ. The influence of some optical parameters on IR spectroscopy of oxygen in silicon. Infrared Phys. 1986;26(2):75-81.
15. Elliott RJ, Gibson AF, Mielczarek EV. An Introduction to Solid State Physics and Its Applications. Phys Today. 1975;28(5):58-58.
16. Okamura H, Michizawa T, Nanba T, Kimura S-i, Iga F, Takabatake T. Indirect and Direct Energy Gaps in Kondo Semiconductor YbB_{12}. J Phys Soc Jpn. 2005;74(7):1954-

1957.
17. Abbas NK, Abdulameer AF, Ali RM, Alwash SM. The Effect of Heat Treatment on Optical Properties of Copper (II) Phthalocyanine Tetrasulfonic Acid Tetrasodium Salt (CuPcTs) Organic Thin Films. Silicon. 2018;11(2):843-855.
18. El Nhass MM, Soliman HS, Metwally HS, Farid AM, Farag AAM, El Shazly AA. Optical Properties of Evaporated Iron Phthalocyanine(FePc) Thin Films. Journal of Optics. 2001;30(3):121-129.
19. Basu PK. Classical theory of optical processes. Theory of Optical Processes in Semiconductors: Oxford University Press; 2003. p. 9-27.
20. Liu CJ, Shih JJ, Ju YH. Surface morphology and gas sensing characteristics of nickel phthalocyanine thin films. Sensors and Actuators B: Chemical. 2004;99(2-3):344-349.
21. Lee Y-L, Sheu C-Y, Hsiao R-H. Gas sensing characteristics of copper phthalocyanine films: effects of film thickness and sensing temperature. Sensors and Actuators B: Chemical. 2004;99(2-3):281-287.

Electrical Behavior, Structural and Optical Characterization of Copper (II) and Zinc Phyhalocyanine Thin Films

Atheer Abbas Shaty[1], Hikmat Adnan Banimuslem[2*]

Abstract

The structural, optical, and electrical properties of ZnPc and CuPc thin films were investigated in this worksheet., At room temperaturewhich prepared on glass slide and Platinum- interdigitated electrode by spin coating technique, optical energy gap shows that the copper phthalocyanine (CuPc) films and zinc phthalocyanine films (ZnPc), 3.87 ev, 3.93 ev respectively. Variation of DC electrical conductivity with (1/T), shows that CuPc,ZnPc films have two activation energy, CuPc for one region, E_{a1} = 0.076 ev and two region, E_{a2}= 0.407 ev. While in the case of ZnPc, the activation energies were found to be 0.029 ev and 0.056 ev for first region and second region respectively. I-V measurements, CuPc has shown Ohmic behavior, while the ZnPC shown like diode behavior, Structural properties, surface topography measurement by AFM and determine roughness surface each ZnPc, CuPc.

Key Words: Copper Phthalocyanine, Zinc Phthalocyanine, D.C Conductivity, Band Gap, Structural (Surface Topographic).

DOI Number: 10.14704/nq.2022.20.6.NQ22101 **NeuroQuantology2022;20(6):1093-1103**

Introduction

Phthalocyanines are aromatic semiconducting organic chemicals. Furthermore, they are chemically stable and have deep colors, making them ideal for use as textile dyes and pigments.Furthermore, phthalocyanine compounds may be useful as solar cells and gas sensors. Because it is a good light absorber in the (UV-Vis) region and can also absorb light on the blue green side of the spectrum, phthalocyanine is currently considered an optical material.(1),(2).

Metal free Pcs have two hydrogen atoms in the middle of the molecule, whereas metal Pcs have a single metal atom. (3). A phthalocyanine molecule has a central cavity that can accommodate various metal ions, and a phthalocyanine that contains one or two metal ions is referred to as a metal phthalocyanine (MPc). Metal cantons (Zn(+2), Fe(+2), Cu(+2), and other metals) introduced into the core cavity of the Pc molecule have a major impact on its physical properties. When a metal cation is added to the Pc molecule, the macrocycle becomes dianion (Pc(-2)) and can be oxidized or reduced to various oxidation statesMany metal atoms can fit into the central cavity without harming the phthalocyanine's planar structure; however, certain metal ions are too big to fit into the central cavity, causing the macrocycle's planar structure to be distorted. The chemical connection between the central metal ion and the four nitrogen atoms of the two groups is of interest. The atom of central, which has a +2 oxidation state, is covalently bonded to two nitrogen atoms and coordinately bonded to the other two nitrogen atoms. (4).Organic semiconductors based on sensors can be employed for sensing applications of various environmental parameters because organic materials are particularly sensitive to temperature.(5).

Corresponding author: Hikmat Adnan Banimuslem
Address: [1,2*]Physics's Department, Science's Faculty, Babylon's University, Babylon, Iraq.
E-mail: [1]atheer.shaty@gmail.com;[2*]hikmatadnan@gmail.com

Environmental sensitivity of phthalocyanines was discovered in studies.(6),(7) These materials have a lot of potential for the development of many sorts of sensors. (8) with great selectivity, repeatability, and reliability They have the potential to be built as multi-functional sensors that can operate in multiple modes, enabling for the creation of a simple "higher order" sensor network with minimal manufacturing costs and quick commercialization.(9).Because of its thermochemical stability and high electromagnetic radiation absorption capabilities, phthalocyanine has made a name for itself in material science and nanotechnology. Importantly, phthalocyanine is a highly adaptable molecule because the two hydrogen atoms in the central cavity allow for the substitution of over 70 metals. This means that the physical qualities of the structure can be changed. This alteration is achievable in both the perimeter and the axial locations of the structure. The creation of phthalocyanine analogues could be aided by structural alterations. In general, extending the -system, using a different number of isoindole units, and exchanging isoindol uints with alternative heteroaromatic ring moieties make it easier to make these phthalocyanine analogues. The electron transfer reactions generated by the π - conjugated ring system, interactions of π - electrons with center metal atoms, and substituents in their structure are the foundations of MPcs' evolving activities. (11).

Materials and Methods

Experimental Details

Materials

Zinc Phthalocyanine: zinc 2,3,9,10,16,17,23,24 - octkis (octyloxy) - 29H, 31H - phthalocyanine (ZnPc) with purity ~96 %, Copper Phthalocyanine: copper (II) 2,9, 16,23 –tetra- tert butyl - 29H, 31H - phthalocyanine (CuPc) with purity ~95%,Chloroform ($CHCl_3$) solvent, Sigma Aldrich supplied N N – Dimethyl forma mide (DMF) with a purity of 99.8 percent and HNO3 with a purity of 70%, both of which were used as purchased.

Thin Film Deposition

Thin films deposition,ZnPc and CuPc thin films were deposited by spin coating technique onto a glass substrates (1x25x75mm3) at room temperature and alsoplatinum-interdigitated electrods were used (IDE).On glass substrates, UV-visible absorption and AFM measurements were taken. Conductivity measurements, on the other hand, were carried out on films deposited onto interdigitated electrodes. All substrates were cleaned ultrasonically with chloroform and deionized water.

InerdigitatedElectrods

Interdigitated electrods (IDE) were created on a 1cm by 1cm glass slide using the GSL-1100X-SPC16-3 sputtering technique.In an argon atmosphere, platinum was deposited using a stainless steel mask.

Measurements

UV-visible absorption spectra were recorded using a Shimadzu 1800 UV-visible spectrophotometerThe I–V characteristics and DC conductivity of the films were measured using a Keithley 4200 semiconductor characterisation system.The formula was used to compute the conductivity (σ): (12).

$$\sigma = \frac{L}{RHWN} \qquad (1)$$

Where Gap between electrodes is L, film's resistance is R, H is the thickness of the film, Distanceoverlapping is W, and Electrodes number isn.

Results and Discussion

UV-Visible Absorption Spectra

phthalocyanines's UV-vis spectrum is caused by overlapping orbitals on the core metal atom and molecular orbitals within the aromatic 18 electron system.(13). The characteristic splitting (Davydov splitting) present in all phthalocyanine derivatives can be seen if you look closely at this band (14). The first π –π* transition on the phthalocyaninemacrocycle has been assigned the high-energy peak of the Q-band (13). A second π – π * transition has already been proposed to explain the low-energy Q-band peak. [8,10]. The occurrence of a d – band associated with the central metal atom in the high-energy region of the B (Soret) band near 300 nm is the main suggestion for the considerable discrepancies in the absorption spectra of the phthalocyanines in this region.Strong absorption occurs near 320 nm. the V peak, in CuPc and the other metal phthalocyanine derivatives implying that π-d transitionsare involved. (16).Because CuPc has partially occupied d-bands.The absorption bands in the region of 275–210 nm. S-band, may be due to d–π* transition

[8,10]. This implies a wider d-band.

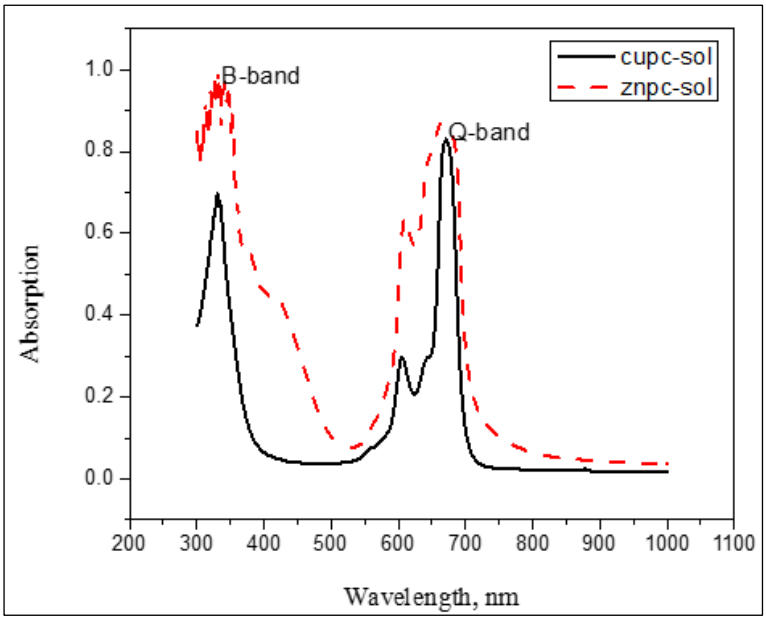

Figure 1. Absorption spectra of CuPc and ZnPc solution in chloroform

Figure depicts the UV–Vis absorption spectra of a copper, zinc phthalocysnines solution in chloroform. The UV and visible light absorption peaks are caused by the B and Q bands, respectively. Band- Q absorptions have twopeaks at a pproximately 615 nm and 695nm. with intensity relative of absorption at (615nm) being lower than that at (695nm). These two peaks are due to the monomer and aggregate of CuPc, ZnPc, respectively.(16). Absorption peak an intense upon (695nm) in Band Q is caused by that transition between bonding and antibonding (π-π*) upon the dimer part that phthalocyanine's molecule. Atom's copper in phthalocyanine's moleculeis linked to band - d.As a result, Region's UV within that spectrum, peak's absorptionstrong upon 335 nm is attributed to partially occupied d transitions.Variations in absorbance that theband- B are greater thanband- QIn the case of Zn phthalocyanine. Transition's electronic is occurs in band -Q fromHOMO, that has a highelectronical densityin phthalocyanine 's molecule, to LUMO, which has a low electronicallydensity onZn–N thebond. Transition's electronic between HOMO-4/LUMO orbitals occurs in the B band. The ZnPc electrostatic potential surface and contours, On Zn and N-atoms, respectively, the +δ and -δ charges are located.

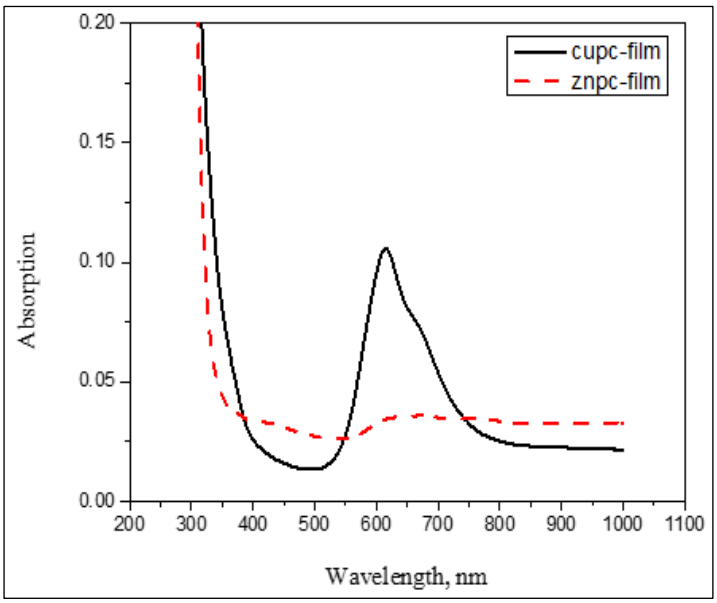

Figure 2. Absorption spectra of CuPc and ZnPc thin films deposited on glass substrate using spin coating technique

Potential's electrostatic that surfaces can provide information about how molecules ZnPc stack insystem's nanostructure. Aggregation-H is the most likely aggregation in the system caused by to shifthigh energy in absorption's spectrum.Absorbance's spectra for ZnPc CuPc, in case of thin film (100 nm thickness) was recored and compared asin Fig. shows. shown figure that both that two spectra have two band in region visible which is band - Q upon (523-775)nm range, andby comparison to the results of the ZnPc,CuPc solution, It produces a little red shift. In addition, the peak that assigned to aggregations of dimer and trimmer molecules in the thin films became more intense in comparison to monomer peak which was higher in the solution. That could be explained by the fact that, in the solid face, phthalocyanine tend to form more aggregation of dimer and trimmer chain of molecules instead being monomers.

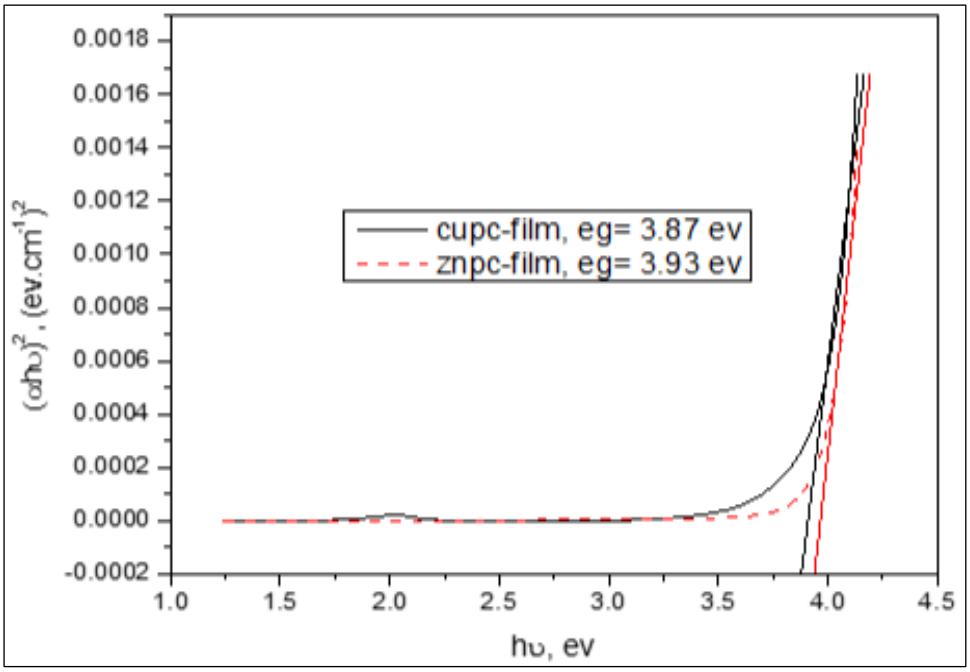

Figure 3. Tauc plot and optical energy gap calculations that thin films'sCuPc and ZnPc on glass slides were deposited by using technique spin coating

Using equation, coefficient's (α)absorption was calculated from the region that absorption high. (17):

$$\alpha = 2.303(A/t) \qquad (4)$$

WhereThin films (nm)thickness is t and α:is absorption coefficient (1/ cm).

The absorption coefficient helps to conclusion the types of electronic transitions. When the valuesof absorption coefficient are higher than($\alpha > 10^3\,cm^{-1}$) at high photonic energies, direct electronic transitions areexpected and the electron momentum energy is conservation, but when the values of the absorption coefficient are lower than($\alpha < 10^3\,cm^{-1}$) at low photonic energies, indirect electronictransitions are expected, in which the momentum of electron and photon are conservation with the help of a phonon(18).

The incident photon's maximum wavelength (λm) that creates the electron–hole pair is defined as(19).

$$h\nu = \frac{1240}{\lambda m}(5)$$

Gap energy optical of values (Eg) for CuPc ZnPc, The Tauc equation was used to determinethin films.(20):

$$\alpha h\nu = B(h\nu - E_g)^2 \ (6)$$

From the top of the valence band to the bottom of the conduction band, an allowed direct transition occurs.When graphing the relation between each of the $(\alpha h\upsilon)^2$ with photon energy of incident radiation, through which it is possible to value calculate that energy gap allowed direct, and best graph obtained that can be the extension of the straight line that intersects the (hυ) - axis to determine the value of energy gap for allowed direct transition of thin films ZnPC, CuPC, as shown in figure, and energy gaps valueswas 3.87ev,3.93ev respectively. Similar findings have also been reported elsewhere(1).

The figureshows a linear change at high energy range did notappear with the other curves, which indicates the occurrence of the allowed direct electronic transition in the preparedfilms. There are variation between energy gap values and it is impact by mechanism a formation thin films and conditions accompanying the preparation process. Energy gap value and type depends on crystal structure of material and how atoms distribution in crystalline lattice and thelevelsenergy structure, this mean that any change in structure properties and the parameterized another, can being caused by the change occurring of energy gapand transitions type whichoccurring in thin films(21).

I-V (Current-voltage) P

By using Kiethly semiconductor characterization system I-V curves have been measured for prepared devices Figures show the current vs voltage characteristics of CuPc and ZnPc thin films deposited onto Platinum interdigitated electrodes. The voltage was swapped from -5 to 5 volt to carry out the experiments.

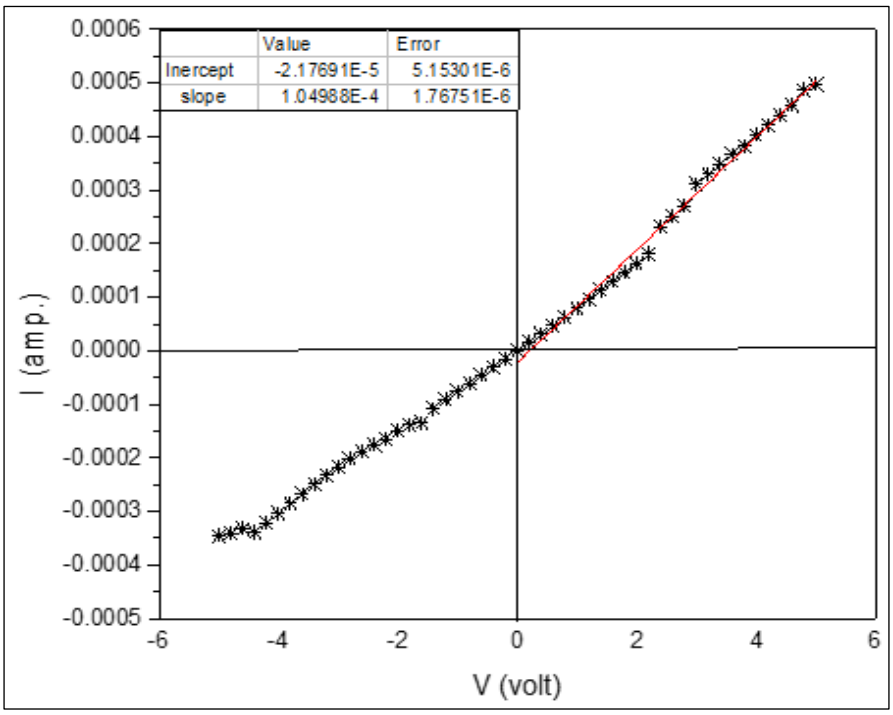

Figure 4. Current–voltage characteristics of CuPc thin films

CuPc has shown Ohmic behavior as expected for interdigitated electrodes since the voltage was applied laterally through the device and the resistivity was calculated using equation(ρ=RA/L)(22). and found to be 2.3$K\Omega$.cm. Similar results are also published in the literature (23). For thermally evaporated CuPc films. However, in the ZnPc device the change in the curve wasexponential exhibiting diode behavior. The observed exponential dependence of the forward current in the lower voltage range may be due to the formation of a depletion region between ZnPc layer and Ti-interdigitated electrodes substrate. A linear trend characteristic of ohmic behavior in the case of CuPc, which observed as mentioned in the beginning of the paragraph is similar to the finding was reported by Rajesh and Menon (24). It is well understood that the conductivity and driving mechanism are affected bymetal contacts nature (3). The model established by Olthuis et al. (25) was used to determine resistivity from a linear modification of the I-V curve, and found to be 1.97 KΩ.cm. The difference between ZnPc and CuPc behavior, attributed to Zinc`s atomic radius is 0.137 nm(26) while copper`s is 0.128 nm(27). Hence the atomic size of zinc is greater than that of copper, this results causes of the effective molecular change of Cu will be more, due to lesser d electrons. Hence,lesser screening effect leading to more effective nuclear change, making smaller covalent radius than zinc (23). The interpretation of this exhibiting behavior is suggested to be: firstly, depletion region in the ZnPc as a result of the bigger atomic radius of the atom may cause a deviation of Zn from the cavity of phthalocyanine molecule and hence created a depletion region(28).Secondly, the bigger size of the atom causes some defect to the molecule, this led to random orientation alignment on the film surface and as a result of this disorder, the depletion region has been created between the metal electrode and active layer. Thirdly, work function for platinum electrodes estimated 4.33 ev (29), andfrom UV- visible measurements, and energy gap of ZnPc and CuPcwere obtained estimated(3.9, 3.8) ev, respectively. From these results, it is likely that electron transition to CuPc easily thanZnPc. Rectification factor R R is defined as the ratio of forward current to reverse current at a given applied voltage Itis clear that the junction has strong rectifying characteristics and behaves like a diode(30). As seen from the figure, there is potential barrier in depletion region that the estimated 3V. The forward current (mA) arise from majority charge carriers(31), while reverse current arise from minority charge carriers and they are extremely small current (μA) (32). Graphing the I-V Curve for forward bias,Voltage forward (V F) that a diode increases to along right for axis horizontal, while currentforward (I F) increases to along left

for axis vertical. Aftera potential barrier, the relation (I,V) represents exponential,Forward Resistance is not constant over the entire curve. It is called dynamic resistance ($r`_d$), below threshold of the curve resistance is greatest because the current increases very little for a given change in voltage ($r`_d = \frac{\Delta V_F}{\Delta I_F}$). Resistance begins to decrease in region of curve's threshold and becomes smallest above the threshold where there is a large change in current for a given change in voltage. When bias - reverse voltage is applied across a sample, only a very small current reverse (I- R) flows through of junctionp type-metal; as V- R gradually increases, so does the reverse current (33).

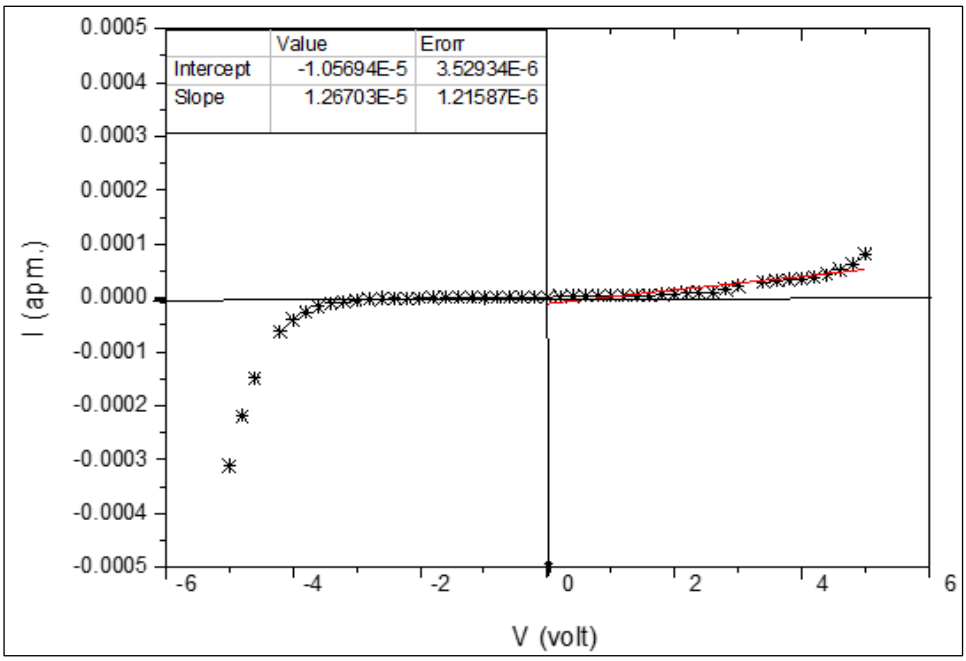

Figure5. Current–Voltage characteristics thin film of ZnPc

Electrical Conductivity DC Dependent on Temperature

Thin films CuPc and ZnPc that electrical conductivity was measured in order to calculate the activation energy thermal. Specimens were measured at temperatures ranging from 313 to 483 k and plotted in the figures.The inset to figures have shown the the temperature dependence of the conductivity calculated utilizing Arrhenius equation(29).

$$\sigma = \sigma_{\circ}\, exp\, \frac{-E_a}{K_B\, T} \qquad (7)$$

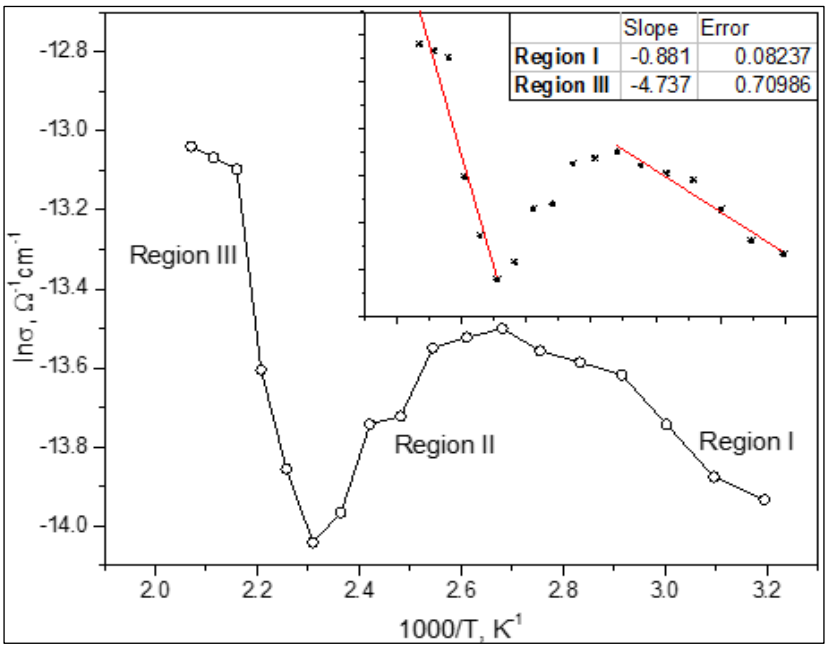

Figure 6. Ln σ as a function of 10^3/T for CuPc Thin Films. The inset shows the fitting analysis of activation energy regions

Where E represents activation energy thermal and K represents constant's Boltzmann. A plot between Ln vs. 1000/T for CuPc and ZnPc films and films thickness is 100 nmdeposited on Platinum-intertdigitated electrodes reveals three regions. However, region II is neglected as it is caused by the recombination of charge carriers. Region I and region III corresponds to two activation energies. The values of the activation energies of CuPc for region I, Ea = 0.076 ev and region III, Ea= 0.407 ev. While in the case of ZnPc, the activation energies were found to be 0.029 and 0.056 ev for region I and region III respectively.E1 corresponds to the extrinsic region and represents the transition process for carriers within localized states in the energy gap, implying a high density of localized states in the energy gap, and E 2 corresponds to the intrinsic region and represents carriers transport across grain boundaries via thermal excitation. Shift in slope, and thus activation energy, is interpreted as a shift from extrinsic to intrinsic conduction(34). At lower temperatures, conduction mechanism is explained as hopping through a band that localized states,and upon higher temperatures as free conduction.These findings have also been concluded previously in the literature (35).

1100

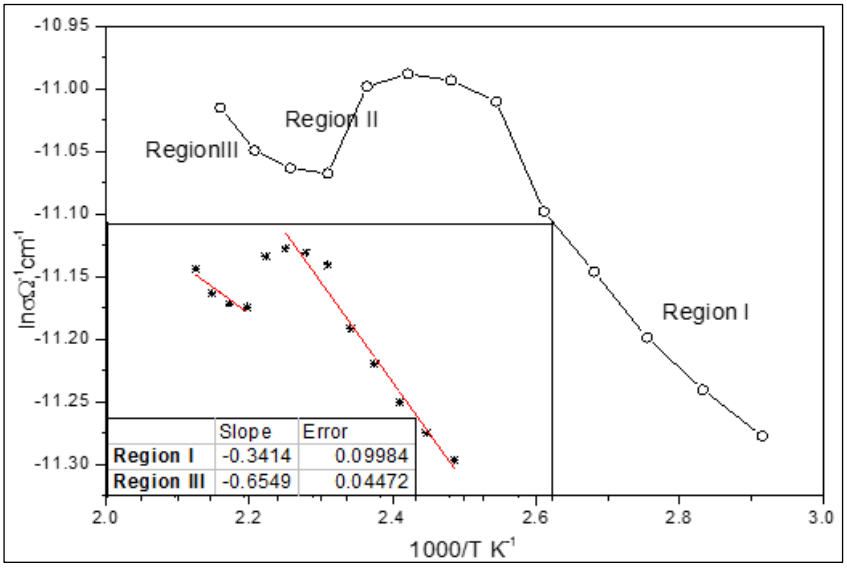

Figure7. Ln σ as function of 10^3/T that ZnPc Thin Films. The inset shows the fitting analysis of activation energy regions

AFM Topology

FigureThe typical aggregation of phthalocyanine thin films is shown. In the solid state, phthalocyanine and almost all organic dyes form extremely dense aggregations.These aggregates are modeled as a conplanar arrangement of rings that progress from monomer to dimer to higher order complexes. They are propelled by van der Waals forces and (π-π) interaction.(36).

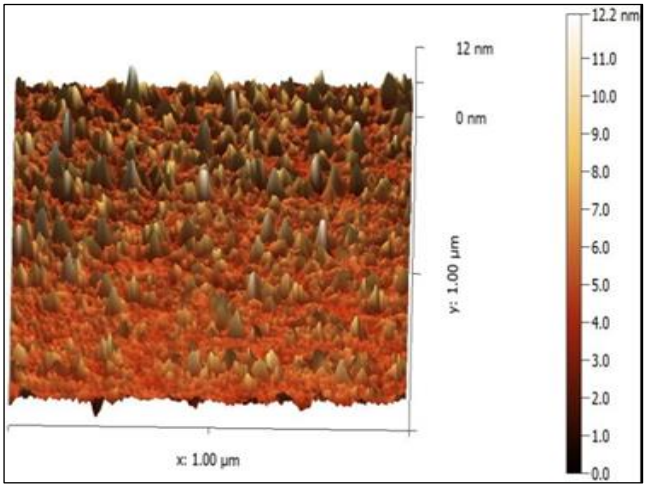

(a)

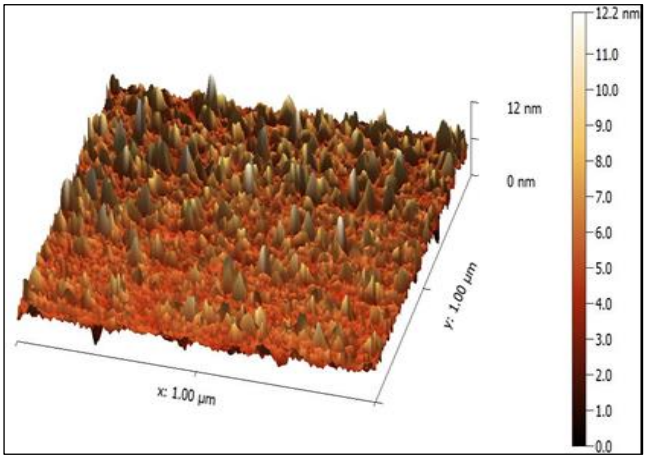

(b)

Figure 8.AFM images of ZnPc film.Plane view (a) and 3D view, (b) 2D of the film surface

Figure Shows a 2D and 3 D view that ZnPcon scan size 1µm × 1 µm.Surface of the film contains open structures700 nm wide that repeaton different regions of the surface on a regular basis. Root mean square (RMS) roughness value is approximately 7.004 nm.Figure.Surface topography of a CuPc film deposited by spin coating onto a glass substrate is shown.In particular,AFM, 2D and 3 D views of filmare reported on scan size 1µm × 1 µm. Roughness value is about 2.668 nm. AFM results of CuPc and ZnPc films prepared by spin coating show a uniform granular surface morphology, as in figures. Where it can be note that the roughness of ZnPc higher than CuPc and this result agreement with the interpretation of electrical characterization.

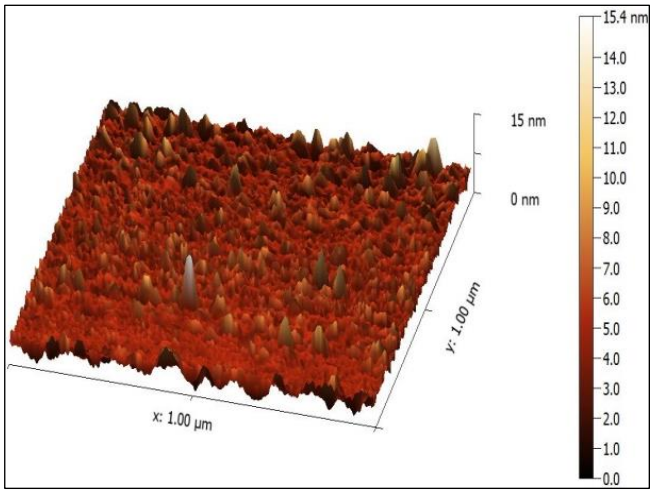

(a)

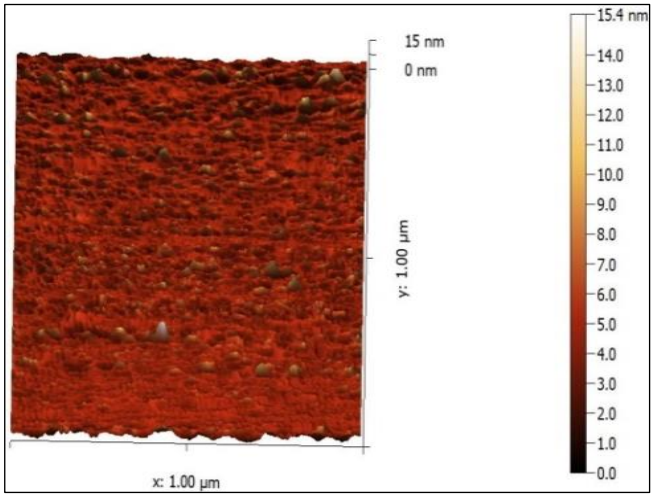

(b)

Figure 9.AFM images of CuPc film.Plane view (a) and 3D view, (b) 2D of the film surface

Conclusion

Zinc and Cu phthalocyanine thin films have been prepared in mean that spin coating mechanism. UV-Visible spectra have revealed that thin film has shown a little red shift in the position of Q band in comparison to solution spectra and formation of dimer and trimmer molecules instead of being monomers. The optical energy gaps were found to be 3.87 ev and 3.93 ev for copper and zinc phthalocyanine respectively. Variation of DC electrical conductivity with (1/T),shows that CuPc,ZnPc films have two activation energy, CuPc

forone region, E_{a1} = 0.076 ev andtwo region, E_{a2} = 0.407 ev . while in the case of ZnPc, the activation energies were found to be 0.029 ev and 0.056 ev for first region and second region respectively. CuPc has shown Ohmic behavior, while the ZnPC shown like diode behavior.

References

Inigo AR, Xavier FP, Goldsmith GJ. Copper phthalocyanine as an efficient dopant in development of solar cells. Mater Res Bull. 1997;32(5):539–46.

Sharma GD, Kumar R, Sharma SK, Roy MS. Charge generation and photovoltaic properties of hybrid solar cells based on ZnO and copper phthalocyanines (CuPc). Sol energy Mater Sol cells. 2006;90(7–8):933–43.

Varghese AC, Menon CS. Electrical properties of nickel phthalocyanine thin films using gold and lead electrodes. J Mater Sci Mater Electron. 2006;17(2):149–53.

Arslan S. Phthalocyanines: Structure, synthesis, purification and applications. Batman Üniversitesi Yaşam Bilim Derg. 2016;6(2/2):188–97.

Weng Q, Yang S. Urban air pollution patterns, land use, and thermal landscape: an examination of the linkage using GIS. Environ Monit Assess. 2006;117(1):463–89.

Schwieger T, Peisert H, Golden MS, Knupfer M, Fink J. Electronic structure of the organic semiconductor copper phthalocyanine and K-CuPc studied using photoemission spectroscopy. Phys Rev B. 2002;66(15):155207.

Moiz SA, Karimov KS, Gohar ND. Orange dye thin film resistive hygrometers. Eurasian Chem J. 2004;6(3):179–83.

Li Y, Yang MJ. Bilayer thin film humidity sensors based on sodium polystyrenesulfonate and substituted polyacetylenes. Sensors Actuators B Chem. 2002;87(1):184–9.

Ondavalli P, Legagneux P, Pribat D. Carbon nanotubes based transistors as gas sensors: State of the art and critical review. Sensors Actuators B Chem. 2009;140(1):304–18.

De La Torre G, Bottari G, Hahn U, Torres T. Functional phthalocyanines: synthesis, nanostructuration, and electro-optical applications. Funct Phthalocyanine Mol Mater. 2010;1–44.

Uğur AL, Erdoğmuş A, Koca A, Avcıata U. Synthesis, spectroscopic, electrochemical and spectroelectrochemical properties of metal free,manganese, and cobalt phthalocyanines bearing peripherally octakis-[4-(thiophen-3-yl)-phenoxy] substituents. Polyhedron. 2010;29(18):3310–7.

Banimuslem H, Hassan A, Basova T, Durmus M, Tunce. Copper phthalocyanine functionalized single-walled carbon nanotubes: thin films for optical detectionl, Sinem Esenpınar, Aliye Aslı Gürek, Ayse Gül Ahsen, Vefa. J Nanosci Nanotechnol. 2015;15(3):2157–67.

Kumar GA, Thomas J, George N, Kumar BA, Radhakrishnan P, Nampoori VPN, et al. Optical absorption studies of free (H2Pc) and rare earth (RePc) phthalocyanine doped borate glasses. Phys Chem Glas. 2000;41(2):89–93.

Hamam KJ, Alomari MI. A study of the optical band gap of zinc phthalocyanine nanoparticles using UV–Vis spectroscopy and DFT function. Appl Nanosci. 2017;7(5):261–8.

El-Nahass MM, El-Gohary Z, Soliman HS. Structural and optical studies of thermally evaporated CoPc thin films. Opt Laser Technol. 2003;35(7):523–31.

El-Nahass MM, Abd-El-Rahman KF, Farag AAM, Darwish AAA. Optical characterisation of thermally evaporated nickel phthalocyanine thin films. Int J Mod Phys B. 2004;18(03):421–34.

Strens RGJ. Elliott and (AF) Gibson. An Introduction to Solid State Physics and its Applications. London (Macmillan), 1974. xxi+ 490 pp., 297 figs. Price£ 5.95. Mineral Mag. 1975;40(310):213.

Alias M. Optoelectronic study of a-Si-Ge-Al (As): H thin films. Ph. D. thesis, College of Science, University of Baghdad, Baghdad, Iraq; 1998.

Abbas NK, Abdulameer AF, Ali RM, Alwash SM. The Effect of Heat Treatment on Optical Properties of Copper (II) Phthalocyanine Tetrasulfonic Acid Tetrasodium Salt (CuPcTs) Organic Thin Films. Silicon. 2019;11(2):843–55.

El Nhass MM, Soliman HS, Metwally HS, Farid AM, Farag AAM, El Shazly AA. Optical properties of evaporated iron phthalocyanine (FePc) thin films. J Opt. 2001;30(3):121–9.

Pankove JI. Optical processes in semiconductors Prentice-Hall. New Jersey. 1971;92.

Singh Y. Electrical resistivity measurements: a review. In: International journal of modern physics: Conference series. World Scientific; 2013. 745–56.

Saleh AM, Abu-Hilal AO, Gould RD. Investigation of electrical properties (ac and dc) of organic zinc phthalocyanine, ZnPc, semiconductor thin films. Curr Appl Phys. 2003;3(4):345–50.

Rajesh KR, Menon CS. Electrical and optical properties of vacuum deposited MnPc thin films. Eur Phys J B-Condensed Matter Complex Syst. 2005;47(2):171–6.

Zanfolim AA, Volpati D, Olivati CA, Job AE, Constantino CJL. Structural and electric-optical properties of zinc phthalocyanine evaporated thin films: temperature and thickness effects. J Phys Chem C. 2010;114(28):12290–9.

Takeuchi A, Inoue A. Classification of bulk metallic glasses by atomic size difference, heat of mixing and period of constituent elements and its application to characterization of the main alloying element. Mater Trans. 2005;46(12):2817–29.

Peker A, Johnson WL. A highly processable metallic glass: Zr41. 2Ti13. 8Cu12. 5Ni10. 0Be22. 5. Appl Phys Lett. 1993;63(17):2342–4.

Matsumoto S, Matsuhama K, Mizuguchi J. β Metal-free phthalocyanine. Acta Crystallogr Sect C Cryst Struct Commun. 1999;55(1):131–3.

Sundar U. Influence of Surface Modification of BaTiO 3 Nanoparticles on the Dielectric Properties of Ba-TiO 3/Epoxy Composite Films. Rutgers The State University of New Jersey-New Brunswick; 2017.

Darwish S, El Zawawi IK, Riad AS. Photovoltaic properties of ZnSe/metal-free phthalocyanine heterojunctions deposited on substrates of InP single crystals. Thin Solid Films. 2005;485(1–2):182–7.

Yuan M, Quan LN, Comin R, Walters G, Sabatini R, Voznyy O, et al. Perovskite energy funnels for efficient light-emitting diodes. Nat Nanotechnol. 2016;11(10):872–7.

Singh A, Uddin MA, Sudarshan T, Koley G. Tunable reverse-biased graphene/silicon heterojunction schottky diode sensor. Small. 2014;10(8):1555–65.

Bube R. Electronic properties of crystalline solids: an introduction to fundamentals. Elsevier; 2012.

Matsumoto N, Shima H, Fujii T, Kannari F. Organic electroluminescence cells based on thin films deposited by ultraviolet laser ablation. Appl Phys Lett. 1997;71(17):2469–71.

Schütze A, Pieper N, Zacheja J. Quantitative ozone measurement using a phthalocyanine thin-film sensor and dynamic signal evaluation. Sensors Actuators B Chem. 1995;23(2–3):215–7.

He N, Chen Y, Bai J, Wang J, Blau WJ, Zhu J. Preparation and optical limiting properties of multiwalled carbon nanotubes with π-conjugated metal-free phthalocyanine moieties. J Phys Chem C. 2009;113(30):13029–35.